

**New regulatory mechanisms in lipid metabolism:
from polymorphisms of triglyceride uptake systems
to mitochondrial stability**

Katalin Sümegi

Ph.D. Thesis

Supervisor: Dr. Béla Melegh

Leader of Doctoral Program: Dr. Béla Melegh

Leader of Doctoral School: Dr. Balázs Sümegi



University of Pécs

Medical School, Department of Medical Genetics

2018

Table of Contents

1. Abbreviations	6
2. Introduction	8
2.1. Lipid metabolism.....	10
2.2. Role of lipids, especially triglycerides	11
2.3. Characterization of GCKR, MLXIPL, ANGPTL3, CILP2, GALNT2, TRIB1, and APOA5 loci	12
3. Aims of the Investigations.....	19
4. Materials and methods	20
4.1. Study population.....	20
4.2. Genetic approaches.....	21
4.2.1. PCR amplification	22
4.2.2. RFLP technique	23
4.3. Biochemical materials and methods	25
4.3.1. Chemicals and other biochemical materials	25
4.3.2. Isolation of rat liver mitochondria.....	26
4.3.3. Determination of membrane potential ($\Delta\Psi$) in isolated rat liver mitochondria	26
4.3.4. Mitochondrial uptake of BGP-15	26
4.3.5. HPLC-MS/MS analysis	27
4.3.6. Cell viability assay	27
4.3.7. Determination of reactive oxygen species in cell culture.....	28
4.3.8. Determination of mitochondrial production of reactive oxygen species.....	29
4.3.9. Construction of mitochondria directed enhanced red fluorescent protein.....	29
4.3.10. JC-1 assay for fluorescent microscopy.....	29
4.3.11. Tetramethylrhodamine methyl ester (TMRM) assay	30
4.3.12. Identification of the type of cell death by annexin V/PI staining.....	30
4.4. Statistical analysis	31
5. Results	32
5.1. GCKR, MLXIPL, ANGPTL3, CILP2, GALNT2, TRIB1 and APOA5	32
5.2 BGP15	46
5.2.1. Mitochondrial uptake of BGP-15	46
5.2.2. Effect of BGP-15 on mitochondrial membrane potential ($\Delta\Psi$)	46
5.2.3. BGP-15 attenuates mitochondrial production of reactive oxygen species.....	49

5.2.4. Effect of BGP-15 on mitochondrial reactive oxygen species production in isolated mitochondria.....	54
5.2.5. Effect of BGP-15 on reactive oxygen species-induced cell death	55
5.2.6. BGP-15 protects against LPS-induced mitochondrial depolarization.....	56
5.2.7. BGP-15 protects against LPS-induced production of reactive oxygen species .	58
6. Discussion	61
6.1. GCKR, MLXIPL, ANGPTL3, CILP2, GALNT2, TRIB1 and APOA5	61
6.2. BGP15	66
7. Summary	69
8. References	70
9. Publications	81
9.1 Publications related to thesis:	81
9.2 Publications non-related to thesis:.....	81
9.3. Book Chapters	85
9.4. Abstracts	86
10. Acknowledgements	88

1. Abbreviations

AIF: Apoptosis inducing factor

ANGPTL3: Angiopoietin-like protein 3

APOA5: Apolipoprotein A5

ATP: Adenosine triphosphate

BGP-15: (O-[3-piperidino-2-hydroxy-1-propyl]-nicotinic amidoxime)

CAD: Coronary artery disease

ChoRE: Carbohydrate response element

ChREBP: Carbohydrate response element-binding protein

CILP2: Cartilage intermediate layer protein 2

CM: Chylomicrons

CRI: Chronic renal insufficiency

CVD: Cardiovascular diseases

EDTA: Ethylenediaminetetraacetic acid

EL: Endothelial lipase

ER: Endoplasmic reticulum

GALNT2: Galactosamine polypeptide N-acetylgalactosaminyltransferase

GCK: glucokinase

GCKR: Glucokinase regulatory protein

GPIHBP1: Glycosylphosphatidylinositol-anchored high density lipoprotein-binding protein 1

GWAS: Genome-wide association studies

HDL: High density lipoprotein

HPLC MS: High performance liquid chromatography mass spectrometry

HSP: Heat shock protein

IHD: Ischemic heart disease

JC-1: Mitochondrial membrane potential probe

JNK: C-Jun N-terminal kinases

LD: Linkage disequilibrium

LDL: Low-density lipoprotein

LPL: Lipoprotein lipase

MAP: Mitogen-activated protein

mERFP: Mitochondria directed enhanced red fluorescent protein

MG: Malignant glioblastoma

MLXIPL: MLX interacting protein like

PARP: Poly ADP ribose polymerase

PCR: Polymerase chain reaction

PKC: Protein kinase C

RFLP: Restriction fragment length

ROS: Reactive oxygen species

SNP: Single-nucleotide polymorphism

T2DM: Diabetes mellitus type 2

TG: Triglyceride

TMRM: Tetramethylrhodamine methyl ester

TRIB1: Human tribbles-1

TRL: Triglyceride-rich lipoproteins

VLDL: Very low density lipoprotein

GPIHBP1: Glycosylphosphatidylinositol-anchored high density lipoprotein-binding protein 1

2. Introduction

Cardiovascular disease (CVD) is a major cause of death worldwide. The recent genome-wide association studies (GWAS) revealed genetic polymorphisms associated with blood lipid level alterations. Nowadays, special attention gained on metabolic consequences, including triglyceride level increases, confirming risk for cardiovascular diseases, metabolic syndrome or for cerebrovascular diseases, especially stroke events [1-19]. The National Cholesterol Education Program (NCEP) in 2001 ascertained numerous markers strongly associated with coronary risk, stratified as risk factors related to lifestyle, such as physical inactivity, obesity, atherogenic diet; and emerging risk factors, as lipoprotein profile, homocysteine level, altered fasting glycaemia and evidence of subclinical atherosclerosis. Approach to lipoprotein management in 2001 National Cholesterol Guidelines [20].

While the exact reasons behind CVD's are unknown [21,22], several studies established elevated triglyceride (TG) levels affect TG metabolism and are independent risk factors for CVD [23,24]. Thus, research of the TG level modifier factors, especially genetic susceptibility variants, may have clinical importance. These factors include, amongst others, ANGPTL3, CILP2, TRIB1, MLXIPL, GALNT2, GCKR and APOA5 genes. As a prominent example the functional roles of *APOA5* polymorphisms have already been widely investigated [1-7]. Several of them are associated with elevated TG levels and higher risks for ischemic stroke and cardio- or cerebrovascular diseases or for metabolic syndrome [4,5,8-11,25,26]. Recently, other TG modifying polymorphisms came into focus, which may also have role in development of different diseases [2,12,15,16,19,27-29]. Some variants are mentioned in connection with increased, while others with decreased triglyceride levels [16,27,28,30,31]. The elevated levels of certain TGs may have a higher risk for several vascular diseases. Moreover, significant associations between TG-elevating and polymorphisms were confirmed [1,2,4,5,12-15,17,29,30,32-36].

As several previous studies revealed Roma greatly differ from the Hungarian population genetically as a result of their descent. Therefore it is interesting to compare them to Caucasian populations. Roma people are an underprivileged, neglected population worldwide with severe healthcare problems. Historical, linguistic and genetic studies suggest that the Roma people originate from South Asia, mainly Northwest India [37,38]. Today the estimated size of the Roma population is 12-15 million globally. The majority of the population - approximately 10-12 million - live in Europe, with the highest percentage (70%) in Central and South-Eastern

Europe [39]. According to the available Roma in Central-Eastern Europe often have a higher rate of cardiovascular events and morbidity than other European populations [40,41]. This is related to the Roma population's poor socioeconomic status, social exclusion, and other risk factors such as disturbed lipid metabolism, hypertension, obesity, alcohol consumption and smoking habits [42].

Intracellular fatty acids are catabolized predominantly in the mitochondria. Long chain fatty acids are transported to the mitochondrial matrix space by the carnitine acyl-transferase system, and on the end forming intramitochondrial long chain of fatty-acyl-CoA which is converted to acetyl-CoA by the mitochondrial beta-oxidation system [43]. Free fatty acids besides contributing to ATP synthesis also cause serious stress to various tissues and can contribute to the development of cellular stress. Fatty acids contribute to intracellular reactive oxygen species (ROS) production in a significant extent in the mitochondria. Oxidative stress induced by palmitate can initiate Ca^{2+} release from the endoplasmic reticulum (ER) leading to ER stress and further ROS production. Elevated Ca^{2+} and ROS can initiate mitochondrial permeability transition causes superoxide production and the activation of mitochondrial apoptosis pathway. This vicious lipotoxicity pathway can lead to β -cell failure and insulin resistance and to diabetic complications [44].

Agents (UCP-1, uncouplers) lowering agents mitochondrial membrane potential ($\Delta\Psi$) and antioxidants (superoxide dismutase, N-acetylcysteine, lipoic acid) can prevent glucose-induced activation of PKC which leads to diabetic complications [45-47].

These observations among other data show the importance of mitochondrial reactive oxygen species production in the development of diabetes [48]. Unfortunately antioxidants therapy fails in human studies for those compounds which are providing excellent protections in cell culture and animal studies [49,50]. Therefore, it would be very advantageous to find molecules which are not antioxidant in the sense that they would not react with ROS, but to find molecules which bind to mitochondrial proteins, and so they can prevent, or highly reduces the mitochondrial ROS production at the respiratory complexes which are the major source of mitochondrial ROS [51].

BGP-15, a O-(3-piperidino-2-hydroxy-1-propyl) pyridine-3-carboxylic acid amidoxime monohydrochloride has a wide range of cytoprotective effects [52-55]. However, up to now has not been identify any clear intracellular targets for BGP-15. In diseases models BGP-15 prevented cell death [54,56,57], reduced oxidative stress (lipid peroxidation and protein oxidation) [56,57], activated heat shock protein (HSP) expression [52,58-60]. In addition, BGP-15 attenuated inflammatory reaction [61] reduced DNA-breaks formation and poly ADP ribose

polymerase (PARP) activation [56,57,61], facilitated mitochondrial energy production [56,57]. Furthermore, BGP-15 decreased the nuclear translocation of apoptosis inducing factor (AIF) from mitochondria, reduced c-Jun N-terminal kinases (JNK) activation [53,60,61], and inhibited the activation of p38 mitogen-activated protein (MAP) kinase [53]. Previous studies showed that BGP-15 is an insulin sensitizer in olanzapine-induced insulin resistance in human phase II studies, and in diabetic insulin resistant patients [58,62,63]. Earlier, it was raised that this can be related to the co-inducer effect of BGP-15 on HSP [58,62,63], but no direct effect of BGP-15 on heat shock transcription factor (HSF1) has been shown.

Previous works showed that ROS (including mitochondrial ROS production) produced in diabetes, and lead to the development of insulin resistance [45-48]. Therefore, it was assumed that BGP-15 attenuates mitochondrial ROS production by binding to Complex I, or Complex III, and so prevent the development of the vicious cycle leading to mitochondrial ROS production and the abnormal activation kinase cascades characteristic to diabetic reprogramming and defective Glut4 translocation to cell surface.

2.1. Lipid metabolism

Lipids are complex, organic, nonpolar molecules, which are insoluble in water, can be divided into several subclasses such as triglycerides, phospholipids and steroids, and there is an additional subgroup, fatty acids, which can be comprised as subunits of TGs or phospholipids. Lipids have important biological role in energy storage, in molecular signaling pathways and in comprising biological cell membranes [64]. Lipids, in general, can be categorized as the extensive classification of LIPID MAPS database into eight subgroups: fatty acyls, glycerolipids, glycerophospholipids, sphingolipids, sterol lipids, prenol lipids, saccharolipids and polyketides [65].

Elevated plasma lipid concentration is a common finding during routine blood tests and contributes to increased risk of CVD, which is a leading cause of death. Hyperlipidemia is often associated with additional CVD risk factors and certain systemic diseases, obesity, metabolic syndrome, and type 2 diabetes mellitus (T2DM) which increase the risk of early-onset atherosclerosis. With the help of identifying genetic hyperlipidemia and recognizing the possible several cardiovascular risk factors - especially those, who have familial prelude-, may treat subsequent serious diseases with medication at an early stage [66].

The formation of atherosclerosis starts with the accumulation of esters and cholesterol during childhood, and is seen as fatty streaks in the intima of large muscular arteries. The fibrous plaque forms in some people when further lipid deposits occur and is covered by a fibromuscular cap. This plaque can undergo changes which makes them susceptible to rupture, which could lead to precipitates occlusive thrombosis and clinically manifest disease (sudden cardiac death, myocardial infarction, stroke, or peripheral arterial disease) [67].

It has been seen that after reaching adulthood these fatty streaks can be linked to serum lipoprotein concentrations, smoking, obesity, and hyperglycemia. After age 30 this risk factors along with hypertension can lead to raised lesions. With this knowledge it seems logical to begin the prevention of coronary artery disease (CAD) in childhood to limit the degree of juvenile fatty streaks and to prevent or impede their progression to raised legions [67].

Chronic renal insufficiency (CRI) is linked to a characteristic dyslipidemia in both children and adults. Typically most commonly observed are moderate hypertriglyceridemia, increased triglyceride-rich lipoproteins (TRL) and reduced high-density lipoproteins (HDL) with total and low-density lipoprotein cholesterol (LDL-C) remaining within or slightly above normal range. Lipoprotein lipase and hepatic lipase activity decrease, and concentrations of apolipoprotein C-III are noticeably higher [68].

2.2. Role of lipids, primarily triglycerides

Elevated plasma TG concentrations are a common finding during routine blood tests and contribute to increased risk of CVD. Hypertriglyceridemia is often associated with other CVD risk factors such as cholesterol, obesity, metabolic syndrome, and T2DM and unrelated to CVD, and severe hypertriglyceridemia is also correlated with elevated risk of acute pancreatitis. The increase in plasma TGs is a result of increased production from the liver and intestine or decreased peripheral catabolism (mainly from reduced lipoprotein lipase activity). Following a meal more than 90% of the circulating TGs are broken down and absorbed in intestinal cells and finally are secreted in chylomicrons. However this digestion isn't the only source of triglycerides. Fatty acids synthesized by the liver are converted to TGs and transported to the blood via very low density lipoproteins (VLDL). In capillaries within fat and muscle tissue, these lipoproteins and chylomicrons are hydrolyzed by lipoprotein lipase into free fatty acids [69,70].

2.3. Characterization of GCKR, MLXIPL, ANGPTL3, CILP2, GALNT2 TRIB1, and APOA5 loci

The glukokinase regulator (GCKR) gene consists of 19 exons, it encodes a protein of 625 amino acids which is a regulatory protein that has a sugar isomerase region which inhibits glucokinase in liver and pancreatic cells beta cells by forming an inactive complex with the enzyme by non-covalent bonds [71-82]. Thus, the function of GCKR is linked to glucose metabolism [82,83]. Recent studies verified the association of several SNPs, like rs780094 (an intronic variant of the GCKR) with increases of plasma TG levels [72,84,85]. In other studies another variant of GCKR (rs1260326) was found to be strongly linked to rs780094, and to inversely modulate fasting plasma glucose and TG levels through elevated glucokinase activity [86-93]. Despite higher risk for dyslipidemia and higher triglyceride levels, the GCKR L446 carriers were protected against T2DM, suggesting a potential molecular mechanism by which these two components of the metabolic syndrome can be dissociated [85].

GCKR plays a role in function of GCK enzyme both as a regulator and as a receptor protein as well. In the liver and pancreas, GCK enzyme is negatively regulated by GCKR, which enables it to make its way into the cell nucleus where it stabilizes and protects the GCK enzyme [74,77,83,86,89,94]. During fasting, the GCKR protein inhibits function of GCK enzyme. Until the glucose levels rise in the plasma, GCKR and GCK form an inactive complex in the nucleus. With the appearance of glucose in the nucleus GCK dissociates from GCKR and exits into the plasma where it initiates the phosphorylation of glucose [95-97]. Studies have shown the relationship between functional variants in GCKR and hypertriglyceridemia. The two best studied SNPs in the GCKR gene are rs780094 and rs1260326. Subjects presenting with rs1260326 or rs780094 exhibited an increase in plasma TG levels. Mutations in the GCKR gene, which result in the synthesis of proteins with inhibitory effect, could associate with diabetes. They are most likely cause sensitivity to fructose-6-phosphate, or they reduce susceptibility to fructose-6-phosphate, which led to believe that GCKR plays a role in the development of T2DM. The risk for developing type 2 diabetes with rs780094 is lower than with rs1260326.

The variant rs780094 contributes to the risk of T2DM and dyslipidaemia. The GCKR rs780094, alone or in combination with GCK rs1799884, associates with T2DM in Han Chinese population. The effect on T2DM is probably mediated through impaired beta cell function, rather than via the obesity. The rs780094(A) risk allele is associated with higher levels of fasting

serum triacylglycerol, impaired fasting and oral glucose tolerance test (OGTT) related insulin release, dyslipidemia, somewhat reduced the risk of T2DM.

The polymorphism rs780094 likely acts as a proxy for a nearby tightly linked ($r(2)=0.93$) SNP, rs1260326, which encodes a common missense GCKR variant. Both of them are linked with opposite effects on fasting plasma TG and glucose concentrations, and, associated with C-reactive protein levels. The T allele of rs1260326 variant has been associated with T2DM and hypertriglyceridemia. It was shown to have the strongest association signal with metabolic phenotypes in the region that also harbors the tightly linked ($r(2)=0.93$) SNP rs780094, which has been previously associated with TG and glucose concentrations.

GCKR rs1260326 associates with increased risk of ischemic heart disease (IHD) for TT homozygous subjects in a large scale of studies. It was found to be associated with elevated remnant cholesterol, elevated nonfasting TGs and apolipoprotein B, but not with elevated LDL cholesterol or with decreased HDL cholesterol levels.

The *MLXIPL* (or its often used name, carbohydrate response element-binding protein, ChREBP) gene is located at chromosome 7q11.23 and it encodes a protein (ChREMP) which is a basic helix-loop-helix leucine zipper transcription factor in the Myc/Max/Mad superfamily. In Williams-Beuren syndrome, a multisystem developmental disorder, this gene is involved. This protein normally forms a heterodimeric complex, binds and activates the carbohydrate response element (ChoRE). ChREBP converts dietary carbohydrate to storage fats in the liver through the coordinated expression of the enzymes that channel glycolytic pyruvate into lipogenesis.

Adipose-ChREBP is a major determinant of fatty acid synthesis and insulin sensitivity in humans and in animals. Glucose-mediated activation of the ChREBP isoform, the ChREBP α , induces expression of another, a potent isoform, the ChREBP β that is transcribed from an alternative promoter. ChREBP β expression in human adipose tissue predicts insulin sensitivity raising the issue that it can be an effective target for diabetes treatment.

ChREBP is located inactively in the cell plasma, and has phosphorylated serin and threonin strands. Deactivation happens after increase of blood glucose level. This xilulouse-5-phosphate also involved in the process, which activates phosphoprotein phosphatase 2A, which removes a phosphate group from the serin in nuclear ChREBP. Here another phosphorylation takes place, after which ChREBP is ready to bind with max-like bHLH-ZIP Mlx transcription factor. This complex connects to the promoter region of ChoRE (the “carbohydrate response element”) and initiates transcription through which it has an effect on the synthesis of several enzymes, like acetyl-coenzme-A carboxylase, and pyruvate kinase. These enzymes participate

in lipogenesis in the liver [98]. SNP rs17145738 associates with severe hypertriglyceridemia. SNP rs3812316 a SNP in the MLXIPL gene that is also known to have G771C or Gln241His variants. In a study of over 10,000 individuals of different ethnicities they were found to be very significantly associated ($p=1.4 \times 10^{-10}$) with plasma TG levels.

Angiopoietin like 3 (ANGPTL3) gene located on chromosome 1p31 was first identified in 2002 and is associated with TG. This gene encodes a protein that is a member of the angiopoietin-like family of growth factors and is specific for the endothelium. The mature protein has the characteristic structure of angiopoietins having a signal peptide, N-terminal coiled-coil domain and the C-terminal fibrinogen (FBN)-like domain. ANGPTL3 is predominantly expressed in the liver. It inhibits lipoprotein-lipase and endothelial lipase (EL), and helps thereby to regulate plasma TG levels and HDL. It plays a role in TG metabolism. There are three known frameshift mutations (Fs122, FsQ192 and FsK455) that are linked to decreased plasma TG levels. In humans with genetic loss-of-function variants in one copy of ANGPTL3 serum LDL levels are reduced while loss-of-function form in both copies of ANGPTL3 results in low LDL, low HDL, and low TGs levels. This represents a variant of familial combined hypolipidemia [99].

The Cartilage intermediate layer protein 2 (CILP2) gene is located at 19p13. The gene encodes a protein which contains a central furin endoprotease consensus site that causes a release of N- and C-terminal peptides. The N-terminal half CILP2 contains a thrombospondin type-1 repeat and an immunoglobulin C2-type domain, but lacks aldehyde dehydrogenase cysteine active site and ATP-binding site. The rs16996148 is a polymorphism near the CILP2 locus has been demonstrated to decrease TG levels [100].

The Galactosamine polypeptide N-acetylgalactosaminyltransferase (GALNT2) gene locates on chromosome 1q42.13 and encodes UDP-N-acetyl-alpha-D-galactosamine:polypeptide N-acetylgalactosaminyltransferase 2, which is a member of the GalNAc-transferases family. Members of this family transfer an N-acetyl galactosamine to the hydroxyl group of a serine or threonine residue in the first step of O-linked oligosaccharide biosynthesis.

Genome-wide association studies demonstrated that GALNT2 plays a role in lipid metabolism, but it is still not known how the enzyme ppGalNAc-T2 mediates this effect. Mutation of GALNT2 has been identified in people with elevated plasma high-density lipoprotein cholesterol and reduced triglycerides. Data suggest that ppGalNAc-T2 can affect lipid metabolism through apoC-III glycosylation [101].

The human tribbles pseudokinase 1 (TRIB1) gene, found on chromosome 8q24.13, was first identified in 2004 [102]. It is a G-protein-coupled receptor-induced protein involved in the regulation of MAPK (mitogen-activated protein kinase). It plays a role in the regulation of lipid metabolism. Its protein product tribbles homolog 1 (trib1) can be found in most human tissues, while Trib1 can either activate or inhibit MAPK activity depending on the ratio of trib1 to MAPK levels. The regulatory effects of Trib1 can take place at transcriptional and translational levels [102]. The polymorphism located near the TRIB1 locus (rs17321515) at chromosome 8q24 is associated with elevated total and LDL-cholesterol and with an increased risk of CHD and CVD, while in a Japanese cohort significant correlation was found between the rs17321515 variant and triglyceride levels and LDL cholesterol concentrations. Studies on European populations showed the A allele at rs17321515 to be associated with elevated TG levels, higher LDL- and lower HDL-cholesterol concentrations.

The most investigated and better understood apolipoproteins are the ApoA1, ApoA4, ApoC3 and ApoA5 are members of the apolipoprotein family. Apolipoprotein A5 (APOA5 gene) protein is the latest identified member of the apolipoprotein family, which was discovered more than a decade ago.[103,104]. One group of researchers [104] was searching for liver regeneration factors, using cDNA subtractive hybridization when they discovered an upregulated protein in rat liver, which showed some homology to other apolipoproteins. During this time Pennachio and his colleagues were searching for regulator genes in lipid metabolism using comparative genome sequencing between human and mouse DNA when they mentioned a gene not far from ApoA1/C3/A4 gene cluster on chromosome 11q23. This gene was located 27kbp far from 3' end of the ApoA4 gene and showed a 27% homology with ApoA4. The mature ApoA5 protein is 39kDa. The ApoA5 protein is expressed exclusively in the liver, and in much lower concentration found in humans (0.1-0.4 µg/ml) leads to believe that only one in 24 VLDL particles can carry an ApoA5 molecule. *ApoA5* encodes a 366 amino acid residue protein, while mature ApoA5 contains 343 amino acid residues in humans [105]. ApoA5 is a hydrophobic protein, which has an amphipathic α -helix secondary structure; therefore the ApoA5 protein is insoluble at neutral pH in aqueous solution [106,107]. In absence of lipids the N-terminal residues 1-146 form a helix [9]. This fragment region is water soluble contrary to the full length protein [108]. Results show that residues 1-146 can bind to lipoproteins like HDL and VLDL. In the attendance of lipids, ApoA5 shows good solubility due to the lipid binding residues 293-343 at the C-terminal end.

ApoA5 has been determined a key player in lipid metabolism through interaction with lipoprotein lipase (LPL) and the anchoring molecules [109-112]. This interaction accelerates

the hydrolysis of TG-rich lipoproteins by affecting LPL or promotes a receptor mediated endocytosis of lipoprotein [113,114]. The presence of naturally existing polymorphisms of the APOA5 gene modifies the effect of the protein on lipid metabolism, resulting in increased TG levels [34,103,115] which has been confirmed in several populations worldwide. The polymorphisms in APOA5 may trigger the development of several diseases like metabolic syndrome, stroke and CVD [4,5,26,116,117].

Similar to other lipoproteins, ApoA5 also has an α -helix forming N-terminal domain and a lipid-binding C-terminal domain, however research by Sun et al.[112] distinguished six different regions in ApoA5 [118]. Studies have revealed that residues 192–238 are necessary for lipid binding and activation of LPL, but the C-terminal end is not a requisite for ApoA5 to bind a folded secondary structure [11,112]. The main heparin-binding domain of ApoA5 contains four positively charged residues (R210, K211, K215, K217) and are vital for interaction between ApoA5 and the LPL-anchoring protein (GPIHBP1; glycosylphosphatidylinositol-anchored high density lipoprotein-binding protein 1) [110,119]. It has been determined that ApoA5 binds to GPIHBP1 in vitro and this interaction has been hypothesized to facilitate lipoprotein lipase (LPL) mediated hydrolysis of the TG component of chylomicrons (CM). Both, the positively charged heparin-binding sequence within ApoA5 and the acidic domain in GPIHBP1 are essential for binding [109].

Due to the single cysteine at residue 204 ApoA5 can exist as a disulfide-linked homodimer or can form heterodimers with other apolipoproteins. ApoA5 is monomeric in human plasma because the cysteine sulfhydryl group remains free [120]. Studies have reported that through a 42 amino acid stretch (residues 186–227), which contains eight Arg/Lys and three His amino acid ApoA5 can connect to heparin and to LDL receptor (LDLr) gene family members (LDLr related protein 1 (LRP1) and the mosaic receptor LR11/SorLA) [113,118]. Similarly to ApoB and ApoE the same mechanism of interaction can probably be found in ApoA5, involving positively charged regions in the ligands and negatively charged regions in the receptors.

The importance of the positively charged residues in interaction was confirmed in double mutant Arg210Glu/Lys211Gln, which showed decreased binding to heparin and LRP1 [8,17]. The N-terminal end of ApoA5 interacts with cell surface midkine (neurite growth-promoting factor 2; NEGF2), it is then internalized in pancreatic β -cells, which leads to increased insulin secretion [121]. This might explain why insulin resistance was seen in *ApoA5* knockout animals [118,122].

Human ApoA5 transgenic and ApoA5 deficient mouse models have been used in several studies to investigate the lipid metabolic role of ApoA5. Transgenic mice showed 40% reduced

plasma TG levels compared to the wild type controls, and ApoA5 deficient mice had significantly elevated TG levels, approximately four times higher than the wild type. Differences were revealed in VLDL levels with fast protein liquid chromatography (FPLC) and gradient gel electrophoresis as they were used to characterize the lipoprotein particles.

The mechanism behind ApoA5 can be explained in three possible ways: (1) ApoA5 is involved in VLDL synthesis and/or secretion via intracellular mechanisms. (2) ApoA5 accelerates the hydrolysis of TG-rich lipoproteins by affecting LPL, either directly or via other regulatory apolipoproteins such as ApoC3. (3) ApoA5 acts as a ligand to lipoprotein receptors or proteoglycans and thus promotes receptor-mediated endocytosis of lipoproteins [118].

The role of ApoA5 in extracellular TG metabolism is supported by different studies and there is increasing proof for the function of ApoA5 as a receptor ligand. Nonetheless, the intracellular role of ApoA5 for lipoprotein assembly and secretion is still more theoretical [118].

Previous studies have suggested that ApoA5 could play a role in the reduction of plasma TG through lipoprotein assembly [123]. Furthermore it has been established that ApoA5 plays a very important role in TG regulation as it affects plasma TG levels, and it may decrease hepatic VLDL production by binding to lipids and cellular membranes and through this mechanism, inhibit VLDL assembly and secretion [106,123]. Several studies' results show that ApoA5 reduces plasma TG levels by accelerating plasma TG hydrolysis. The most significant plasma TG level reducing effect of ApoA5 is the acceleration of plasma TG hydrolysis by modulating LPL activity or by amending the effects or the concentrations of other apolipoproteins like ApoC3. ApoC3 unlike ApoA5 has a physiological antagonist effect on LPL activity [105]. Since, ApoA5 can alter the concentration or effects of ApoC3, it can modify the plasma TG level.

ApoA5 is mostly found on the surface of VLDL or HDL lipoproteins [114]. When the VLDL/CM-ApoA5 complex reaches the endothelium, it connects to the GPIHBP1 protein or HSPG, which is anchored to the endothelium, and to the LPLs. The LPLs can be found in dimeric form on the GPIHBP1 protein or HSPG surface and catalyzing the lipoprotein TG hydrolysis. As previously stated, researchers assume that ApoA5 may influence TG hydrolysis in different ways. This depends on the anchoring molecule to which it is connected, either HSPG or GPIHBP1 [110]. If the VLDL/CM-ApoA5 complex connects to the HSPG molecule, this complex can assist the ApoC-2 activation of LPL, resulting in increased speed of TG hydrolysis. After the breakdown of TG-rich lipoproteins (VLDL or chylomicron (CM)), ApoA5 disconnects from the remnant particle and transfers to nascent HDL. Furthermore ApoA5 can bind to the GPIHBP1 homodimer and LPLs, where the interaction may accelerate the TG

hydrolysis in CM/VLDL. Furthermore, ApoA5 can interact with LPLR family members and induce endocytosis of remnant lipoproteins.

Several polymorphisms were identified in the APOA5 gene in the past years. The most comprehensively studied four single nucleotide polymorphisms (SNPs) are the following: rs662799, rs2266788, rs207560 and rs3135506. Studies have demonstrated that some of these SNPs are independent risk factors for CVD, metabolic syndrome and stroke.[23,124] The most commonly studied polymorphism rs662799 has been associated with coronary artery disease [125]. Pennacchio et al. confirmed that the most common SNPs in the APOA5 gene are in strong linkage disequilibrium and constitute haplotype variants [115]. Out of all the haplotypes, APOA5*2, was found to be strongly associated with increased TG levels and shows susceptibility for metabolic and vascular events [4,126].

3. Aims of the Investigations

During my PhD training I was involved in different research profiles performed on cells, in vitro models, animals, and on human samples. In my PhD I summarize two major focus points related to each other.

The first area includes human investigations targeted mainly on the possible functional roles of the triglyceride modifier genes in Roma population samples. This involved the examination of TG level modifier APOA5 polymorphisms in Roma samples as susceptibility factor because it is known, that the Roma population has high prevalence of increased TG levels [42]. Assuming that genetic background also plays a role in their susceptibility for cardiovascular diseases several gene polymorphisms were examined that literature has suggested to play a role in lipid metabolism and in the development of metabolic syndrome and cardio/cerebrovascular diseases. The following polymorphisms were examined: rs12130333 at the ANGPTL3, rs16996148 at the CILP2, rs17321515 at the TRIB1, rs17145738 and rs3812316 of the MLXIPL, rs4846914 at GALNT2, rs1260326, rs780094 residing at the GCKR loci and four APOA5 polymorphisms (rs662799, rs2266788, rs207560 and rs3135506) DNA samples. These samples were genotyped essentially using PCR-RFLP method. The targeted variants could be targets for therapeutic interventions. Often we used our biobank pooled samples as controls, in some experiments we performed also comparisons with huge public biobank and database results as well. In these experiments we often used internationally recognized biobanks; in all experiments we followed the Helsinki declaration for human experiments, and had the appropriate ethics committee approval.

The second part, the mitochondrial stability experiments were part of a long-term, quite complex series of mitochondrial investigations. Keeping in mind the importance of mitochondria in regulating cell death in ROS-related diseases [127,128], in my training we investigated whether the protective effects of BGP-15 rely on the preservation of mitochondrial integrity and reduction of mitochondrial ROS production, using different biochemical approaches, as they are detailed under the section of the “Materials and methods”.

The link between the human and in vitro parts is the possible therapeutic significance of them.

4. Materials and Methods

4.1. Study population

The Hungarian and Roma populations used for our study are part of the Biobank at the Department of Medical Genetics, which is part of the Hungarian National Biobank Network (www.biobanks.hu) as well as part of the European Biobanking and Biomolecular Resources Research Infrastructure (BBMRI) (<http://bbmri.eu/bbmri/>). Samples in the Biobank date back to 2001 and is currently one of the largest collections of Roma samples in Hungary. The Biobank functions with the permission and support of the Medical Scientific Council's Research and Ethics Committee (ETT TUKEB). The collection and analysis of the DNA samples were conducted according to the regulations of the Declaration of Helsinki Declaration in 1975 and the currently operative National regulations. The study protocol was reviewed and approved by the Hungarian Scientific and Research Ethics Committee of the Medical Research Council (ETT TUKEB). Informed written consent was obtained from all subjects prior to study. Roma samples were obtained from Roma minority who self-reported at least three past generations of Roma ancestry. Care was also taken during the selection of the previously collected biobank samples to minimize biased results from possible sampling errors; like exclusion of known family members, selected from different living areas. The same also applied for the average Hungarians as well; none of them self-reported to belong to any known ethnic groups living in Hungary, they were apparently healthy and free from any know disease. Major clinical data of the study population are presented in Table 1.

Table 1. Major clinical and laboratory data of Roma and Hungarian population samples

	Roma (399)	Hungarians (404)
Males/females	179/221	141/263
Age (years)	55.7±0.94	61.5±0.79
Plasma triglyceride (mmol/l)	1.61±0.04	1.44±0.02
Total cholesterol (mmol/l)	4.70±0.06	5.58±0.06

*p<0.025

Sample size determination was based on the preliminary analyses of SNP prevalence. Based on the important significant difference in frequencies of the genetic alterations between Roma and Hungarian samples; we calculated how many samples were need per group to be adequately small and large enough to detect a statistically significant difference and to exclude Type I and Type II errors ($\alpha=0.05$ and $\beta<0.03$, two tailed). A total of 363 (gender: 162 male, 201 female; age: 55.86 ± 0.99) Roma and 404 (gender: 141 male, 263 female; age: 61.51 ± 0.79) Hungarian samples were used in the study. The fasting serum TG and total cholesterol levels of the subjects were measured right after taking blood samples, which was carried out between 8:00 and 9:00 in the morning.

4.2. Genetic approaches

For DNA extraction blood was drawn from peripheral vein into 10 ml EDTA containing tubes (BD Vacutainer; Becton, Dickinson and Co, UK), and DNA was extracted from the white blood cells with routine desalting methods as follows. The contents of the tubes were transferred into 50 ml centrifuge tubes and brought the volume to 50 ml with cold (4°C) RBC Lysis Buffer and put into a bucket of ice for 30 minutes turning it 5-6 times during this time period. Following 30 minutes at 5000 RPM in the centrifuge at 4°C , the supernatant was carefully removed. Once again this was brought to volume to 50 ml with Lysis Buffer and the previous process was repeated 4 times. Five ml SE buffer (pH 8.0) /containing 4.39 grams (75 mmol) NaCl and 8.41 grams (25 mmol) Na-EDTA, 25 μl Proteinase-K (10mg/ml) and 500 μl 10% SDS 10%/ was added to the sediment, vortexed and incubated the sample at 37°C overnight at 200 RPM in an incubator shaker. The following day 3 ml of saturated NaCl solution (6M) was added, vortexed

for 15 seconds, and centrifuged the tube at 3000 RPM for 15 minutes. Afterwards the DNA containing supernatant was gently poured into a sterile 50 ml tube and 96% ethanol was added to 40 ml final volume and the samples were stored room temperature for about 5-10 minutes until DNA precipitated. Next 200 μ l 70% ethanol was added to a clean Eppendorf tube and DNA from the previous tube was gently added to this. Samples were left at room temperature for 20 minutes before the ethanol was removed with a pipette. DNA was dried at room temperature for approximately 30 minutes. Finally 500 μ l of TE buffer solution (pH:8, 0.78g Tris HCl + 0.14 EDTA) was added to the DNA which was then incubated at 37°C overnight until completely dissolved.

4.2.1. PCR amplification

As the starting point of polymorphism analysis was DNA amplification with polymerase chain reaction with the standard method of utilizing synthetic oligonucleotide primers specific or the sequence surrounding (purchased from Metabion International AG, Martinsried, Germany), Taq polymerase, buffer solution, dNTP and genomic DNA template. Primers were designed with the help of Primer3 program accessed through Biology Workbench 3.2 (<http://workbench.sdsc.edu/>) and BLAST. The sequences of primers and conditions of PCR-RFLP are shown in Table 2.

The reaction mixture had a final volume of 50 μ l with 5 μ l buffer solution (500 mM KCl, 14 mM MgCl₂, 10 mM Tris-HCl, pH 9.0), 0.2 mM dNTP solution, 1 U Taq polymerase enzyme (10U/ μ l), primer pair equal to 0.2 mM, 1 μ l MgCl₂ solution and 1 μ g DNS template.

For the PCR reaction the following parameters were utilized for 35 cycles: predenaturation at 96°C for 2 minutes, denaturation at 96°C for 30 seconds, annealing at 55°C for 30 seconds, elongation at 72°C for 30 seconds and as a final step a final elongation at 72°C for 5 minutes with an MJ Research PTC-200 Peltier Thermal Cycler (Bio-Rad, Hercules, CA, USA).

8 μ l of PCR products were loaded into the wells of a 2% agarose gel stained with ethidium-bromide (1 gram of Lonza SeaKem[®] LE Agarose mixed with 50ml of TBE (Tris/Borate/EDTA) buffer solution and microwaved for approximately 4 minutes 1.5 μ l of ethidium-bromide was added.). 8 μ l of amplified DNA was mixed with 1 μ l of Bromophenol Blue loading buffer. After loading the samples in the wells of the agarose gel an electrical

current of 175V was used for about 5 minutes. Finally, the gel was illuminated with an Ultraviolet lights (Cleaver Scientific Ltd.) and pictures were taken.

4.2.2. RFLP technique

In order to detect variations in each specific DNA sequence restriction length fragment polymorphisms (RFLP) method was used. The DNA samples were digested by restriction enzymes and cleaved into segments. These restriction fragments were separated according to their lengths by gel electrophoresis and thus it was possible to detect SNPs in homologous DNA. The reaction mixture contained 1 Unit specific enzyme (Fermentas Inc., Burlington, ON, Canada), 10-15 μ l PCR product, 10x buffer and sterile distilled water. The incubation temperature applied was according to the needs of the restriction endonuclease.

Table 2. Primer sequences and PCR-RFLP conditions

Gene	Functional variants	Forward primer	Reverse primer	Melting temperature (°C)	PCR product size (bp)	Restriction endonuclease	Ancestral genotype fragments (bp)	Heterozygous genotype fragments (bp)	Minor allele genotype fragments (bp)
<i>GCKR</i>	C1337T rs1260326	TGCAGACTATAGTGGAGCCG	CATCACATGGCCACTGCTTT	60	231	<i>HpaII</i>	18, 63, 150	18, 63, 150, 213	18, 213
	rs780094	ATTGTCTCAGGCAAACCTGGTA	CCCGGCCTCAACAAATGTAT	60	273	<i>PscI</i>	63, 210	33, 63, 177, 210	33, 63, 177
<i>MLXIPL</i>	rs17145738	ATGGTCCAGGAGTCTGCC	AGCCATCGTGCCTAGCTAAA	60	615	<i>TaaI</i>	49, 113, 253	49, 113, 253, 366	49, 366
	rs3812316	CCATCCCCAGCCATCCCT	TTCTCCAGTGTGGTCCCGT	60	239	<i>BspLI</i>	16, 17, 203	16, 17, 26, 177, 203	16, 17, 26, 177
<i>ANGPTL3</i>	rs12130333	TTTCTAAACCTTGGTATCTTCATTG	CATTTTCATGTTGCTTTGTAATTT	58	372	<i>DraI</i>	79, 294	26, 79, 268, 294	26, 79, 268
<i>CILP2</i>	rs16996148	TTCATCATTCACCCATCCA	AATGTGTGTTCTCCAAGCC	58	466	<i>HinIII</i>	184, 283	47, 184, 235, 283	47, 184, 235
<i>GALNT2</i>	rs4846914	CTGTGCCTTCTGGGACTGCTA	AGTGAGGAAGGACTATGAGATGATG	57	200	<i>HpyF3I</i>	19, 74, 107	19, 74, 107, 126	74, 126
<i>TRIB1</i>	rs17321515	AAGGAAGGGTTAGGTAGACCAATTA	GACACCAGCTGTAGAGAACCAAATA	57	596	<i>FspBI</i>	56, 90, 450	56, 90, 450, 541	56, 541
<i>APA05</i>	rs662799	CCCCAGGAAGTGGAGCGACCTT	TTCAAGCAGAGGGAAGCCTGTA	55	398	<i>TruI</i>	22, 109, 267	22, 109, 267, 289	109, 289
	rs207560	CTCAAGGCTGTCTTCAG	CCTTTGATTCTGGGGACTGG	62	280	<i>MnII</i>	25, 114, 141	25, 41, 73, 114, 141	25, 41, 73, 141
	rs2266788	TCAGTCCTTGAAAGTGGCCT	ATGTAGTGGCACAGGCTTCC	62	287	<i>BseGI</i>	122, 165	35, 87, 122, 165	35, 87, 165
	rs3135506	AGAGCTAGCACCGCTCCTTT	TAGTCCCTCTCCACAGCGTT	62	256	<i>Cfr13I</i>	26, 79, 151	26, 79, 151, 177	79, 177

4.3. Biochemical materials and methods

4.3.1. Chemicals and other biochemical materials

All chemicals for cell culture studies were from PAA Laboratories (Cölbe, Germany) and Gibco/Invitrogen (Carlsbad, CA, USA). The fluorescent dyes JC-1, fluorescein-conjugated annexin V (annexin V-FITC), Hoechst 33342, rhodamine 123 (R123), propidium iodide (PI), dihydrorhodamine 123 (DHR123) and MitoSOX were obtained from Molecular Probes (Carlsbad, CA, USA). BGP-15 was a gift from N-Gene (New York, NY, USA). All other chemicals were purchased from Sigma Aldrich Co. (Budapest, Hungary).

WRL-68 (HeLa derivative), H9c2 (rat heart myoblast) and U-251 MG (human malignant glioblastoma) cells were purchased from the European Collection of Cell Cultures (ECCC). The cell lines were grown at 37°C in a humidified 5% CO₂ atmosphere. The WRL-68 cells were cultured in Eagle's minimum essential medium, and H9c2, while U-251 MG cells in Dulbecco's modified Eagle's medium. All media contained antibiotics (1% penicillin and streptomycin mixture), and 10% bovine serum. Cells were passaged every 3 days; were seeded at a starting density of 2×10^4 cells/well in a 96-well plate for the viability and ROS production assays, or at a density of 1×10^5 cells/well in a 6-well plate for fluorescent microscopy.

Wistar rats were purchased from Charles River Hungary Breeding Ltd. (Budapest, Hungary). The animals were kept under standard conditions; tap water and rat feed were provided *ad libitum*. The experiment conformed to the Guide for the Care and Use of Laboratory Animals, published by the US National Institutes of Health (NIH Publication no. 85-23, revised in 1996), and was approved by the local Animal Research Review Committee of the University of Pécs, Hungary.

4.3.2. Isolation of rat liver mitochondria

Rats were sacrificed by decapitation under isoflurane (AbbVie Ltd., Budapest, Hungary) anesthesia, their livers were removed, and mitochondria were isolated from the liver homogenates by differential centrifugation, as described in a standard protocol [129]. Isolated liver mitochondria were purified by Percoll density gradient centrifugation [130], and the protein concentrations were determined using the biuret method using bovine serum albumin as a standard.

4.3.3. Determination of membrane potential ($\Delta\Psi$) in isolated rat liver mitochondria

$\Delta\Psi$ was determined by measuring R123 fluorescence upon its release from the mitochondria. Fluorescence was measured by a fluorescence spectrometer (LS-50B; Perkin-Elmer; gift from Alexander von Humboldt Foundation, Bonn, Germany) at an excitation wavelength of 494 nm, and an emission wavelength of 525 nm. For 60 seconds 1 mg protein/mL mitochondria were preincubated in an assay buffer (containing 70 mM sucrose, 214 mM mannitol, 20 mM N-2-hydroxyethyl piperazine-N'-2-ethanesulfonic acid, 5 mM glutamate, 0.5 mM malate and 0.5 mM phosphate) containing 1 μ M R123. Alterations in $\Delta\Psi$ were induced by the addition of BGP-15 at the indicated concentrations.

4.3.4. Mitochondrial uptake of BGP-15

Mitochondrial uptake of BGP-15 (50 μ M) was determined in 5 mM Tris buffer (pH 7.5) containing 150 mM KCl, 1 mM EDTA and 2.5 mg mitochondrial protein in 800 μ l volume, in addition to 10 μ M glucose-6-phosphate as a standard in order to determine the void volume. Uncoupling was induced using 50 μ M 2,4-dinitrophenol. After an incubation period of 10 min, the mitochondria were centrifuged at 20,000 g, then washed and lysed in 800 μ l of ethanol-water 1:1 solution, and centrifuged again at 20,000 g. Aliquots of the clear supernatant were freeze-dried, and taken up in aqueous formic acid solution (0.1%).

4.3.5. HPLC-MS/MS analysis

Five μL aliquots of the samples were injected into the HPLC-MS system (Dionex Ultimate 3000 UHPLC, Q-Exactive HRMS; Thermo Fisher Scientific, Bremen, Germany). Liquid chromatographic separation was carried out using a Kinetex (Gen-Lab Kft., Budapest, Hungary) $2.6\ \mu\text{m}$ C18 100 Å HPLC column ($100 \times 2.1\ \text{mm}$), which was maintained at 30°C . The used mobile phase was (A) aqueous formic acid solution (0.1%) with (B) acetonitrilic formic acid solution (0.1%). The flow rate was set to $300\ \mu\text{L}/\text{minute}$. The initial gradient conditions were set to 5% B, held for 3 minutes, then B was increased linearly until reaching 80% after 12 minutes. The initial conditions were reached after 2 minutes, then the column was equilibrated for 8 minutes. The mass spectrometer was equipped with a heated electrospray ion (ESI) source which was operated in the negative ion mode. The spray voltage was set to 3.5 kV, the capillary temperature adjusted to 300°C , and the temperature of the probe heater was set to 50°C . The S-lens RF level was set to 70. Mass range was set to m/z 150–1,500. Data analysis was performed using the Thermo Xcalibur (version 2.2 SP1.48) software. Ion intensities were determined by matching them to a BGP-15 calibration curve.

4.3.6. Cell viability assay

The viability of WRL-68 cells after various treatments were tested by sulforhodamine B (SRB) assay. The standard method used for cell density determination in cytotoxicity screening was based on essentially the measurement of cellular protein content, according to the method described by Papazisis and colleagues [131], with some modifications. The culture medium was aspirated prior to fixation of the cells by the addition of $200\ \mu\text{L}$ of cold 10% trichloroacetic acid. After a 20 minute incubation at 4°C , cells were washed twice with deionized water, and the microplates were then left to dry at room temperature for at least 24 hours. When dried, the cells were stained with $200\ \mu\text{L}$ of 0.1% SRB dissolved in 1% acetic acid for at least 20 minutes at room temperature, then they were washed four times with 1% acetic acid to remove the unbound stain remains. The plates were dried at room temperature. The bound SRB was solubilized with $200\ \mu\text{L}$ of 10 mM unbuffered Tris-base solution, and plates were shaken on a plate shaker for at least 10 minutes. Absorbance was determined using the GloMax Multi Detection System (Promega, USA) at 560 nm in addition to the background measurement at 620 nm. The optical density values were defined as the absorbance of each individual well

extracted from the blank value. All experiments were done in at least eight replicates, and each measurements were in triplicates.

4.3.7. Determination of reactive oxygen species in cell culture

Intracellular ROS (peroxynitrite, $\bullet\text{OH}$ and iron + hydrogen peroxide (H_2O_2)) were determined by using two separate approaches, like fluorescence microscopy and quantitative determination of ROS-evoked fluorescence intensities by a plate reader. The WRL-68 or U-251 MG cells were seeded to glass coverslips and cultured at least overnight before their further use. WRL-68 cells were transiently transfected with mitochondria directed enhanced red fluorescent protein (mERFP). The next day, cells were washed twice with phosphate buffered saline (PBS), and treated as described in the Results and the figure legends. Then, the medium was replaced to a fresh solution containing 1 μM of the oxidation-sensitive DHR123 fluorescent dye, and incubation was continued for an additional 15 minutes to allow oxidation of DHR123 by the endogenous ROS.

The fluorescence of mERFP and the oxidized DHR123 was excited at 615 and 485 nm, and the evoked emission was measured at >650 and 525 nm, respectively using a Nikon Eclipse Ti-U fluorescent microscope (Auro-Science Consulting Ltd., Budapest, Hungary) equipped with a Spot RT3 camera using a 60x objective lens. The nuclei of U-251 MG cells were labelled using Hoechst 33342 (1 $\mu\text{g}/\text{mL}$) dye, which were excited at 350 nm and read at 460 nm emission wavelengths. All experiments were repeated in triplicates.

Alternatively, WRL-68, H9c2 or U-251 MG cells were also seeded in 96-wells plates and kept in Krebs-Henseleit buffer containing 10% fetal bovine serum (FBS). The WRL-68 and H9c2 cells were treated with either H_2O_2 for 30 minutes alone or with increasing concentrations of BGP-15 in the absence or in the presence of 20 μM MitoTEMPO (Sigma Aldrich Co.) After 30 minutes, DHR123 (1 μM) was added to the medium and R123 formation was measured after 15 minutes with the GloMax Multi Detection System (excitation wavelength was 490 nm and emission wavelength was between 510–570 nm). The U-251 MG cells were treated with either LPS for 30 minutes alone or with 50 μM BGP-15 in the absence or presence of 20 μM MitoTEMPO (Sigma Aldrich Co.). Superoxide anions were detected by the addition of MitoSOX (0.3 μM) fluorescent dye. Fluorescence of oxidized MitoSOX was excited at 365 nm, and the evoked emission was determined at 410–460 nm by the GloMax Multi Detection System. All experiments were run in six replicates and the measurements were repeated three times.

4.3.8. Determination of mitochondrial production of reactive oxygen species

Mitochondria (100 $\mu\text{g}/\text{mL}$) were dissolved in a buffer solution containing 20 mM 3-(N-morpholino)propanesulfonic acid (MOPS), and 314 mM sucrose (pH 7.4) with either malate (5 mM) and glutamate (5 mM) or succinate (5 mM). ROS production was determined by the oxidation of DHR123 (1 μM) to R123, as measured by a fluorescence spectrometer at an excitation wavelength of 494 and an emission wavelength of 525 nm, under continuous mixing at 30°C. ROS production was localized to the respiratory complexes by either blocking the electron flow with antimycin A (10 μM) where glutamate (5 mM) and malate (5 mM) were used as substrates in order to localize ROS production to complex I, or by blocking electron flow with potassium cyanide (1 mM), where succinate was used as the substrate to localize ROS production to complex III. The antioxidant capacities of BGP-15 were determined by the chemical oxidation of DHR123 (1 μM ; excitation wavelength was 494 nm and emission wavelength was 525 nm) to R123. In these systems, either 500 μM H_2O_2 or 50 μM H_2O_2 plus 1 μM Fe^{2+} -EDTA was used.

4.3.9. Construction of mitochondria directed enhanced red fluorescent protein

The mERFP-expressing plasmid was constructed by PCR amplification of the targeted mitochondrial sequence of cytochrome c oxidase subunit VIIIa (COX8A) gene (RZPD). The amplified sequence was then inserted into pDsRed-Monomer-N1 mammalian expression plasmid (Clontech-Takara Bio Europe; Saint-Germain-en-Laye, France) between the XhoI and HindIII restriction sites.

4.3.10. JC-1 assay for fluorescent microscopy

$\Delta\Psi$ was measured using the $\Delta\Psi$ specific fluorescent probe, JC-1. WRL-68 or U-251 MG cells were seeded to glass coverslips and cultured at least overnight before the experiment. After the indicated treatment, cells were washed twice in ice-cold PBS, then incubated for 15 minutes at 37°C in modified Krebs-Henseleit solution containing 100 ng/mL of JC-1. When excited at 490 nm, the dye emits either green fluorescence at a low $\Delta\Psi$ or red fluorescence at a high $\Delta\Psi$. Following the incubation procedure, the cells were washed once with modified Krebs-Henseleit

solution, then visualized by a Nikon Eclipse Ti-U fluorescent microscope which was equipped with a Spot RT3 camera, using a 40x objective lens with epifluorescent illumination. All experiments were repeated three times.

4.3.11. Tetramethylrhodamine methyl ester (TMRM) assay

WRL-68 cells were seeded in 96-wells plates, were kept in Krebs-Henseleit buffer containing 10% fetal bovine serum (FBS), and then were treated with either H₂O₂ alone or with BGP-15 for 3 hours. In a separate set of experiment, U-251 MG cells were treated with either LPS for 60 minutes alone or with 50 μM BGP-15. Then, the medium was replaced with Krebs-Henseleit solution containing TMRM (50 nM) cationic, cell-permeant, red color fluorescent dye. After 15 minutes incubation, excess dye was eliminated by washing off, and the fluorescence was measured by the GloMax Multi Detection System (at excitation wavelength was 525 nm and emission wavelength was between 580–640 nm). To assess aspecific adsorption of the dye, the fluorescence signal was remeasured after addition of 1 μM mitochondrial uncoupling agent carbonyl cyanide 4-(trifluoromethoxy)phenylhydrazone (FCCP). The ΔΨ value was calculated based on the difference of fluorescence signal before and after FCCP-treatment. All experiments were run in six replicates and the measurement was repeated in triplicates.

4.3.12. Identification of the type of cell death by annexin V/PI staining

Cell death was detected by the GloMax Multi Detection System after annexin V-FITC/PI double staining procedure. WRL-68 cells were seeded at 2×10^4 cells/well in a 96-well, then cultured at least overnight before their use. After subjecting the cells to the indicated treatment, cells were washed once in PBS and then incubated in modified Krebs-Henseleit solution containing FITC-conjugated annexin V and PI, according to the manufacturer's instructions. Following the incubation, the cells were washed once with modified Krebs-Henseleit solution. Then green fluorescence signal (annexin V-FITC) was measured with the GloMax Multi Detection System (excitation wavelength was 490 nm and emission wavelength was 518 nm). The red fluorescence signal (PI) was excited at 525 nm and the evoked emission was measured at 617 nm. All experiments were run in six replicates and each measurement was repeated three times.

4.4. Statistical analysis

Statistical analysis was performed with the program SPSS 18.0 (SPSS Inc, Chicago, IL, USA). All clinical data presented is shown as average \pm SEM values. In some experiments differences between treatment groups were determined by ANOVA with a post-hoc test, while in others Student's t-test was used to compare the difference of the mean values from the two groups, depending on the nature of the study. The distribution of the variables was determined with the Kolmogorov-Smirnov-test. In the case of normal distribution parameter probes were used, while in the case of abnormal distribution non-parameter probes were used. In order to determine the difference among the values of each group the Kruskal-Wallis-test was performed. The χ^2 -test was used to compare the differences among clinical and laboratory parameters of each group in the case of normal distribution with discrete variable. Mann-Whitney-test was used to compare the differences in the clinical parameters of the Roma population versus the Hungarian population. During correlation analysis we used the logistic regression model and to determine the exact ratios. Linkage disequilibrium (LD) patterns were studied with Haploview 4.2. The minor allele frequency at each locus had to be >0.05 , with an r^2 value of <0.8 between pairs of loci, based on the default settings in Haploview [132]. HAPSTAT 3.0 (<http://www.bios.unc.edu/wlin/hapstat/>) was used for haplotype assignment. For statistical analysis of the data PASW statistics 20 software package (SPSS Inc., Chicago IL) was used. The significance limit (p) was $p<0.05$.

5. Results

5.1. GCKR, MLXIPL, ANGPTL3, CILP2, GALNT2, TRIB1 and APOA5

All allele distribution and allele frequencies of polymorphisms were in Hardy–Weinberg equilibrium both in Roma and in Hungarian individuals.

Tables 3. and 4. show the significant differences were found in allele frequencies for MLXIPL both variants, GALNT2 rs4846914 and ANGPTL3 rs1213033 polymorphisms comparing Roma participants to the Hungarians The C alleles in rs17145738 and rs3812316 variants of MLXIPL occurred more frequently in Roma population than in Hungarians. The variants rs1213033 of ANGPTL3 and rs4846914 of GALNT2 genes showed lower allele frequency in Roma participants than in Hungarians.

The levels of serum TG and total cholesterol in the two populations with different genotypes can be found in Table 5. and Table 6. No association could be detected between serum triglyceride levels and carrying minor alleles compared with the non-carriers in Roma and Hungarian samples.

Table 3. Allele distribution of polymorphisms of GCKR and MLXIPL gene loci

	Roma (399)		Hungarians (404)	
GCKR rs1260326	CC (n=119)	CT+TT (n=205+75)	CC (n=102)	CT+TT (n=208+94)
T allele frequency	44.5%		49.0%	
GCKR rs780094	GG (n=119)	GA+AA (n=180+100)	GG (n=99)	GA+AA (n=218+87)
A allele frequency	47.6%		48.5%	
MLXIPL rs17145738	TT (n=2)	TC+CC (n=43+354)	TT (n=9)	TC+CC (n=98+297)
C allele frequency	94.1%*		85.6%	
MLXIPL rs3812316	GG (n=5)	GC+CC (n=36+358)	GG (n=9)	GC+CC (n=89+306)
C allele frequency	94.2%*		86.8%	

*p<0.025 vs. non-carriers

Table 4. Allele distribution of polymorphisms of CILP2, GALNT2, ANGPTL3 and TRIB1 gene variants

	Roma (394)		Hungarians (400)	
CILP2 rs1699614	GG (n=333)	GT+TT (n=60+1)	GG (n=342)	GT+TT (n=56+2)
T allele frequency	7.86%		7.50%	
GALNT2 rs4846914	AA (n=90)	AG+GG (n=243+63)	AA (n=91)	AG+GG (n=182+127)
G allele frequency	46.6%*		54.5%	
ANGPTL3 rs1213033	CC (n=309)	CT+TT (n=81+8)	CC (n=270)	CT+TT (n=112+18)
T allele frequency	12.2%*		18.5%	
TRIB1 rs17321515	AA (n=103)	GA+GG (n=203+93)	AA (n=107)	GA+GG (n=186+107)
G allele frequency	48.8%		50.0%	

*p<0.025 vs. non-carriers

Table 5. The effect on lipid parameters of polymorphisms of GCKR and MLXIPL variants

	Roma (399)		Hungarians (404)	
GCKR rs1260326	CC (n=119)	CT+TT (n=205+75)	CC (n=102)	CT+TT (n=208+94)
Plasma triglyceride (mmol/l)	1.47 ± 0.06	1.66 ± 0.05	1.58 ± 0.06	1.52 ± 0.03
Serum cholesterol (mmol/l)	4.57 ± 0.11	4.76 ± 0.07	5.66 ± 0.10	5.54 ± 0.07
GCKR rs780094	GG (n=119)	GA+AA (n=180+100)	GG (n=99)	GA+AA (n=218+87)
Plasma triglyceride (mmol/l)	1.50 ± 0.06	1.65 ± 0.05	1.51 ± 0.05	1.54 ± 0.03
Serum cholesterol (mmol/l)	4.57 ± 0.10	4.76 ± 0.07	5.69 ± 0.10	5.54 ± 0.07
MLXIPL rs17145738	TT (n=2)	TC+CC (n=43+354)	TT (n=9)	TC+CC (n=98+297)
Plasma triglyceride (mmol/l)	1.22 ± 0.12	1.61 ± 0.04	1.44 ± 0.09	1.54 ± 0.03
Serum cholesterol (mmol/l)	4.75 ± 0.15	4.70 ± 0.06	6.23 ± 0.53	5.56 ± 0.06
MLXIPL rs3812316	GG (n=5)	GC+CC (n=36+358)	GG (n=9)	GC+CC (n=89+306)
Plasma triglyceride (mmol/l)	1.51 ± 0.25	1.61 ± 0.04	1.41 ± 0.09	1.54 ± 0.03
Serum cholesterol (mmol/l)	4.88 ± 0.30	4.7 ± 0.06	5.90 ± 0.52	5.57 ± 0.06

Values are means ± SEM. *p<0.025 vs. non-carriers. Triglycerides and serum total cholesterol levels are mmol/l.

Table 6. Association of lipid parameters with polymorphisms of CILP2, GALNT2, ANGPTL3 and TRIB1 genes

	Roma (394)		Hungarians (400)	
CILP2 rs1699614	GG (n=333)	GT+TT (n=60+1)	GG (n=342)	GT+TT (n=56+2)
Plasma triglyceride (mmol/l)	1.60 ± 0.04	1.62 ± 0.10	1.54 ± 0.03	1.52 ± 0.05
Serum cholesterol (mmol/l)	4.71 ± 0.06	4.69 ± 0.14	5.59 ± 0.06	5.53 ± 0.16
GALNT2 rs4846914	AA (n=90)	AG+GG (n=243+63)	AA (n=91)	AG+GG (n=182+127)
Plasma triglyceride (mmol/l)	1.65 ± 0.09	1.59 ± 0.04	1.57 ± 0.05	1.53 ± 0.03
Serum cholesterol (mmol/l)	4.72 ± 0.11	4.70 ± 0.07	5.66 ± 0.11	5.56 ± 0.07
ANGPTL3 rs1213033	CC (n=309)	CT+TT (n=81+8)	CC (n=270)	CT+TT (n=112+18)
Plasma triglyceride (mmol/l)	1.61 ± 0.04	1.61 ± 0.08	1.52 ± 0.03	1.58 ± 0.04
Serum cholesterol (mmol/l)	4.67 ± 0.06	4.81 ± 0.12	5.57 ± 0.07	5.60 ± 0.10
TRIB1 rs17321515	AA (n=103)	GA+GG (n=203+93)	AA (n=107)	GA+GG (n=186+107)
Plasma triglyceride (mmol/l)	1.71 ± 0.07	1.57 ± 0.04	1.51 ± 0.04	1.55 ± 0.03
Serum cholesterol (mmol/l)	4.76 ± 0.11	4.69 ± 0.06	5.59 ± 0.11	5.57 ± 0.07

Values are means ± SEM. *p<0.025 vs. non-carriers. Triglycerides and serum total cholesterol levels are mmol/l.

The alleles and genotype frequencies of the studied APOA5 variants can be found in Table 7. For rs662799 APOA5 polymorphism we found that the frequency of the G allele was almost three times higher in the Roma population compared to Hungarian samples ($p=0.0001$) and almost two times higher than in European population (1000Genomes; $p=0.006$). Significantly large difference can be observed in allele frequency between Roma and HapMap European population ($p=0.0001$). The G allele was about two-fold more frequent in Asian (1000Genomes) and HapMap Chinese population than in Roma subjects ($p=0.002$; 0.001). Homozygous carriers of G allele were more frequent in Roma population than in Hungarians ($p=0.037$) and in Europeans (1000Genomes; $p=0.010$); however, it was less frequent in Romas than in Asian (1000Genomes; $p=0.027$) population. There was no significant difference in GG genotype frequencies between Roma and HapMap Chinese populations. Results of rs207560 show the frequency of the T allele in Roma samples was almost double than in those of the Hungarian population ($p=0.018$). The T allele was significantly frequent in Asian (1000Genomes; $p=0.0001$) population than in Romas. There was no difference between Roma and European populations (1000Genomes; $p=0.185$). Homozygous carriers of T allele were more frequent in Asian population (1000Genomes) than in Roma subjects ($p=0.0001$); however, the frequency of TT genotypes was similar in Hungarians and in Europeans (1000 Genomes; $p=0.940$; 0.211). Data of rs3135506 show that the G allele frequency in Roma's was more than two times higher compared to the Hungarian population ($p=0.001$); however, it does not differ significantly from the European population (1000Genomes; $p=0.066$). There was no significant difference in the frequency of GG genotype of Hungarians and of Europeans (1000 Genomes; $p=0.079$; 0.240) compared to Roma subjects. Allele- and genotype frequency data of rs207560 and rs3135506 in European and Chinese populations are not available in HapMap database, thus the analyses were not executed in these cases. We also analyzed the rs2266788 variant, where we did not find any difference between G allele frequencies of Hungarian and European populations (1000Genomes, HapMap) compared to Roma subjects ($p=0.473$; 0.062 ; 0.375). We found the frequency of the G allele was more than three times higher in Asian populations (1000Genomes and HapMap Chinese) compared to Roma samples ($p=0.0001$). The frequency of GG genotype was significantly different only in Asian population (1000Genomes) compared to Roma ($p=0.0001$). Cases with $n=0$ were not analyzed statistically.

Table 8. summarizes the lipid parameters of the populations according to genotypes. The plasma triglyceride levels were significantly elevated in the carriers of the risk alleles when compared to non-carriers for all SNPs in both populations. Significantly higher TG levels were found in heterozygous carriers of rs207560, rs3135506 and rs2266788 variants compared to

non-carriers in both study groups. Homozygous carriers of rs662799 variant have higher TG levels than non-carriers in Roma subjects. In Hungarians, we did not find any difference in TG levels between homo- or heterozygous carriers and non-carriers. Comparison of the cholesterol levels did not show any difference.

We analyzed associations among the four APOA5 variants in both study groups. (Table 9.) Strong correlations were found among rs662799, rs207560 and rs2266788 variants. However, rs3135506 variant did not show significant correlation with other APOA5 variants in Roma samples as well as in Hungarians. The same associations were detected after inclusion of the adjustment parameters like age and total cholesterol levels.

The associations between APOA5 variants and TG/cholesterol levels are summarized in Table 10. Significant correlations were found between all of the APOA5 variants and TGs in both populations. After inclusion of the adjustment parameters, such as age and total cholesterol levels, the association became even stronger. We did not observe any significant correlation between allelic variants and cholesterol levels in both populations.

Furthermore, we examined the linkage disequilibrium among the APOA5 major polymorphisms in both populations. We found moderate association between the rs2266788 and the rs3135506 variants ($r^2=0.56$), likewise between rs207560 and rs3135506 ($r^2=0.42$) in Hungarian population. In Roma population we found strong association between the rs207560 and the rs3135506 variants ($r^2=0.97$).

We also investigated the haplotypes with statistical probes in Roma and Hungarian populations. The structure of the probable haplotypes is summarized in Table 11. With the applied methods, we identified seven haplotypes in each population. Six of these haplotypes, APOA5*1, APOA5*2, APOA5*3, APOA5*4, APOA5*5 and ht7 were found to occur most frequently in both populations. The frequencies of the haplotypes are shown in Table 11. Significant differences were found in the presence of APOA5*2, APOA5*4, APOA5*5 and ht7 haplotypes between the Roma and Hungarian populations. However, we did not identify differences in the presence of APOA5*1 and APOA5*3 haplotypes between these populations. Ht5 haplotype in Roma and ht4 haplotype in Hungarian population could not be detected.

Table 7. Genotype and allele frequencies of APOA5 gene variants in different population samples

APOA5 variant	Population	N	Alleles		Risk allele frequency (%)	p-value ^a	Genotypes			p-value ^b
			N				N (%)			
			<u>A</u>	G			AA	AG	GG	
g.116792991G>A	Roma from Hungary (this study)	363	628	98	13.5		278 (76.58)	72 (19.84)	13 (3.58)	
	non-Roma from Hungary (this study)	404	765	43	5.32	0.0001	366 (90.60)	33 (8.17)	5 (1.24)	0.037
	Asian (1000Genomes)	504	718	290	28.8	0.002	251 (49.80)	216 (42.86)	37 (7.34)	0.027
	European (1000Genomes)	503	922	84	8.35	0.006	424 (84.30)	74 (14.71)	5 (0.99)	0.01
	HapMap Chinese	45	66	24	26.7	0.001	23 (51.11)	20 (44.44)	2 (4.44)	0.78
	HapMap European	60	118	2	1.67	0.0001	58 (96.67)	2 (3.33)	0	-
g.116791110T>C			<u>C</u>	T	T		CC	CT	TT	
	Roma from Hungary (this study)	363	680	46	6.34		318 (87.60)	44 (12.12)	1 (0.28)	
	non-Roma from Hungary (this study)	404	779	29	3.59	0.018	376 (93.07)	27 (6.68)	1 (0.25)	0.94
	Asian (1000Genomes)	504	768	240	23.81	0.0001	290 (57.54)	188 (37.3)	26 (5.16)	0.0001
European (1000Genomes)	503	924	82	8.15	0.185	426 (84.70)	72 (14.31)	5 (0.99)	0.211	

		<u>C</u>	G	G		CC	CG	GG	
g.116791691G> <u>C</u>	Roma from Hungary (this study)	363	658	68	9.37	300 (82.64)	58 (15.98)	5 (1.38)	
	non-Roma from Hungary (this study)	404	770	38	4.7	367 (90.84)	36 (8.91)	1 (0.25)	0.079
	Asian (1000Genomes)	504	1008	0	0	504 (100)	0	0	-
	European (1000Genomes)	503	938	68	6.76	438 (87.08)	62 (12.33)	3 (0.59)	0.24
		<u>A</u>	G	G		AA	AG	GG	
g.116789970G> <u>A</u>	Roma from Hungary (this study)	363	679	47	6.47	317 (87.33)	45 (12.40)	1 (0.27)	
	non-Roma from Hungary (this study)	404	747	61	7.55	344 (85.15)	59 (14.60)	1 (0.25)	0.94
	Asian (1000Genomes)	504	768	240	23.81	290 (57.54)	188 (37.30)	26 (5.16)	0.0001
	European (1000Genomes)	503	914	92	9.15	416 (82.70)	82 (16.30)	5 (0.99)	0.211
	HapMap Chinese	45	68	22	24.4	24 (53.33)	20 (44.44)	1 (2.22)	0.082
	HapMap European	59	113	5	4.24	54 (91.53)	5 (8.47)	0	-

Ancestral alleles are underlined. ^a indicates significance of the differences between Roma and other population risk alleles. ^b indicates significance of the differences between Roma and other population homozygous carriers.

Table 8. Lipid parameters (mmol/l) of the Roma and Hungarian population samples according to APOA5 gene variants

APOA5 variant	Parameter	Roma				Hungarian			
		AA	AG	GG	AG+GG	AA	AG	GG	AG+GG
rs662799	triglyceride	1.59 ± 0.04	1.72 ± 0.10 p=0.245	2.00 ± 0.16 p=0.009	1.76 ± 0.08 p=0.049	1.51 ± 0.02	1.79 ± 0.13 p=0.060	1.88 ± 0.31 p=0.133	1.81 ± 0.12 p=0.024
	cholesterol	4.66 ± 0.07	4.77 ± 0.13 p=0.352	4.91 ± 0.39 p=0.494	4.79 ± 0.12 p=0.280	5.57 ± 0.06	5.43 ± 0.22 p=0.234	6.14 ± 1.16 p=0.928	5.52 ± 0.24 p=0.257
rs207560	triglyceride	1.59 ± 0.04	1.92 ± 0.12 p=0.009	1.27 ± 0 p=0.668	1.91 ± 0.12 p=0.011	1.51 ± 0.02	1.84 ± 0.13 p=0.009	1.60 ± 0 p=0.602	1.84 ± 0.12 p=0.008
	cholesterol	4.67 ± 0.06	4.85 ± 0.19 p=0.242	3.90 ± 0 p=0.371	4.83 ± 0.19 p=0.302	5.57 ± 0.06	5.50 ± 0.29 p=0.377	4.70 ± 0 p=0.318	5.47 ± 0.28 p=0.295
rs3135506	triglyceride	1.59 ± 0.04	1.81 ± 0.10 p=0.028	1.96 ± 0.50 p=0.586	1.82 ± 0.10 p=0.025	1.52 ± 0.03	1.71 ± 0.07 p=0.001	1.50 ± 0 p=0.943	1.71 ± 0.06 p=0.001
	cholesterol	4.67 ± 0.06	4.88 ± 0.14 p=0.131	4.14 ± 0.43 p=0.269	4.82 ± 0.13 p=0.251	5.55 ± 0.06	5.67 ± 0.17 p=0.419	5.50 ± 0 p=0.862	5.66 ± 0.17 p=0.442
rs2266788	triglyceride	1.59 ± 0.04	1.92 ± 0.12 p=0.008	1.27 ± 0 p=0.671	1.90 ± 0.12 p=0.010	1.51 ± 0.03	1.69 ± 0.07 p=0.004	1.60 ± 0 p=0.575	1.69 ± 0.07 p=0.004
	cholesterol	4.67 ± 0.06	4.84 ± 0.19 p=0.282	3.90 ± 0 p=0.373	4.82 ± 0.19 p=0.347	5.57 ± 0.06	5.52 ± 0.18 p=0.384	4.70 ± 0 p=0.322	5.50 ± 0.17 p=0.327

Table 9. Correlations among APOA5 variants in the study groups

Population	Correlation coefficient (R)	APOA5 variant	APOA5 variant			
			rs662799	rs207560	rs3135506	rs2266788
Roma	Crude	rs662799	-	0.562 p<0.001 CI=-0.612-0.832	0.021 p=0.684 CI=-0.092-0.140	0.552 p<0.001 CI=-0.593-0.813
		rs207560	0.562 p<0.001 CI=-0.612-0.832	-	0.084 p=0.110 CI=-0.163-0.017	0.988 p<0.001 CI=0.980-1.013
		rs3135506	0.021 p=0.684 CI=-0.092-0.140	0.084 p=0.110 CI=-0.163-0.017	-	0.087 p=0.098 CI=-0.167-0.014
		rs2266788	0.552 p<0.001 CI=-0.593-0.813	0.988 p<0.001 CI=0.980-1.013	0.087 p=0.098 CI=-0.167-0.014	-
	Adjusted [†]	rs662799	-	0.636 p<0.001 CI=0.665-0.883	0.119 p=0.913 CI=-0.119-0.133	0.625 p<0.001 CI=0.642-0.860
		rs207560	0.636 p<0.001 CI=0.665-0.883	-	0.138 p=0.110 CI=-0.185-0.019	0.985 p<0.001 CI=0.977-1.016
		rs3135506	0.119 p=0.913 CI=-0.119-0.133	0.138 p=0.110 CI=-0.185-0.019	-	0.137 p=0.099 CI=-0.190-0.016
		rs2266788	0.625 p<0.001 CI=0.642-0.860	0.985 p<0.001 CI=0.977-1.016	0.137 p=0.099 CI=-0.190-0.016	-

Hungarian	Crude	rs662799	-	0.78 p<0.001 CI=0.826-0.967	0.073 p=0.143 CI=-0.173-0.025	0.485 p<0.001 CI=0.328-0.469
		rs207560	0.78 p<0.001 CI=0.826-0.967	-	0.019 p=0.702 CI=-0.133-0.090	0.626 p<0.001 CI=0.769-0.984
		rs3135506	0.073 p=0.143 CI=-0.173-0.025	0.019 p=0.702 CI=-0.133-0.090	-	0.084 p=0.090 CI=-0.224-0.016
		rs2266788	0.485 p<0.001 CI=0.328-0.469	0.626 p<0.001 CI=0.769-0.984	0.084 p=0.090 CI=-0.224-0.016	-
	Adjusted [†]	rs662799	-	0.803 p<0.001 CI=0.833-0.970	0.076 p=0.160 CI=-0.177-0.029	0.512 p<0.001 CI=0.345-0.488
		rs207560	0.803 p<0.001 CI=0.833-0.970	-	0.061 p=0.703 CI=-0.110-0.074	0.637 p<0.001 CI=0.769-0.986
		rs3135506	0.076 p=0.160 CI=-0.177-0.029	0.061 p=0.703 CI=-0.110-0.074	-	0.09 p=0.098 CI=-0.233-0.020
		rs2266788	0.512 p<0.001 CI=0.345-0.488	0.637 p<0.001 CI=0.769-0.986	0.09 p=0.098 CI=-0.233-0.020	-

[†]Adjusted for differences in age and cholesterol levels.

Table 10. Correlations between carrying APOA5 risk alleles and triglyceride levels in Roma and Hungarian population samples

Population	Correlation coefficients		APOA5 variant			
			rs662799	rs207560	rs3135506	rs2266788
Roma	Crude	R/Be	0.102	0.149	0.124	0.149
		R ²	0.011	0.022	0.015	0.022
		95%	0.000-0.092	0.027-0.144	0.011-0.113	0.027-0.143
		p	0.051	0.004	0.018	0.004
	Adjusted [†]	R	0.360	0.351	0.362	0.351
		R ²	0.129	0.123	0.131	0.123
		Beta	0.138	0.111	0.142	0.113
		95%	0.014-0.115	0.002-0.126	0.018-0.129	0.003-0.126
		p	0.012	0.043	0.009	0.040
Hungarian	Crude	R/Be	0.155	0.161	0.142	0.137
		R ²	0.024	0.026	0.020	0.019
		95%	0.024-0.106	0.031-0.125	0.019-0.102	0.014-0.081
		p	0.002	0.001	0.004	0.006
	Adjusted [†]	R	0.200	0.214	0.182	0.199
		R ²	0.040	0.046	0.033	0.039
		Beta	0.152	0.171	0.129	0.151
		95%	0.022-0.106	0.033-0.128	0.012-0.098	0.018-0.086
		p	0.003	0.001	0.012	0.003

[†]Adjusted for differences in age and cholesterol levels.

Table 11. The structure of the individual APOA5 haplotype variants with percentage of Romas and Hungarians

Haplotypes	APOA5 variant				Population
	rs662799	rs207560	rs3135506	rs2266788	Roma/Hungarian (%)
<i>APOA5*1/ht1</i>	A	C	C	A	77.8/85.6
<i>APOA5*2/ht8</i>	G	T	C	G	5.4 [†] /3.2
<i>APOA5*3/ht3</i>	A	C	G	A	7.6/4.7
<i>APOA5*4/ht2</i>	G	C	C	A	6.3 [†] /2.0
<i>APOA5*5/ht6</i>	A	C	C	G	0.1 [†] /4.1
<i>ht4</i>	G	C	G	A	1.8/-
<i>ht5</i>	G	T	C	A	-/0.1
<i>ht7</i>	A	T	C	G	1.0 [†] /0.2

[†]p<0.05 vs Hungarian samples

5.2 BGP15

5.2.1. Mitochondrial uptake of BGP-15

We found that the BGP-15 possesses a delocalized positive charge, therefore, it is suitable for determining membrane potential-dependent uptake. We measured BGP-15 uptake in both energized and uncoupled mitochondria. The void volume was determined using glucose-6-phosphate, which substance is unable to permeate the mitochondrial inner membrane. When incubated in the presence of 50 μM BGP-15 for 10 minutes, the energized mitochondria took up more than 85% of the drug (Fig. 1A), suggesting that the majority of BGP-15 was taken up in a membrane potential-dependent manner. Complete uncoupling by dinitrophenol significantly decreased BGP-15 uptake (Fig. 1A). However, even the uncoupled mitochondria were found to bind more BGP-15 than the amount corresponding to the void volume, indicating that BGP-15 interacted with the mitochondrial proteins and/or lipids. Extrapolating this finding to physiological conditions, it is likely that more than 90% of BGP-15 had accumulated in the mitochondria, which raises the possibility that BGP-15 may protect cells via mitochondrial mechanisms.

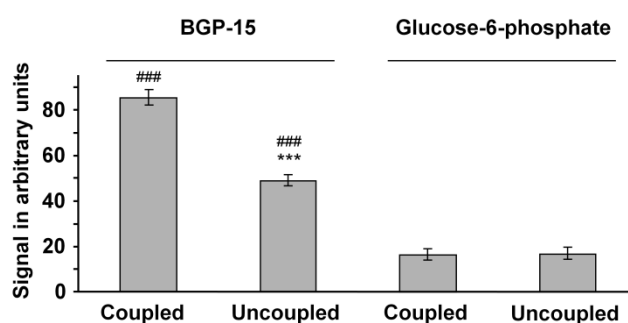


Figure 1A. Membrane potential enhanced the mitochondrial uptake of BGP-15 (50 μM) in isolated rat liver mitochondria. Uncoupling was found to occur with 50 μM 2,4-dinitrophenol. Data are presented as the mean \pm SEM of three independent experiments. *** $P < 0.001$ compared to coupled mitochondria, ### $P < 0.001$ compared to the glucose-6-phosphate signal.

5.2.2. Effect of BGP-15 on mitochondrial membrane potential ($\Delta\Psi$)

As mild uncoupling of the mitochondria could be beneficial in insulin resistance [133], we tested the effect of BGP-15, an insulin sensitizer [58,62,63] on $\Delta\Psi$ by using a $\Delta\Psi$ -sensitive

dye (R123) in isolated rat liver mitochondria. Treatment by BGP-15 alone resulted in a concentration-dependent decrease in $\Delta\psi$ at millimolar concentrations (Fig. 1B). The effect on $\Delta\psi$ of submillimolar concentrations of BGP-15 was below the detection limit (Fig. 1B) suggesting that at the 50 μM concentration we have used throughout the study the drug could hardly cause any mitochondrial depolarization.

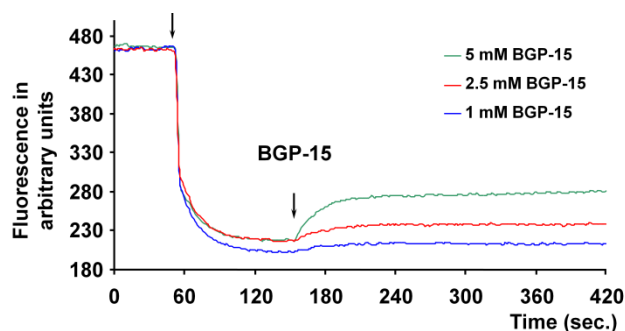


Figure 1B. Mitochondrial membrane potential was monitored by measuring the fluorescence intensity of R123, a cationic fluorescent dye. Isolated rat liver mitochondria, represented by the first arrow, took up the dye in a voltage-dependent manner, resulting in fluorescent quenching. At the second arrow either 1 mM, 2.5 mM or 5 mM BGP-15 was added. A representative plot of three independent concurrent experiments is presented.

Under cell culture conditions we analyzed the effect of BGP-15 on $\Delta\psi$ using JC-1, a cell-permeable voltage-sensitive fluorescent mitochondrial dye. JC-1 emits red fluorescence in highly energized mitochondria (aggregated dye), while depolarized mitochondria emit green fluorescence (monomer dye). WRL-68 cells were incubated in the presence of 50 μM H_2O_2 , either alone or together with 50 μM BGP-15, for 3 hours before loading with 100 ng/mL JC-1 dye for 15 minutes, after which fluorescent microscopy was performed. In the control and BGP-15-treated cells, fluorescence microscopy showed strong red fluorescence and weak green fluorescence, which indicates a high $\Delta\psi$ in mitochondria (Fig. 2A and B). The addition of H_2O_2 to cells facilitates the depolarization of mitochondria, resulting in weaker red fluorescence and stronger green fluorescence (Fig. 2A and B). When H_2O_2 was added to cells in addition to BGP-15, the depolarization of mitochondria was found to be weaker, as shown by a smaller decrease in red fluorescence and weaker increase in green fluorescence (Fig. 2A and B). This was also demonstrated by the accurate (mitochondrial) labelling of red fluorescence in the cells treated with both H_2O_2 and BGP-15, and in cells treated with H_2O_2 only (Fig. 2A). The quantitative assessment revealed that BGP-15 did not affect the $\Delta\psi$ at a concentration of 50 μM (Fig. 2B);

however, it was found to reduce the H₂O₂-induced depolarization of the mitochondrial membrane (Fig. 2B), suggesting that even at this concentration it protected the $\Delta\Psi$ against oxidative stress. We have obtained identical results when we assessed $\Delta\Psi$ by using TMRM, another membrane potential sensitive fluorescent dye and a quantitative, plate reader-based method (Fig. 2C).

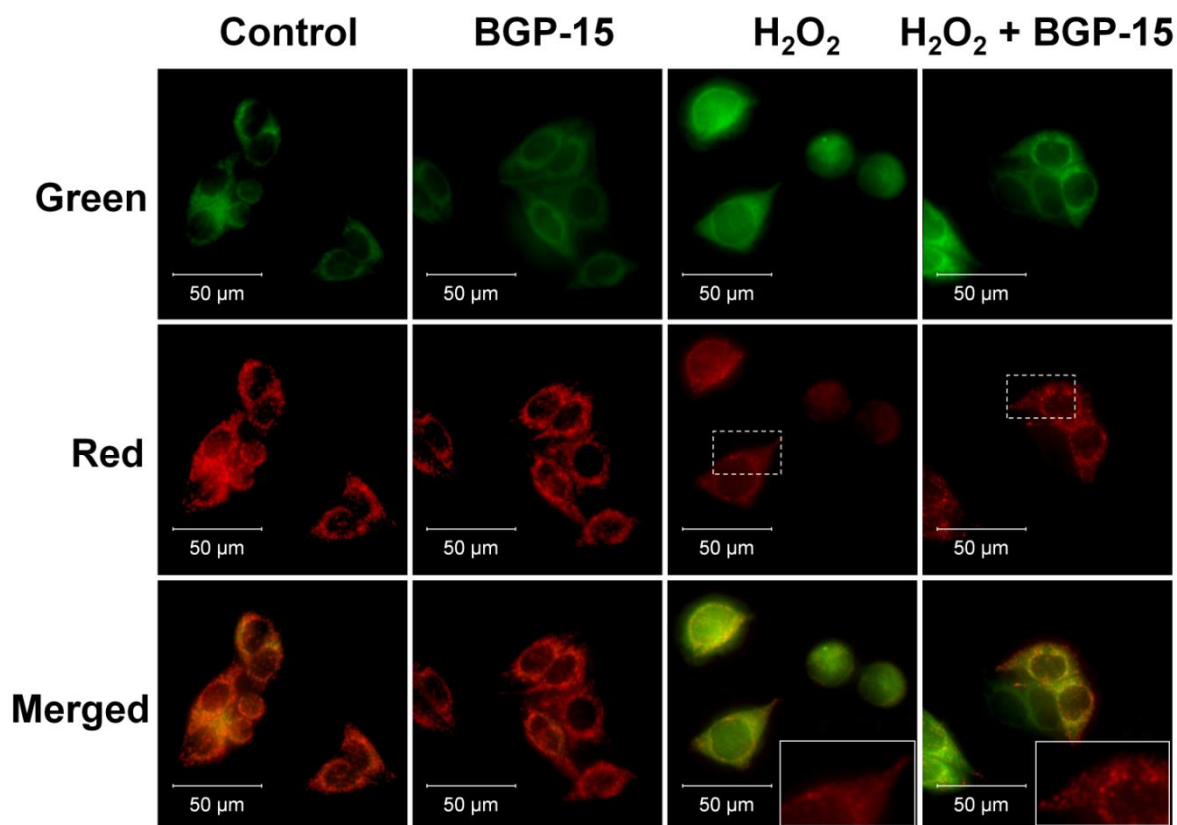


Figure 2A. Effect of BGP-15 on H₂O₂-induced mitochondrial membrane depolarization in WRL-68 cells. Cells were exposed to 50 μ M H₂O₂ in the absence or presence of 50 μ M BGP-15, then stained with 100 ng/mL of JC-1, a membrane potential-sensitive fluorescent dye. The dye was loaded, and after a 15 minute incubation fluorescent microscopic images were taken using both the red and green channels. The inserts show the homogenous red fluorescence in H₂O₂-treated cells, and the dotted labelling represents the H₂O₂ + BGP-15 treated cells, showing that BGP-15 protected the mitochondrial integrity in the presence of H₂O₂. Inserts are expanded from the area indicated by dashed rectangles. Representative merged images of three independent experiments are presented.

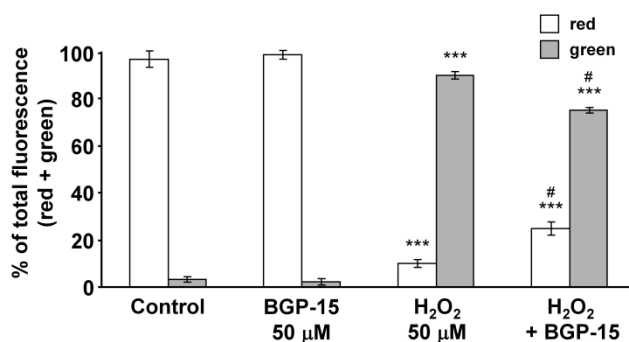


Figure 2B Quantitative analysis of mitochondrial depolarization induced by H₂O₂ (50 μM) and its reduction by BGP-15 (50 μM) in WRL-68 cells. Results are presented as the mean ± SEM. ***P < 0.001 compared to control cells, #P < 0.05 compared to H₂O₂-treated cells.

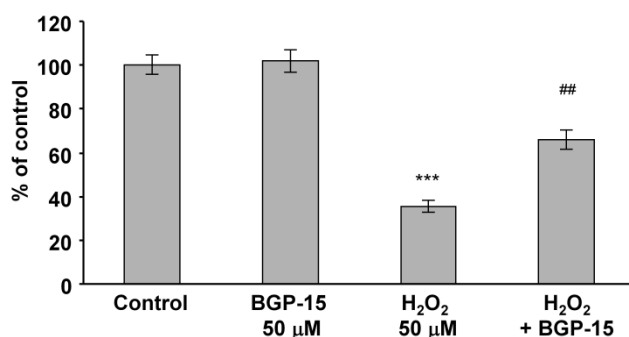


Figure 2C. Effect of BGP-15 on H₂O₂-induced mitochondrial membrane depolarization in WRL-68 cells. Cells were treated with 50 μM H₂O₂ in the absence or presence of 50 μM BGP-15 for 3 hours, then stained with 50 ng/mL of TMRM, a cationic, cell-permeant, red fluorescent dye. After a 15 minutes incubation fluorescent signal was measured by the GloMax Multi Detection System, then remeasured after the application of 1 μM FCCP ΔΨ was calculated as the difference of fluorescence signal before and after FCCP-treatment. Data are presented as the mean ± SEM of three independent experiments. **P < 0.01, ***P < 0.001 compared to control cells; ##P < 0.01 compared to H₂O₂-treated cells.

5.2.3. BGP-15 attenuates mitochondrial production of reactive oxygen species

Destabilization of the mitochondrial membrane systems has previously been reported to contribute to mitochondrial ROS production [134], and BGP-15 was shown to protect the mitochondrial membrane system under oxidative stress (Fig. 2A and B), we assumed that it could also affect mitochondrial ROS production. To investigate this possibility, WRL-68 cells were transfected with mERFP to label the mitochondria, and then incubated in the presence or

absence of 50 μM H_2O_2 for 30 minutes. Fresh medium containing DHR123 was added, and after 15 minutes the amount of green R123 fluorescence, as a result of oxidation from non-fluorescent DHR123, was measured by fluorescence microscopy. BGP-15 at a concentration of 50 μM did not affect the weak green fluorescence of mitochondrial localization (Fig. 3A). However, its addition did reduce the substantial increase in green fluorescence induced by the H_2O_2 treatment (Fig. 3A and B). Furthermore, oxidative stress-induced green fluorescence was diffuse in the absence of BGP-15, whereas it was predominantly localized to the mitochondria in the presence of BGP-15 (Fig. 3A inserts). Although the R123 fluorescence could result from cytosolically produced R123 taken up to the mitochondria and DHR123 oxidized by mitochondrial ROS, we think that R123 fluorescence reflected mitochondrial ROS production, as it was predominantly localized to the mitochondria when $\Delta\psi$ was not compromised.

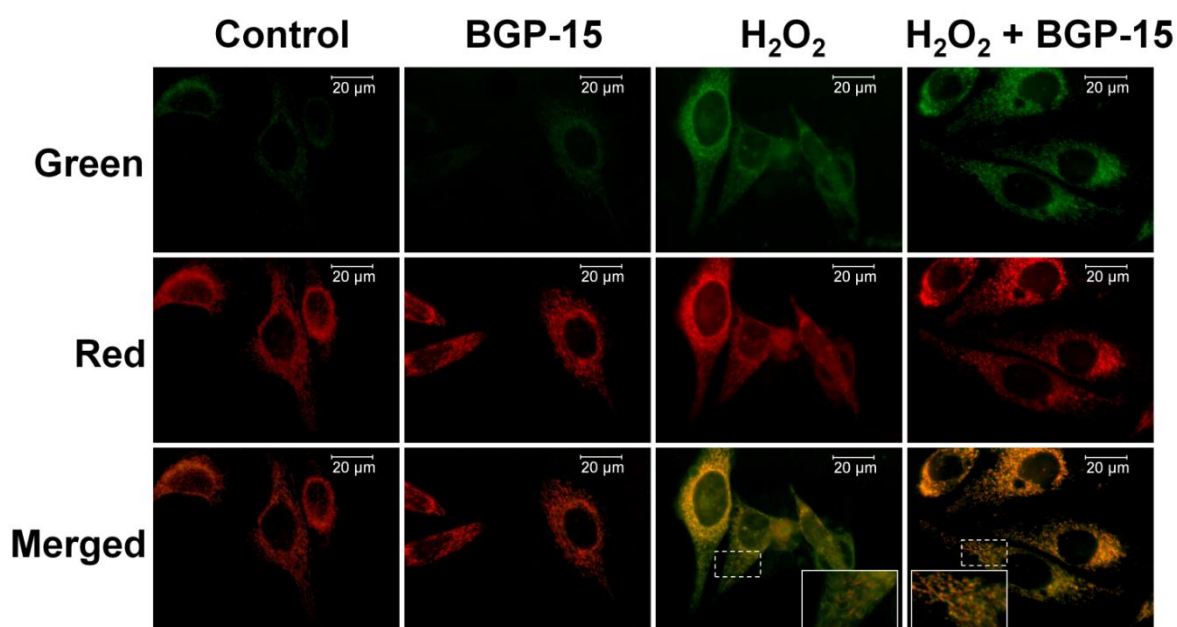


Figure 3A Effect of hydrogen peroxide and BGP-15 pretreatment (for 30 minutes) on mitochondrial ROS production, as determined by the oxidation of the mitochondrial enriched dye from DHR123 to R123 in WRL-68 cells that had been labelled with mitochondrial directed red fluorescent protein. High magnification fluorescent microscopic images show the different localization of the produced R123. Inserts are expanded from the area indicated by dashed rectangles.

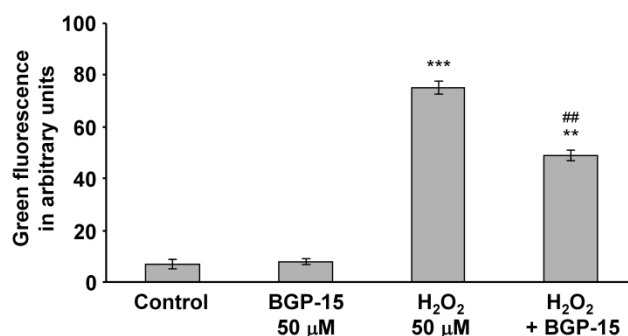


Figure 3B. Quantification of R123 production. Data are presented as the mean \pm SEM of three independent experiments. **P < 0.01 and ***P < 0.001 compared to control cells; ##P < 0.01 compared to H₂O₂-treated cells.

As it was found previously (N-Gene Inc., personal communication), BGP-15 serum concentration does not exceed 25 nmoles/mL. Therefore, we analyzed the effect of BGP-15 on ROS-induced ROS production at concentrations ranging between 1–50 μ M under cell culture conditions using a quantitative, plate-reader based method instead of microscopy. BGP-15 had a concentration-dependent inhibitory effect on the ROS-induced ROS production in WRL-68 cells, which was significant even at the 1 μ M concentration (Fig. 4A). In order to show that these observations apply to other cell lines too, we analyzed the effect of BGP-15 on H₂O₂-induced ROS production in H9c2 cardiomyocytes using the same system. Fig. 4B shows that BGP-15 decreased the ROS-induced ROS production in H9c2 cardiomyocytes in a concentration-dependent manner (1–50 μ M range).

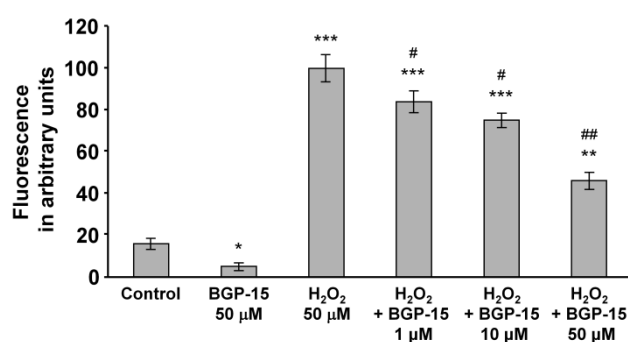


Figure 4A Effect of BGP-15 on oxidative stress-induced DHR123 oxidation in WRL-68 cells. Data are presented as the mean \pm SEM of three independent experiments. *P < 0.05, **P < 0.01 and ***P < 0.001 compared to control cells; #P < 0.05 and ##P < 0.01 compared to H₂O₂-treated cells.

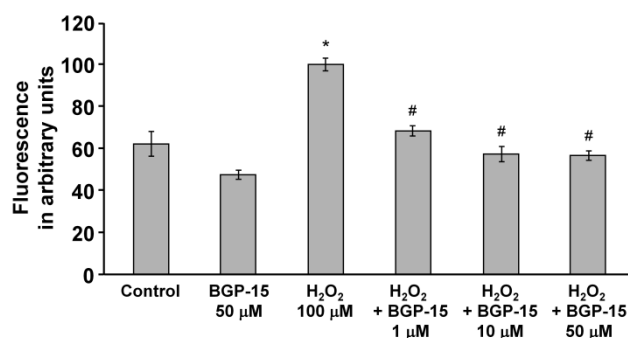


Figure 4B Effect of BGP-15 on oxidative stress-induced DHR123 oxidation in H9c2 cardiomyocytes. Results are presented as the mean \pm SEM of three independent experiments. *P < 0.05 compared to control cells, #P < 0.05 compared to H₂O₂-treated cells.

In order to study whether the observed antioxidant effect of BGP-15 have resulted from scavenging property of the drug, we determined its effect on 500 μ M H₂O₂- (Fig. 4C) and H₂O₂ and Fe²⁺-EDTA (Fenton reaction, Fig. 4D)-induced DHR123 oxidation in cell-free systems. Since BGP-15 did not affect DHR123 oxidation in any of these systems (Fig. 4C and D) its antioxidant effect could not have resulted from scavenging property of the drug. DHR123 can be oxidized predominantly by peroxynitrite and hydroxyl radicals that are formed in the Fenton reaction; however, it cannot detect superoxide. Therefore, we aimed to investigate whether BGP-15 could reduce the production of mitochondrial superoxide. To this end, we determined H₂O₂-induced ROS production in WRL-68 (Fig. 4E) and H9c2 (Fig. 4F) cells using the mitochondria-targeted redox fluorescent dye MitoSOX [135] instead of DHR123. Essentially, the results were comparable to those we obtained with DHR123 (Fig. 4A and B vs. 4E and F). Furthermore, we repeated these experiments in the presence of the mitochondria-targeted antioxidant MitoTEMPO [136]. MitoTEMPO abolished H₂O₂-induced ROS production in all groups (Fig. 4E and F) indicating mitochondrial localization of the BGP-sensitive ROS production. These data provide evidence that BGP-15 reduced mitochondrial superoxide production in both WRL-68 cells (Fig. 4E) and H9c2 cardiomyocytes (Fig. 4F).

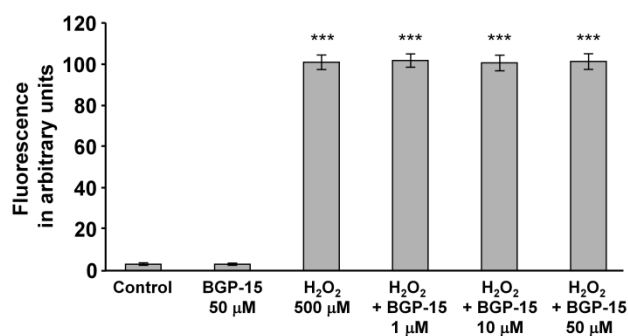


Figure 4C BGP-15 in chemical reactions does not inhibit DHR123 oxidation induced by H₂O₂ (500 μM). Data are presented as the mean ± SEM of three independent experiments. ***P < 0.001 compared to control group.

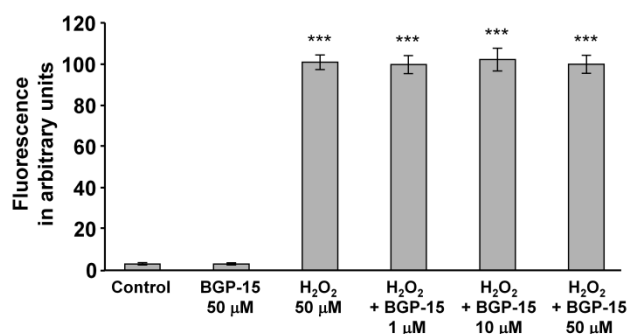


Figure 4D BGP-15 in chemical reactions does not inhibit DHR123 oxidation induced by H₂O₂ (50 μM) and Fe(II)-EDTA (66 μM) (Fenton reaction system). Results are presented as the mean ± SEM of three independent experiments. ***P < 0.001 compared to the control group.

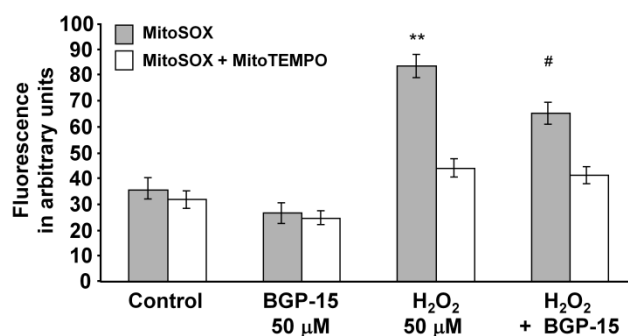


Figure 4E Effect of BGP-15 on oxidative stress-induced superoxide production in WRL-68 cells in the absence or presence of 20 μM MitoTEMPO as determined by MitoSOX (0.3 μM). Data are presented as the mean ± SEM of three independent experiments. *P < 0.05, **P < 0.01 compared to control cells, #P < 0.05 compared to H₂O₂-treated cells.

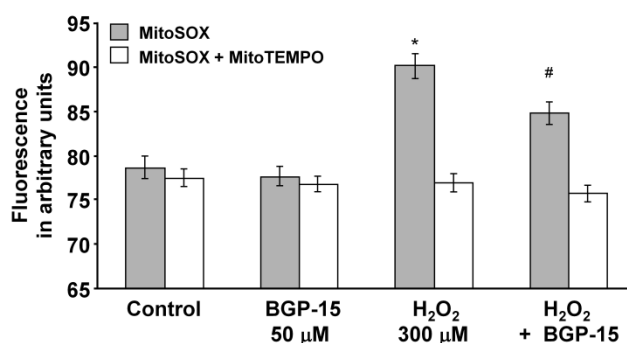


Figure 4F Effect of BGP-15 on the oxidative stress-induced superoxide production in H9c2 cardiomyocytes in the absence or presence of 20 μM MitoTEMPO as determined by MitoSOX (0.3 μM). Results are presented as the mean ± SEM of three independent experiments. *P < 0.05 compared to control cells, #P < 0.05 compared to H₂O₂-treated cells.

5.2.4. Effect of BGP-15 on mitochondrial reactive oxygen species production in isolated mitochondria

In order to provide unequivocal evidence for the mitochondrial mechanism underlying the inhibitory effect of BGP-15 on ROS-induced ROS production, we used Percoll gradient-purified mitochondria. We determined the effect of BGP-15 on the oxidation of DHR123 in the presence of glutamate and malate as substrates, with antimycin A for complex III inhibition, and showed the production of ROS in complex I and the complex III cytochrome b region of the respiratory chain. We found that the addition of BGP-15 at concentrations of 10 to 50 μM had a ~50% inhibitory effect on mitochondrial ROS production (Fig. 4G). These results suggest that the target of BGP-15 was between complex I and the complex III cytochrome b region of the respiratory chain [137].

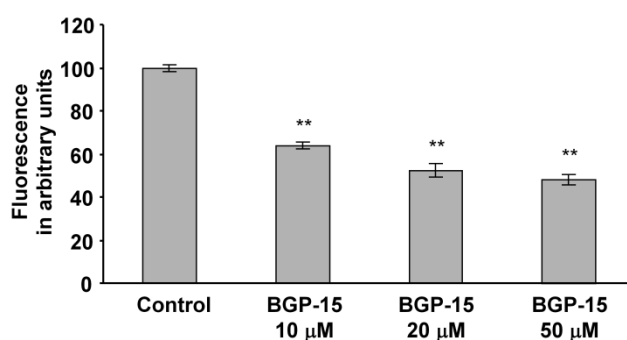


Figure 4G Effect of BGP-15 on mitochondrial DHR123 oxidation using glutamate-malate as substrate and with complex III inhibited by antimycin A. Data are presented as the mean \pm SEM of three independent experiments. **P < 0.01 compared to the control group.

BGP-15 was also shown to reduce mitochondrial ROS production in the presence of succinate as a substrate and CN⁻ as the cytochrome oxidase inhibitor (Fig. 4H), however, to a much smaller extent. This suggests that BGP-15 affected ROS production mainly via complex I and the cytochrome b part of complex III. These data show that BGP-15 has a specific inhibitory effect on mitochondrial ROS production at the complex I and complex III cytochrome b region of the respiratory chain, which is not an antioxidant effect.

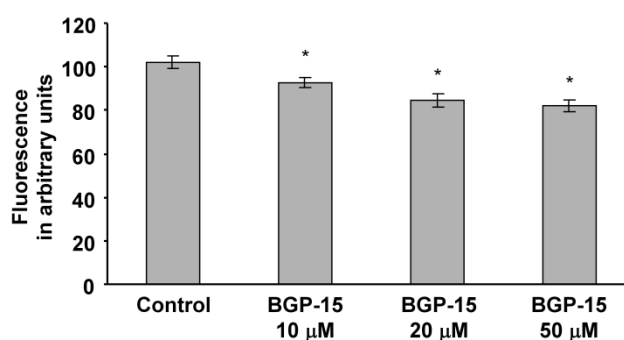


Figure 4H Effect of BGP-15 on mitochondrial DHR123 oxidation using succinate as substrate and with complex IV inhibited by CN⁻. Results are presented as the mean \pm SEM of three independent experiments. *P < 0.05 compared to the control group.

5.2.5. Effect of BGP-15 on reactive oxygen species-induced cell death

As BGP-15 was shown to protect against H₂O₂-induced mitochondrial damage in addition to reducing mitochondrial ROS production, we analyzed its effects on H₂O₂-induced cell death. We treated WRL-68 cells with 50 μ M H₂O₂ in the presence of 0–50 μ M BGP-15 for 24 hours, then determined cell survival using the SRB method. We found that, consistent with its aforementioned protective effects (Figs 2–4), BGP-15 increased cell survival in a concentration-dependent manner (Fig. 5A). To further investigate the underlying mechanism behind the cytoprotective effect of BGP-15, we determined the proportion of apoptosis and necrosis using annexin V-conjugated fluorescein-isothiocyanate and PI staining, which was performed after exposing the cells to 50 μ M H₂O₂ in the presence or absence of 50 μ M BGP-15 for 24 hours, which was then measured by the GloMax Multi Detection System. We found

that under these conditions, H₂O₂-induced cell death was predominantly necrotic and only approximately 10% of the cells died by apoptosis (Fig. 5B). BGP-15 significantly reduced both apoptotic and necrotic cell death, which was likely to be a result of mitochondrial protection.

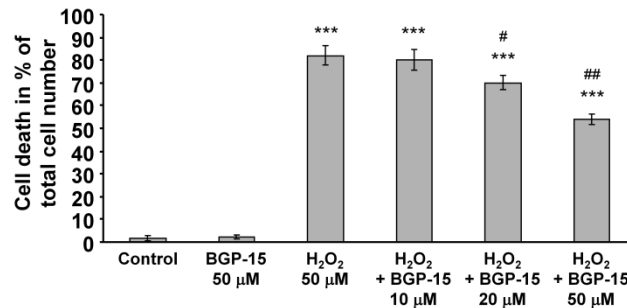


Figure 5A BGP-15 protects against H₂O₂-induced cell death (sulforhodamine B assay). Data are presented as the mean ± SEM of eight independent experiments. ***P < 0.001 compared to control cells; #P < 0.05 and ##P < 0.01 compared to H₂O₂-treated cells.

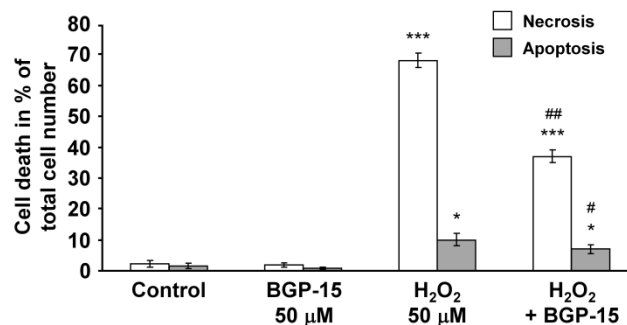


Figure 5B Determination of the effect of BGP-15 on H₂O₂-induced apoptosis (fluorescein-labelled annexin V) and necrosis (propidium iodide) pathways. Data are presented as the mean ± SEM of three independent experiments. *P < 0.05 and ***P < 0.001 compared to control cells; #P < 0.05 and ##P < 0.01 compared to H₂O₂-treated cells.

5.2.6. BGP-15 protects against LPS-induced mitochondrial depolarization

It has been shown that the U-251 MG human malignant glioblastoma cell line contains components of the LPS signaling pathway [138], and LPS-induced signaling has been shown to be important in neurodegenerative, liver and several other diseases [139,140]. Additionally, mitochondria have been reported to play an important role in LPS signaling [139-143]. Therefore, we analyzed the effect of BGP-15 on LPS-induced mitochondrial depolarization in the U-251 MG cell line. This system is much more complex than the ROS-induced

depolarization because LPS induces toll-like receptor 4 (TLR4)-dependent signaling and NADPH oxidase (NOX)-dependent ROS production, thereby increasing intracellular Ca^{2+} levels [144,145]. Mitochondrial depolarization was found to be induced by the addition of 1 $\mu\text{g}/\text{mL}$ LPS for 1 hour, as determined by JC-1 staining and fluorescent microscopy (Fig. 6A and B). We found that the addition of BGP-15 alone did not affect $\Delta\psi$, but significantly attenuated LPS-induced mitochondrial depolarization in the U-251 MG human malignant glioblastoma cells (Fig. 6A and B). We have obtained identical results when we assessed $\Delta\Psi$ by using TMRM, another membrane potential sensitive fluorescent dye and a quantitative, plate reader-based method (Fig. 6C). These data suggest that BGP-15 may play a role in inflammatory processes by a novel mitochondrial mechanism.

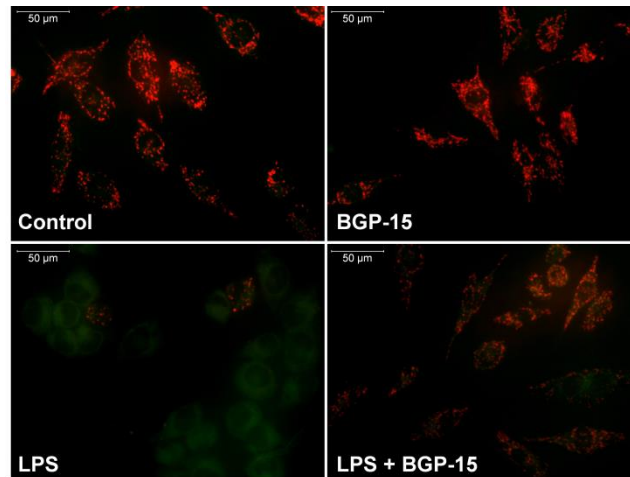


Figure 6A Effect of BGP-15 on LPS-induced mitochondrial membrane depolarization in U-251 MG cells. Cells were exposed to 1 $\mu\text{g}/\text{mL}$ LPS in the absence or presence of 50 μM BGP-15, then stained with 100 ng/mL of JC-1. Fluorescent microscopic images were taken using both the red and green channels. Representative merged images of three independent experiments are presented.

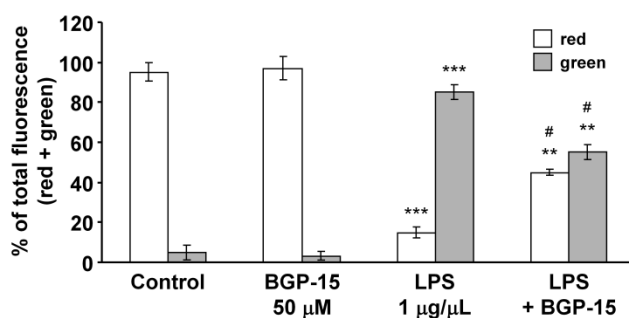


Figure 6B Quantitative analysis of LPS-induced (1 μg/mL) mitochondrial depolarization and its reduction by BGP-15 (50 μM) in U-251 MG cells. Results are presented as the mean ± SEM. **P < 0.01 and ***P < 0.001 compared to control cells; #P < 0.05 compared to LPS-treated cells.

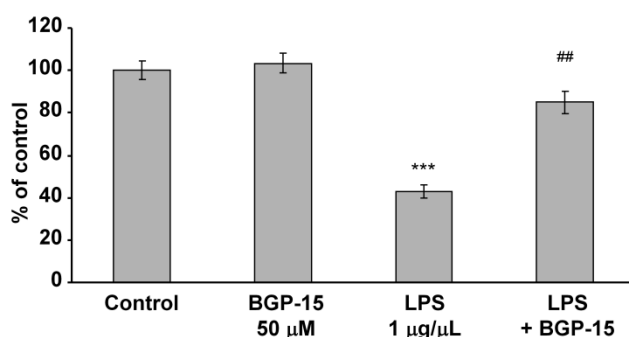


Figure 6C Effect of BGP-15 on LPS-induced mitochondrial membrane depolarization in U-251 MG cells. Cells were treated with 1 μg/mL LPS in the absence or presence of 50 μM BGP-15 for 1 hour, then stained with 50 nM of TMRM. After a 15 minutes incubation fluorescent signal was measured by the GloMax Multi Detection System, then remeasured after the application of 1 μM FCCP. $\Delta\Psi$ was calculated as the difference of fluorescence signal before and after FCCP-treatment. Data are presented as the mean ± SEM of three independent experiments. *P < 0.05, ***P < 0.001 compared to control cells; ##P < 0.01 compared to LPS-treated cells.

5.2.7. BGP-15 protects against LPS-induced production of reactive oxygen species

Due to the association between mitochondrial depolarization and ROS production [134], we measured LPS-induced ROS production in the U-251 MG cells. We exposed the cells to 1 μg/mL LPS in the presence or absence of 50 μM BGP-15 for 1 hour, and then measured the fluorescence of R123 which had been oxidized from non-fluorescent DHR123 by the ROS (Fig. 6D and E). Very low fluorescence intensities were detected in the untreated and BGP-15-treated cells, however, the addition of LPS was found to greatly induce ROS production (Fig. 6D and

E). BGP-15 reduced the LPS-induced ROS production almost to control levels (Fig. 6D and E). Similarly to the H₂O₂-induced ROS production, we wanted to determine the intracellular localization of the LPS-induced ROS. To this end, we repeated the previous experiment using MitoSOX instead of DHR123 and a plate-reader instead of microscopy. Essentially, the results were comparable to those we obtained with DHR123 (Fig. 6D and E vs. 6F). Furthermore, we repeated the experiment in the presence of MitoTEMPO. MitoTEMPO abolished LPS-induced ROS production (Fig. 6F) indicating mitochondrial localization of the BGP-sensitive ROS production. These data provide evidence that BGP-15 reduced LPS-induced mitochondrial superoxide production in.

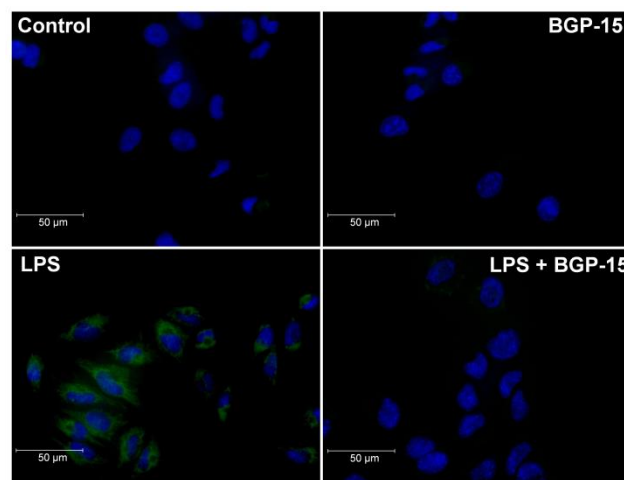


Figure 6D Effect of BGP-15 on the LPS-induced ROS production in U-251 MG cells (containing the TLR4 receptor), as determined by the oxidation of DHR123 (1 μM) to R123, measured with fluorescent microscopy. Cell nuclei were labelled using Hoechst 33342. Representative merged images of three independent experiments are presented.

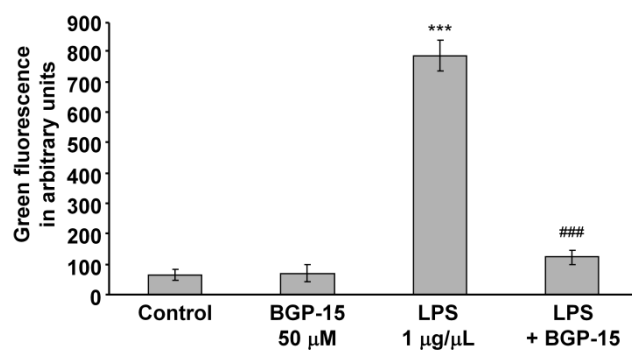


Figure 6E. Quantitative analysis of LPS-induced (1 μ g/mL) ROS production and the protective effect of BGP-15 (50 μ M). Data are presented as the mean \pm SEM of three independent experiments. ***P < 0.001 compared to control cells; ###P < 0.001 compared to LPS-treated cells.

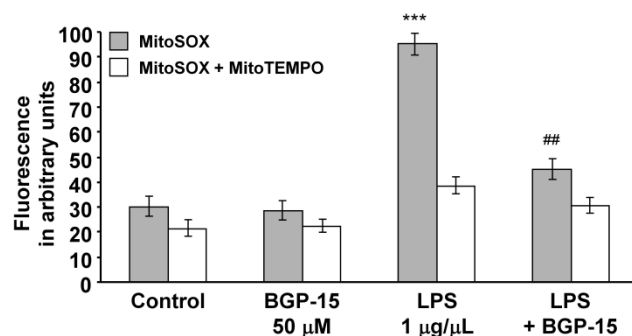


Figure 6F. Effect of BGP-15 on oxidative stress-induced superoxide production in U-251 MG cells in the absence or presence of 20 μ M MitoTEMPO as determined by MitoSOX (0.3 μ M). Data are presented as the mean \pm SEM of three independent experiments. *P < 0.05, ***P < 0.001 compared to control cells, ##P < 0.01 compared to LPS-treated cells.

6. Discussion

6.1. GCKR, MLXIPL, ANGPTL3, CILP2, GALNT2, TRIB1 and APOA5

The possible roles of serum TGs and total cholesterol in relation to development of numerous diseases, including cardio-and cerebrovascular diseases, metabolic syndrome and diabetes mellitus are extensively investigated worldwide [4,8,10,11,34,85,146-154]. In the past decade a spectrum of studies described genetic polymorphisms which affect triglyceride levels, like GCKR and more intensively investigated, the APOA5 variants [4,11,34,85,150-154].

The glucokinase enzyme is under the control of GCKR, which enzyme has a dominant glucose phosphorylase role of the liver and of the pancreatic β -cells in the glucose homeostasis of the blood [71,73,84]. In genome-wide association studies the possible effect of functional variants in GCKR gene in association with hypertriglyceridemia was also investigated [15,155].

The intronic rs780094 and the exonic rs1260326 variants are the most widely investigated variants, the last one causes a Leu/Pro change at 446 amino acid position. This indirectly affects triglyceride levels, has a role in impaired fasting glycemia, and is a possible risk for type II diabetes mellitus [156]. Santoro et al. studied 455 obese children and adolescents for rs1260326 of GCKR gene, 181 of them were Caucasians, 139 African Americans, and 135 Hispanics. An association with hepatic fat accumulation along with large VLDL and triglyceride levels was observed. Two genes, the GCKR and PNPLA3 act together and have a susceptible effect also for manifestation of fatty liver in obese young people [157].

Several studies found that ANGPTL3 affect lipid metabolism, the protein indirectly inhibits the activity of lipoprotein and other endothelial lipases. The loss-of-function mutations of ANGPTL3 gene causing total ANGPTL3 absence, which shows a high association rate with recessive hypolipidemia. This type of hypolipidemia is characteristic for decrease of apolipoprotein B and apolipoprotein A-I-enclosing lipoproteins, which leads to altering levels of HDL. Pisciotta et al. investigated ANGPTL3 gene in 4 persons with low levels of LDL cholesterol and HDL cholesterol, and they found homozygous, compound heterozygous for ANGPTL3 loss-of-function mutations (p.I19LfsX22/p.N147X, p.G400VfsX52) associated with the deficiency of ANGPTL3 in plasma. Decreased plasma levels of TG-containing lipoproteins and of HDL particles were observed, moreover, the heterozygous carriers showed normal level of plasma HDL-cholesterol, with low level of ANGPTL3 and attenuated level of LDL-cholesterol in the plasma [158].

A MLXIPL; or by alternative name, carbohydrate response element binding protein, ChREBP) gene is located in the WBSR14 deletion region at chromosome 7q11.23. Recently, GWAS studies between the plasma TG-level alterations and MLXIPL locus correlations were found. Moreover, the influence of TG level increase of the major alleles of the rs17145738 and rs3812316 variants in MLXIPL locus were observed [15,16].

In recent GWAS studies, the minor G-allele of the rs4846914 intronic variant of the GALNT2 gene was found to associate with increased TG concentrations of the plasma. In a case-control study, which was performed on Han Chinese population analyzing 4192 individuals for T2DM, the association between elevated TG levels and genotypes for MLXIPL rs17145738 variant and for GCKR rs780094 was confirmed, but not for GALNT2 rs4846914 polymorphism [159].

Recently, an association has been found between dyslipidemia and the rs16996148 (near CILP2), rs17321515 (near TRIB1), rs12130333 (near ANGPTL3) variants [16]. In addition, these loci were correlated with the manifestation of cardiovascular diseases [15].

The CILP2 gene the proteins' relation to lipid metabolism is not well understood. However, in a GWAS study, a TG level reducing role of the rs16996148 variant was confirmed analyzing Caucasian individuals [27].

In a recent study Vrblík et al. investigated 895 Czech patients with primary dyslipidemia comparing with 672 healthy controls. No significant effect of the polymorphisms CILP2 on lipid levels after receiving statin treatment was detected [160].

The human TRIB1 facilitates the proteasome-dependent protein degradation. In an Asian Malay population, the variant adjacent to the TRIB1 locus (rs17321515) showed a significant correlation with increased total cholesterol and LDL-cholesterol, and also a higher risk for coronary heart disease and CVD was documented [161].

Our present findings support the earlier results, the allele frequencies showed significant differences in both MLXIPL variants, GALNT2 rs4846914 and ANGPTL3 rs1213033 polymorphisms comparing Roma individuals to the Hungarians. Analyzing Roma and Hungarian population samples we could not confirm any significant associations between triglycerides levels and minor allele carriers compared with the non-carriers. These findings exclude the existence of major associations, like in the case of APOA5. Meanwhile, further well-powered studies examining larger populations can still reveal fine but less pronounced associations of these parameters.

We examined the effect of major APOA5 polymorphisms (rs662799; rs2266788; rs3135506; rs207560) on lipids, especially in TG levels. The result of this study showed that heterozygous carriers of rs2266788; rs3135506; rs207560 variants had higher TG levels than non-carriers. Homozygous carriers of rs662799 variant have higher TG levels than non-carriers in Roma subjects. To the best of our knowledge, such association has not been described yet. However, most of the studies do not present the homozygous and heterozygous samples separately because of the low risk allele frequencies of the APOA5 variants. After combining the homozygous and heterozygous samples we found significantly elevated plasma TG levels in carriers of risk alleles of the APOA5 variants when compared to the non-carriers in both Hungarian and Roma populations. All four APOA5 variants showed correlation to TG levels with or without adjustment factors like age and cholesterol levels. These findings correspond to the results of previous studies.[4,5,13,26,117]

In Central-Eastern Europe, Romas are likely more susceptible to metabolic syndrome and stroke. They have higher morbidity rates, and lower life expectancy than other European populations [40,162]. One of the most common causes of death among Romas CVD [41,163,164] with a 2.5-fold higher premature CVD mortality compared to the overall population[165] and they are at increased risk for various CVD risks factors.[111,166-168] This is not restricted to the Eastern European countries.[166,167]

Several risk factors which increase the development of CVD include smoking, family history with CVD, hypertension, lipid and lipoprotein abnormalities (elevated total cholesterol and LDL-cholesterol, HDL-cholesterol, hypertriglyceridemia and increased lipoprotein(a) (Lp(a)), diabetes (insulin resistance, hyperinsulinemia and elevated blood glucose level), obesity and metabolic syndromes. Several studies in Central-Eastern Europe show, [42] that the two most commonly found risk factors contributing to the development of CVD in Roma populations are obesity and smoking, followed by diabetes, metabolic syndrome, hypertension, and increase of TGs. The high rate of obesity is probably due to increased physical activity and unhealthy dietary habits. They also usually start smoking in their early teens due to cultural, and ethnical pressure. Most Romas are exposed to these risk factors in their direct family environment.[42]

Earlier studies of susceptibility genetic variants revealed that Roma are a genetically unique population [169-172] and their genetic constitution can differ from other populations [173,174]. In our study, the minor allele frequencies of the studied APOA5 variants were collected in 1000Genomes and HapMap databases, to compare those found in the Roma population with those in Europeans and Asians. For rs662799 significantly different risk allele

frequencies were detected between Roma and other studied populations. The allele frequencies in Roma subjects were in between those of Europeans and Asians. We found Roma risk allele frequencies differed significantly from those of the Asian populations for rs662799, rs207560, rs2266788 variants. We found, that the risk allele frequencies were significantly higher in Roma than in Hungarian population for rs662799; rs3135506 and rs207560 variants. It is important to emphasize, that the frequencies found in Hungarians correspond with those detected in European populations [115,175,176]. The reasons for these differences are not clear. At the same time, the already confirmed definitive association of susceptibility variants and the development of diseases mean that increased minor allele frequencies obligatory lead to increased vascular events [125]. The data of the present study support that elevated rates of susceptibility alleles are in relationship- at least in part- with increased prevalence of CVDs in Roma minority.

The most common APOA5 variants, like rs662799, rs207560, rs2266788 and rs3135506 are in strong linkage disequilibrium and create two major haplotype variants (APOA5*2 and *3). These two haplotypes together with wild type haplotype (APOA5*1-3) constitute approximately 98% of the average population [115]. Five common haplotypes were identified so far (APOA5*1-5) [177-179]. Additional possible haplotypes are also known (ht4, 5, 7) composing only a small portion of the population. We searched for linkage disequilibrium among the APOA5 polymorphisms in both populations and attempted to investigate the haplotypes in Roma and Hungarian samples. Different linkage was found between the rs207560 and rs3135506 in Roma and Hungarian populations. In Roma the linkage between the variants was strong, while in Hungarians moderate, possibly because of the distinct origin of the two populations. We believe that this association has not yet been described.

The haplotype analyses for APOA5 revealed eight theoretical haplotypes, but only seven occurred in both populations. Five of these (APOA5*1, APOA5*2, APOA5*3, APOA5*4 and APOA5*5) are the most extensively studied haplotypes of the gene. Ht7 haplotype has not yet been investigated in susceptibility studies, so far. Comparison of the prevalence's in Roma and Hungarian populations revealed APOA5*2, APOA5*4 and ht7 haplotypes were significantly prevalent in Roma population, whereas APOA5*5 haplotype was more frequent in Hungarians.

Previous studies described APOA5*2 haplotype to be associated with elevated TG levels and might be a susceptibility for metabolic syndrome and ischemic stroke in the Hungarian population [4,126]. Our results suggest that Roma people have higher risk for hypertriglyceridemia and for vascular events because of increased prevalence of the APOA5 susceptibility alleles. Previously, Kisfali et al. did not confirm connection between the presence

of APOA5*4 and the risk for metabolic syndrome in Hungarians. Furthermore, APOA5*5 haplotype was found to have a protective effect against metabolic syndrome, and associated with decreased TG levels [126]. Our findings on APOA5*5 also provide indirect support for APOA5 variant's having a role in the Roma susceptibility to CVD.

6.2. BGP-15

As previously mentioned BGP-15 has been shown to have a protective effect in several disease models, including ischemic heart disease [180], Duchenne muscular dystrophy [52], neuropathy [55], cisplatin-induced kidney disease [181], glivec-induced cardiac disease [53] and paracetamol-induced liver disease [54], in addition to insulin resistance, as it has been studied on both animals and humans [58,62,63]. Here, oxidative stress and inflammatory processes play a key role in disease progression, and in several cases, mitochondrial damage is essential. This is why we studied the effect of BGP-15 on ROS- or inflammatory response-induced mitochondrial damage in cell culture models, with focus on the effects of BGP-15 on mitochondrial membrane stability and ROS production, which are critical for mitochondrial-induced signaling, energy metabolism and mitochondrial cell death pathways. Recently, it has been shown that mild mitochondrial uncoupling can be protective in several disease models, including insulin resistance [133], hypertriglyceridemia and fatty liver disease [182], and can have a regulatory role in endocrine cross-talk via the induction of fibroblast growth factor 21 and the growth hormone/insulin-like growth factor I axis [183]. However, we saw that BGP-15 exerted only mild uncoupling effect in millimolar concentrations. Since we previously used BGP-15 at a 50 μM concentration, it is unlikely that its uncoupling effect played a significant role in its mitochondria- and cytoprotective effects. But as we saw using two membrane potential sensitive dyes BGP-15 reduced the oxidative stress-induced mitochondrial depolarization by ROS-induced mitochondrial depolarization could result in decreased ATP synthesis, increased superoxide production by the electron-transport chain, release of proapoptotic proteins from the intermembrane space, decreased mitochondrial fusion and increased fission [128,184-186]. All of these processes disturb cellular energy metabolism and a lead toward proapoptotic signaling eventually resulting in cell death [128,184-186]. Thus, the membrane potential stabilizing effect of BGP-15 likely contributed to its protective effect in the aforementioned diseases.

BGP-15 was also found to be critical in the reduction of ROS- and LPS-induced ROS production (Figs 3A and 6D), which can play a significant role in the progression of several diseases. Unfortunately, it is difficult to localize the site of ROS production by using conventional mitochondria-targeted redox dyes since oxidation of the dye by extramitochondrial or mitochondrial ROS results in identical fluorescence localized to the mitochondria. For this reason we used MitoSOX [135] at a concentration of 0.3 μM excited at

365 nm. Under these conditions, the resulting 440 nm fluorescence is believed to result from oxidation of the dye by mitochondrially produced superoxide [135]. Furthermore, we quenched mitochondrial ROS by the mitochondria-targeted antioxidant MitoTEMPO [136]. All the results supported that BGP-15 reduced mitochondrial ROS production. This effect could not result from antioxidant property of the molecule as it was revealed by our experiments on various cell-free ROS-generating systems (Fig. 4C and D). We believe that we localized the most important target of BGP-15, complex I-III, which is critical for ROS production by the respiratory chain. It can generate substantial amounts of ROS under different conditions including hypoxia, mitochondrial hyperpolarization, inhibition of respiratory complexes [187]. The significant ROS-reducing effect of BGP-15 may be important in regulating ROS-dependent processes including cell death, MAPK and poly(ADP-ribose) polymerase (PARP) pathways, in addition to transcription factor activation (NF- κ B, AP-1, NRF2, etc.) [188]. The high enrichment of BGP-15 in the mitochondria, combined with the significant reduction in mitochondrial ROS production at complex I by BGP-15, suggests that the protective effect of BGP-15 observed in different disease models is likely to be mediated by the previously mentioned mitochondrial mechanisms. Our results also suggest that the effect of BGP-15 on signaling pathways, such as BGP-15-induced reduction in JNK and p38 MAPK activation [189] or BGP-15-induced Akt activation [190], could also potentially be related to reduced ROS production. LPS induces a complex stress pattern in sensitive cells, including ROS production by NADPH oxidases, an increase in cytoplasmic free calcium level and activation of mitochondria damaging signaling pathways [191,192]. In a separate study on cyclophilin D (CypD) knockout mice, we reported that LPS-induced mitochondrial ROS production was substantially reduced in CypD deficient cells and tissues, accompanied by reduced MAPK activation [141,142]. This stabilized the mitochondrial membrane systems by preventing high calcium-induced mitochondrial permeability transition, resulting in attenuated ROS production and benign intracellular signaling. For this reason we assumed that, similar to the oxidative stress situation, BGP-15 would protect against LPS-induced mitochondrial damage and we found that BGP-15 prevented LPS-induced mitochondrial depolarization and ROS production, demonstrating that BGP-15 can protect mitochondria against complex inflammatory damage as well as against ROS-induced damage. These results suggest the potential of BGP-15 as an experimental drug, not only in ROS-related diseases, but also in inflammatory diseases.

In conclusion, the critical mechanism underlying the protective effect of BGP-15 on the mitochondria appear to be due to reduced ROS production, predominantly at the first and third

respiratory complexes (Fig. 7). By this mechanism, it may regulate several pathways that play critical roles in the progression of ROS-related and inflammatory diseases.

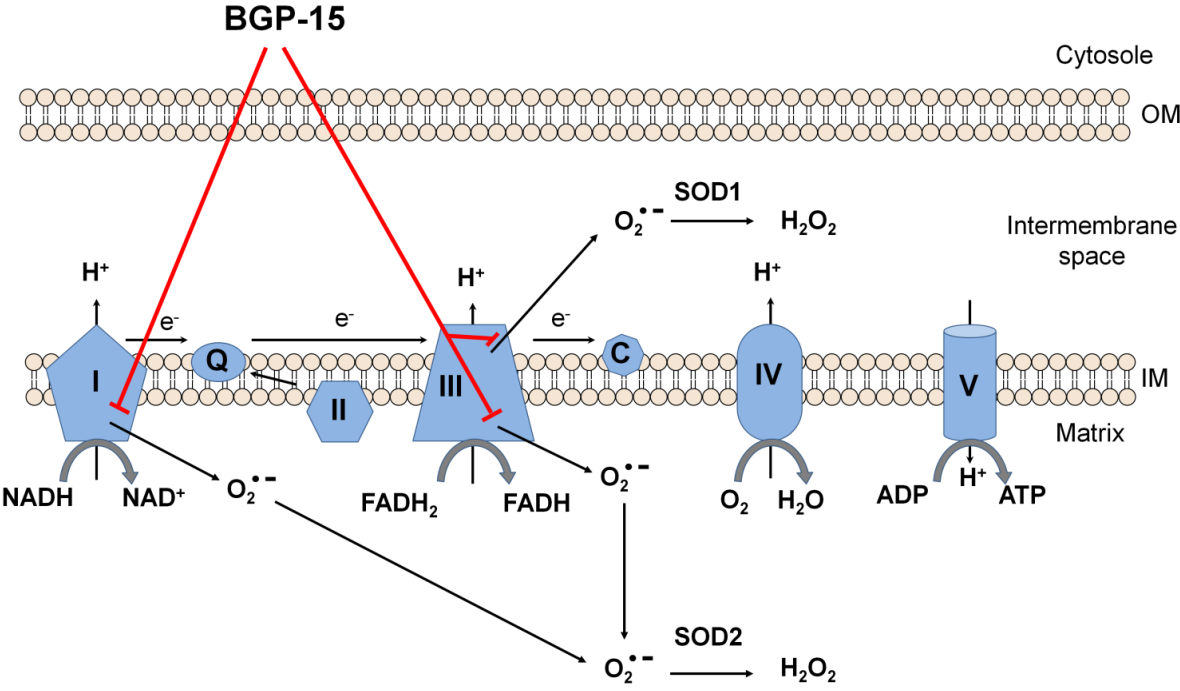


Figure 7. Possible mitochondrial molecular mechanism of BGP-15 cytoprotective action. BGP-15 reduces mitochondrial ROS production at complex I and at complex III, and reduces ROS induced mitochondrial damage, as well as cell death.

7. Summary

1. Significant differences were observed in both variants of *MLXIPL*, *GALNT2* rs4846914 and *ANGPTL3* rs1213033 polymorphisms comparing Roma individuals to Hungarians. However, there were no associations between levels of triglycerides and minor allele carriers in Roma and Hungarian population samples.
2. *GCKR*, *CILP2*, *GALNT2* and *TRIB1* loci were not associated with increased triglyceride levels in any population investigated.
3. In *APOA5* rs662799, rs2266788, rs207560 and rs3135506 we found elevated plasma triglyceride levels in the risk allele carriers compared to non-carriers in both populations. At least a two-fold significant increase was detected in minor allele frequencies in Roma when compared to Hungarians, except the rs2266788 variant.
4. Haplotype analysis revealed significant increase of *APOA5**2, *APOA5**4 in Roma, as opposed to the higher levels of *APOA5**5 found in Hungarians.
5. Different linkage disequilibrium was found between rs207560 and rs3135506 variants in Roma compared to Hungarians.
6. BGP-15 accumulates in mitochondria and attenuates ROS-induced mitochondrial ROS production.
7. BGP-15 has a protective effect against ROS-induced mitochondrial depolarization and preserves mitochondrial integrity.
8. BGP-15 attenuates bacterial lipopolysaccharide (LPS)-induced collapse of mitochondrial membrane potential and ROS production in LPS-sensitive cells.
9. BGP-15 did not have any antioxidant effects and reduces ROS production mainly at Complex I, and so a novel mitochondrial drug candidate for the prevention of ROS-related and inflammatory disease progression.

8. References

1. Szalai C, Keszei M, Duba J, Prohaszka Z, Kozma GT, et al. (2004) Polymorphism in the promoter region of the apolipoprotein A5 gene is associated with an increased susceptibility for coronary artery disease. *Atherosclerosis* 173: 109-114.
2. Vaessen SF, Schaap FG, Kuivenhoven JA, Groen AK, Hutten BA, et al. (2006) Apolipoprotein A-V, triglycerides and risk of coronary artery disease: the prospective Epic-Norfolk Population Study. *J Lipid Res* 47: 2064-2070.
3. Martinelli N, Girelli D, Ferraresi P, Olivieri O, Lunghi B, et al. (2007) Increased factor VIII coagulant activity levels in male carriers of the factor V R2 polymorphism. *Blood Coagul Fibrinolysis* 18: 125-129.
4. Maasz A, Kisfali P, Jaromi L, Horvatovich K, Szolnoki Z, et al. (2008) Apolipoprotein A5 gene IVS3+G476A allelic variant confers susceptibility for development of ischemic stroke. *Circ J* 72: 1065-1070.
5. Maasz A, Kisfali P, Szolnoki Z, Hadarits F, Melegh B (2008) Apolipoprotein A5 gene C56G variant confers risk for the development of large-vessel associated ischemic stroke. *J Neurol* 255: 649-654.
6. Feitosa MF, An P, Ordovas JM, Ketkar S, Hopkins PN, et al. (2011) Association of gene variants with lipid levels in response to fenofibrate is influenced by metabolic syndrome status. *Atherosclerosis* 215: 435-439.
7. Garelnabi M, Lor K, Jin J, Chai F, Santanam N (2012) The paradox of ApoA5 modulation of triglycerides: Evidence from clinical and basic research. *Clin Biochem*.
8. Mohas M, Kisfali P, Jaromi L, Maasz A, Feher E, et al. (2010) GCKR gene functional variants in type 2 diabetes and metabolic syndrome: do the rare variants associate with increased carotid intima-media thickness? *Cardiovasc Diabetol* 9: 79.
9. Jaromi L, Csongei V, Polgar N, Szolnoki Z, Maasz A, et al. (2010) Functional variants of glucokinase regulatory protein and apolipoprotein A5 genes in ischemic stroke. *J Mol Neurosci* 41: 121-128.
10. Jaromi L, Csongei V, Polgar N, Rappai G, Szolnoki Z, et al. (2011) Triglyceride level-influencing functional variants of the ANGPTL3, CILP2, and TRIB1 loci in ischemic stroke. *Neuromolecular Med* 13: 179-186.
11. Johansen CT, Hegele RA (2012) Allelic and phenotypic spectrum of plasma triglycerides. *Biochim Biophys Acta* 1821: 833-842.
12. Souverein OW, Jukema JW, Boekholdt SM, Zwinderman AH, Tanck MW (2005) Polymorphisms in APOA1 and LPL genes are statistically independently associated with fasting TG in men with CAD. *Eur J Hum Genet* 13: 445-451.
13. Havasi V, Szolnoki Z, Talian G, Bene J, Komlosi K, et al. (2006) Apolipoprotein A5 gene promoter region T-1131C polymorphism associates with elevated circulating triglyceride levels and confers susceptibility for development of ischemic stroke. *J Mol Neurosci* 29: 177-183.
14. Freiberg JJ, Tybjaerg-Hansen A, Jensen JS, Nordestgaard BG (2008) Nonfasting triglycerides and risk of ischemic stroke in the general population. *JAMA* 300: 2142-2152.
15. Willer CJ, Sanna S, Jackson AU, Scuteri A, Bonnycastle LL, et al. (2008) Newly identified loci that influence lipid concentrations and risk of coronary artery disease. *Nat Genet* 40: 161-169.
16. Kathiresan S, Willer CJ, Peloso GM, Demissie S, Musunuru K, et al. (2009) Common variants at 30 loci contribute to polygenic dyslipidemia. *Nat Genet* 41: 56-65.

17. Labreuche J, Touboul PJ, Amarenco P (2009) Plasma triglyceride levels and risk of stroke and carotid atherosclerosis: a systematic review of the epidemiological studies. *Atherosclerosis* 203: 331-345.
18. Perez-Martinez P, Garcia-Rios A, Delgado-Lista J, Perez-Jimenez F, Lopez-Miranda J (2011) Nutrigenetics of the postprandial lipoprotein metabolism: evidences from human intervention studies. *Curr Vasc Pharmacol* 9: 287-291.
19. Aslibekyan S, Goodarzi MO, Frazier-Wood AC, Yan X, Irvin MR, et al. (2012) Variants Identified in a GWAS Meta-Analysis for Blood Lipids Are Associated with the Lipid Response to Fenofibrate. *PLoS One* 7: e48663.
20. Grundy SM (2002) Approach to lipoprotein management in 2001 National Cholesterol Guidelines. *Am J Cardiol* 90: 11i-21i.
21. Krauss RM (1998) Atherogenicity of triglyceride-rich lipoproteins. *Am J Cardiol* 81: 13B-17B.
22. Hodis HN (1999) Triglyceride-rich lipoprotein remnant particles and risk of atherosclerosis. *Circulation* 99: 2852-2854.
23. Cullen P (2000) Evidence that triglycerides are an independent coronary heart disease risk factor. *Am J Cardiol* 86: 943-949.
24. Haim M, Benderly M, Brunner D, Behar S, Graff E, et al. (1999) Elevated serum triglyceride levels and long-term mortality in patients with coronary heart disease: the Bezafibrate Infarction Prevention (BIP) Registry. *Circulation* 100: 475-482.
25. Brautbar A, Covarrubias D, Belmont J, Lara-Garduno F, Virani SS, et al. (2011) Variants in the APOA5 gene region and the response to combination therapy with statins and fenofibric acid in a randomized clinical trial of individuals with mixed dyslipidemia. *Atherosclerosis* 219: 737-742.
26. Kisfali P, Mohas M, Maasz A, Hadarits F, Marko L, et al. (2008) Apolipoprotein A5 IVS3+476A allelic variant associates with increased triglyceride levels and confers risk for development of metabolic syndrome in Hungarians. *Circ J* 72: 40-43.
27. Kathiresan S, Melander O, Guiducci C, Surti A, Burt NP, et al. (2008) Six new loci associated with blood low-density lipoprotein cholesterol, high-density lipoprotein cholesterol or triglycerides in humans. *Nat Genet* 40: 189-197.
28. Shimizugawa T, Ono M, Shimamura M, Yoshida K, Ando Y, et al. (2002) ANGPTL3 decreases very low density lipoprotein triglyceride clearance by inhibition of lipoprotein lipase. *J Biol Chem* 277: 33742-33748.
29. Seidemann SB, Li L, Shen GQ, Topol EJ, Wang QK (2008) Identification of a novel locus for triglyceride on chromosome 1p31-32 in families with premature CAD and MI. *J Lipid Res* 49: 1034-1038.
30. Izar MC, Fonseca FA, Ihara SS, Kasinski N, Sang WH, et al. (2003) Risk Factors, biochemical markers, and genetic polymorphisms in early coronary artery disease. *Arq Bras Cardiol* 80: 379-395.
31. Thomsen SB, Rathcke CN, Skaaby T, Linneberg A, Vestergaard H (2012) The Association between genetic variations of CHI3L1, levels of the encoded glycoprotein YKL-40 and the lipid profile in a Danish population. *PLoS One* 7: e47094.
32. Baroni MG, Berni A, Romeo S, Arca M, Tesorio T, et al. (2003) Genetic study of common variants at the Apo E, Apo AI, Apo CIII, Apo B, lipoprotein lipase (LPL) and hepatic lipase (LIPC) genes and coronary artery disease (CAD): variation in LIPC gene associates with clinical outcomes in patients with established CAD. *BMC Med Genet* 4: 8.
33. Meigs JB, Nathan DM, D'Agostino RB, Sr., Wilson PW (2002) Fasting and postchallenge glycemia and cardiovascular disease risk: the Framingham Offspring Study. *Diabetes Care* 25: 1845-1850.

34. Pennacchio LA, Rubin EM (2003) Apolipoprotein A5, a newly identified gene that affects plasma triglyceride levels in humans and mice. *Arterioscler Thromb Vasc Biol* 23: 529-534.
35. Ma X, Bacci S, Mlynarski W, Gottardo L, Soccio T, et al. (2004) A common haplotype at the CD36 locus is associated with high free fatty acid levels and increased cardiovascular risk in Caucasians. *Hum Mol Genet* 13: 2197-2205.
36. Saidi S, Slamia LB, Ammou SB, Mahjoub T, Almawi WY (2007) Association of apolipoprotein E gene polymorphism with ischemic stroke involving large-vessel disease and its relation to serum lipid levels. *J Stroke Cerebrovasc Dis* 16: 160-166.
37. Kalaydjieva L, Gresham D, Calafell F (2001) Genetic studies of the Roma (Gypsies): a review. *BMC Med Genet* 2: 5.
38. Zeman CL, Depken DE, Senchina DS (2003) Roma health issues: a review of the literature and discussion. *Ethn Health* 8: 223-249.
39. Gresham D, Morar B, Underhill PA, Passarino G, Lin AA, et al. (2001) Origins and divergence of the Roma (gypsies). *Am J Hum Genet* 69: 1314-1331.
40. McKee M (1997) The health of gypsies. *BMJ* 315: 1172-1173.
41. Vozarova de Courten B, de Courten M, Hanson RL, Zahorakova A, Egyenes HP, et al. (2003) Higher prevalence of type 2 diabetes, metabolic syndrome and cardiovascular diseases in gypsies than in non-gypsies in Slovakia. *Diabetes Res Clin Pract* 62: 95-103.
42. Dobranici M, Buzea A, Popescu R (2012) The cardiovascular risk factors of the Roma (gypsies) people in Central-Eastern Europe: a review of the published literature. *J Med Life* 5: 382-389.
43. Abo Alrob O, Lopaschuk GD (2014) Role of CoA and acetyl-CoA in regulating cardiac fatty acid and glucose oxidation. *Biochem Soc Trans* 42: 1043-1051.
44. Ly LD, Xu S, Choi SK, Ha CM, Thoudam T, et al. (2017) Oxidative stress and calcium dysregulation by palmitate in type 2 diabetes. *Exp Mol Med* 49: e291.
45. Lin Y, Berg AH, Iyengar P, Lam TK, Giacca A, et al. (2005) The hyperglycemia-induced inflammatory response in adipocytes: the role of reactive oxygen species. *J Biol Chem* 280: 4617-4626.
46. Kowluru RA, Kowluru V, Xiong Y, Ho YS (2006) Overexpression of mitochondrial superoxide dismutase in mice protects the retina from diabetes-induced oxidative stress. *Free Radic Biol Med* 41: 1191-1196.
47. Vincent AM, Olzmann JA, Brownlee M, Sivitz WI, Russell JW (2004) Uncoupling proteins prevent glucose-induced neuronal oxidative stress and programmed cell death. *Diabetes* 53: 726-734.
48. Newsholme P, Gaudel C, Krause M (2012) Mitochondria and diabetes. An intriguing pathogenetic role. *Adv Exp Med Biol* 942: 235-247.
49. Coyle LC, Rodriguez A, Jeschke RE, Simon-Lee A, Abbott KC, et al. (2006) Acetylcysteine In Diabetes (AID): a randomized study of acetylcysteine for the prevention of contrast nephropathy in diabetics. *Am Heart J* 151: 1032 e1039-1012.
50. Jaffery Z, Verma A, White CJ, Grant AG, Collins TJ, et al. (2012) A randomized trial of intravenous n-acetylcysteine to prevent contrast induced nephropathy in acute coronary syndromes. *Catheter Cardiovasc Interv* 79: 921-926.
51. Drose S, Stepanova A, Galkin A (2016) Ischemic A/D transition of mitochondrial complex I and its role in ROS generation. *Biochim Biophys Acta* 1857: 946-957.
52. Gehrig SM, van der Poel C, Sayer TA, Schertzer JD, Henstridge DC, et al. (2012) Hsp72 preserves muscle function and slows progression of severe muscular dystrophy. *Nature* 484: 394-398.
53. Sarszegi Z, Bognar E, Gaszner B, Konyi A, Gallyas F, Jr., et al. (2012) BGP-15, a PARP-inhibitor, prevents imatinib-induced cardiotoxicity by activating Akt and suppressing JNK and p38 MAP kinases. *Mol Cell Biochem* 365: 129-137.

54. Nagy G, Szarka A, Lotz G, Doczi J, Wunderlich L, et al. (2010) BGP-15 inhibits caspase-independent programmed cell death in acetaminophen-induced liver injury. *Toxicol Appl Pharmacol* 243: 96-103.
55. Bardos G, Moricz K, Jaszlits L, Rabloczky G, Tory K, et al. (2003) BGP-15, a hydroximic acid derivative, protects against cisplatin- or taxol-induced peripheral neuropathy in rats. *Toxicol Appl Pharmacol* 190: 9-16.
56. Halmosi R, Berente Z, Osz E, Toth K, Literati-Nagy P, et al. (2001) Effect of poly(ADP-ribose) polymerase inhibitors on the ischemia-reperfusion-induced oxidative cell damage and mitochondrial metabolism in Langendorff heart perfusion system. *Mol Pharmacol* 59: 1497-1505.
57. Szabados E, Literati-Nagy P, Farkas B, Sumegi B (2000) BGP-15, a nicotinic amidoxime derivate protecting heart from ischemia reperfusion injury through modulation of poly(ADP-ribose) polymerase. *Biochem Pharmacol* 59: 937-945.
58. Literati-Nagy Z, Tory K, Literati-Nagy B, Kolonics A, Torok Z, et al. (2012) The HSP co-inducer BGP-15 can prevent the metabolic side effects of the atypical antipsychotics. *Cell Stress Chaperones* 17: 517-521.
59. Gombos I, Crul T, Piotto S, Gungor B, Torok Z, et al. (2011) Membrane-lipid therapy in operation: the HSP co-inducer BGP-15 activates stress signal transduction pathways by remodeling plasma membrane rafts. *PLoS One* 6: e28818.
60. Chung J, Nguyen AK, Henstridge DC, Holmes AG, Chan MH, et al. (2008) HSP72 protects against obesity-induced insulin resistance. *Proc Natl Acad Sci U S A* 105: 1739-1744.
61. Farkas B, Magyarlaki M, Csete B, Nemeth J, Rabloczky G, et al. (2002) Reduction of acute photodamage in skin by topical application of a novel PARP inhibitor. *Biochem Pharmacol* 63: 921-932.
62. Literati-Nagy B, Peterfai E, Kulcsar E, Literati-Nagy Z, Buday B, et al. (2010) Beneficial effect of the insulin sensitizer (HSP inducer) BGP-15 on olanzapine-induced metabolic disorders. *Brain Res Bull* 83: 340-344.
63. Literati-Nagy Z, Tory K, Literati-Nagy B, Kolonics A, Vigh L, Jr., et al. (2012) A novel insulin sensitizer drug candidate-BGP-15-can prevent metabolic side effects of atypical antipsychotics. *Pathol Oncol Res* 18: 1071-1076.
64. Subramaniam S, Fahy E, Gupta S, Sud M, Byrnes RW, et al. (2011) Bioinformatics and systems biology of the lipidome. *Chem Rev* 111: 6452-6490.
65. Fahy E, Subramaniam S, Murphy RC, Nishijima M, Raetz CR, et al. (2009) Update of the LIPID MAPS comprehensive classification system for lipids. *J Lipid Res* 50 Suppl: S9-14.
66. Nelson RH (2013) Hyperlipidemia as a risk factor for cardiovascular disease. *Prim Care* 40: 195-211.
67. McGill HC, Jr., McMahan CA, Herderick EE, Malcom GT, Tracy RE, et al. (2000) Origin of atherosclerosis in childhood and adolescence. *Am J Clin Nutr* 72: 1307S-1315S.
68. Saland JM, Ginsberg HN (2007) Lipoprotein metabolism in chronic renal insufficiency. *Pediatr Nephrol* 22: 1095-1112.
69. Yuan G, Al-Shali KZ, Hegele RA (2007) Hypertriglyceridemia: its etiology, effects and treatment. *CMAJ* 176: 1113-1120.
70. Jones A (2013) Triglycerides and cardiovascular risk. *Heart* 99: 1-2.
71. Warner JP, Leek JP, Intody S, Markham AF, Bonthron DT (1995) Human glucokinase regulatory protein (GCKR): cDNA and genomic cloning, complete primary structure, and chromosomal localization. *Mamm Genome* 6: 532-536.
72. Vaxillaire M, Vionnet N, Vigouroux C, Sun F, Espinosa R, 3rd, et al. (1994) Search for a third susceptibility gene for maturity-onset diabetes of the young. Studies with eleven candidate genes. *Diabetes* 43: 389-395.
73. Hayward BE, Dunlop N, Intody S, Leek JP, Markham AF, et al. (1998) Organization of the human glucokinase regulator gene GCKR. *Genomics* 49: 137-142.

74. Hayward BE, Fantes JA, Warner JP, Intody S, Leek JP, et al. (1996) Co-localization of the ketohexokinase and glucokinase regulator genes to a 500-kb region of chromosome 2p23. *Mamm Genome* 7: 454-458.
75. Wilson JE (1995) Hexokinases. *Rev Physiol Biochem Pharmacol* 126: 65-198.
76. Van Schaftingen E, Detheux M, Veiga da Cunha M (1994) Short-term control of glucokinase activity: role of a regulatory protein. *FASEB J* 8: 414-419.
77. van Schaftingen E, Veiga-da-Cunha M, Niculescu L (1997) The regulatory protein of glucokinase. *Biochem Soc Trans* 25: 136-140.
78. Shiota M, Galassetti P, Monohan M, Neal DW, Cherrington AD (1998) Small amounts of fructose markedly augment net hepatic glucose uptake in the conscious dog. *Diabetes* 47: 867-873.
79. de la Iglesia N, Mukhtar M, Seoane J, Guinovart JJ, Agius L (2000) The role of the regulatory protein of glucokinase in the glucose sensory mechanism of the hepatocyte. *J Biol Chem* 275: 10597-10603.
80. Vandercammen A, Van Schaftingen E (1991) Competitive inhibition of liver glucokinase by its regulatory protein. *Eur J Biochem* 200: 545-551.
81. Detheux M, Vandekerckhove J, Van Schaftingen E (1994) Cloning and sequencing of rat liver cDNAs encoding the regulatory protein of glucokinase. *FEBS Lett* 339: 312.
82. Wang H, Iynedjian PB (1997) Modulation of glucose responsiveness of insulinoma beta-cells by graded overexpression of glucokinase. *Proc Natl Acad Sci U S A* 94: 4372-4377.
83. Agius L, Peak M, Newgard CB, Gomez-Foix AM, Guinovart JJ (1996) Evidence for a role of glucose-induced translocation of glucokinase in the control of hepatic glycogen synthesis. *J Biol Chem* 271: 30479-30486.
84. Orho-Melander M, Melander O, Guiducci C, Perez-Martinez P, Corella D, et al. (2008) Common missense variant in the glucokinase regulatory protein gene is associated with increased plasma triglyceride and C-reactive protein but lower fasting glucose concentrations. *Diabetes* 57: 3112-3121.
85. Vaxillaire M, Cavalcanti-Proenca C, Dechaume A, Tichet J, Marre M, et al. (2008) The common P446L polymorphism in GCKR inversely modulates fasting glucose and triglyceride levels and reduces type 2 diabetes risk in the DESIR prospective general French population. *Diabetes* 57: 2253-2257.
86. Futamura M, Hosaka H, Kadotani A, Shimazaki H, Sasaki K, et al. (2006) An allosteric activator of glucokinase impairs the interaction of glucokinase and glucokinase regulatory protein and regulates glucose metabolism. *J Biol Chem* 281: 37668-37674.
87. Slosberg ED, Desai UJ, Fanelli B, St Denny I, Connelly S, et al. (2001) Treatment of type 2 diabetes by adenoviral-mediated overexpression of the glucokinase regulatory protein. *Diabetes* 50: 1813-1820.
88. Grimsby J, Sarabu R, Corbett WL, Haynes NE, Bizzarro FT, et al. (2003) Allosteric activators of glucokinase: potential role in diabetes therapy. *Science* 301: 370-373.
89. Grimsby J, Coffey JW, Dvorozniak MT, Magram J, Li G, et al. (2000) Characterization of glucokinase regulatory protein-deficient mice. *J Biol Chem* 275: 7826-7831.
90. Efanov AM, Barrett DG, Brenner MB, Briggs SL, Delaunois A, et al. (2005) A novel glucokinase activator modulates pancreatic islet and hepatocyte function. *Endocrinology* 146: 3696-3701.
91. Magnuson MA, Jetton TL (1993) Evolutionary conservation of elements in the upstream glucokinase promoter. *Biochem Soc Trans* 21: 160-163.
92. Matschinsky FM (1996) Banting Lecture 1995. A lesson in metabolic regulation inspired by the glucokinase glucose sensor paradigm. *Diabetes* 45: 223-241.
93. Matschinsky FM, Glaser B, Magnuson MA (1998) Pancreatic beta-cell glucokinase: closing the gap between theoretical concepts and experimental realities. *Diabetes* 47: 307-315.

94. Farrelly D, Brown KS, Tieman A, Ren J, Lira SA, et al. (1999) Mice mutant for glucokinase regulatory protein exhibit decreased liver glucokinase: a sequestration mechanism in metabolic regulation. *Proc Natl Acad Sci U S A* 96: 14511-14516.
95. Bosco D, Meda P, Iynedjian PB (2000) Glucokinase and glucokinase regulatory protein: mutual dependence for nuclear localization. *Biochem J* 348 Pt 1: 215-222.
96. Chu CA, Fujimoto Y, Igawa K, Grimsby J, Grippo JF, et al. (2004) Rapid translocation of hepatic glucokinase in response to intraduodenal glucose infusion and changes in plasma glucose and insulin in conscious rats. *Am J Physiol Gastrointest Liver Physiol* 286: G627-634.
97. Brown KS, Kalinowski SS, Megill JR, Durham SK, Mookhtiar KA (1997) Glucokinase regulatory protein may interact with glucokinase in the hepatocyte nucleus. *Diabetes* 46: 179-186.
98. Havula E, Hietakangas V (2012) Glucose sensing by ChREBP/MondoA-Mlx transcription factors. *Semin Cell Dev Biol* 23: 640-647.
99. Oike Y, Akao M, Kubota Y, Suda T (2005) Angiopoietin-like proteins: potential new targets for metabolic syndrome therapy. *Trends Mol Med* 11: 473-479.
100. Lusis AJ, Pajukanta P (2008) A treasure trove for lipoprotein biology. *Nat Genet* 40: 129-130.
101. Holleboom AG, Karlsson H, Lin RS, Beres TM, Sierts JA, et al. (2011) Heterozygosity for a loss-of-function mutation in GALNT2 improves plasma triglyceride clearance in man. *Cell Metab* 14: 811-818.
102. Kiss-Toth E, Bagstaff SM, Sung HY, Jozsa V, Dempsey C, et al. (2004) Human tribbles, a protein family controlling mitogen-activated protein kinase cascades. *J Biol Chem* 279: 42703-42708.
103. Pennacchio LA, Olivier M, Hubacek JA, Cohen JC, Cox DR, et al. (2001) An apolipoprotein influencing triglycerides in humans and mice revealed by comparative sequencing. *Science* 294: 169-173.
104. van der Vliet HN, Sammels MG, Leegwater AC, Levels JH, Reitsma PH, et al. (2001) Apolipoprotein A-V: a novel apolipoprotein associated with an early phase of liver regeneration. *J Biol Chem* 276: 44512-44520.
105. Baroukh N, Bauge E, Akiyama J, Chang J, Afzal V, et al. (2004) Analysis of apolipoprotein A5, c3, and plasma triglyceride concentrations in genetically engineered mice. *Arterioscler Thromb Vasc Biol* 24: 1297-1302.
106. Beckstead JA, Oda MN, Martin DD, Forte TM, Bielicki JK, et al. (2003) Structure-function studies of human apolipoprotein A-V: a regulator of plasma lipid homeostasis. *Biochemistry* 42: 9416-9423.
107. Nilsson SK, Lookene A, Beckstead JA, Gliemann J, Ryan RO, et al. (2007) Apolipoprotein A-V interaction with members of the low density lipoprotein receptor gene family. *Biochemistry* 46: 3896-3904.
108. Wong K, Beckstead JA, Lee D, Weers PM, Guigard E, et al. (2008) The N-terminus of apolipoprotein A-V adopts a helix bundle molecular architecture. *Biochemistry* 47: 8768-8774.
109. Sharma V, Ryan RO, Forte TM (2012) Apolipoprotein A-V dependent modulation of plasma triacylglycerol: a puzzlement. *Biochim Biophys Acta* 1821: 795-799.
110. Gin P, Yin L, Davies BS, Weinstein MM, Ryan RO, et al. (2008) The acidic domain of GPIHBP1 is important for the binding of lipoprotein lipase and chylomicrons. *J Biol Chem* 283: 29554-29562.
111. Dolinska S, Kudlackova M, Ginter E (2007) The prevalence of female obesity in the world and in the Slovak Gypsy women. *Bratisl Lek Listy* 108: 207-211.
112. Sun G, Bi N, Li G, Zhu X, Zeng W, et al. (2006) Identification of lipid binding and lipoprotein lipase activation domains of human apoAV. *Chem Phys Lipids* 143: 22-28.

113. Lookene A, Beckstead JA, Nilsson S, Olivecrona G, Ryan RO (2005) Apolipoprotein A-V-heparin interactions: implications for plasma lipoprotein metabolism. *J Biol Chem* 280: 25383-25387.
114. Merkel M, Loeffler B, Kluger M, Fabig N, Geppert G, et al. (2005) Apolipoprotein AV accelerates plasma hydrolysis of triglyceride-rich lipoproteins by interaction with proteoglycan-bound lipoprotein lipase. *J Biol Chem* 280: 21553-21560.
115. Pennacchio LA, Olivier M, Hubacek JA, Krauss RM, Rubin EM, et al. (2002) Two independent apolipoprotein A5 haplotypes influence human plasma triglyceride levels. *Hum Mol Genet* 11: 3031-3038.
116. Hubacek JA, Skodova Z, Adamkova V, Lanska V, Poledne R (2004) The influence of APOAV polymorphisms (T-1131>C and S19>W) on plasma triglyceride levels and risk of myocardial infarction. *Clin Genet* 65: 126-130.
117. Maasz A, Kisfali P, Horvatovich K, Mohas M, Marko L, et al. (2007) Apolipoprotein A5 T-1131C variant confers risk for metabolic syndrome. *Pathol Oncol Res* 13: 243-247.
118. Nilsson SK, Heeren J, Olivecrona G, Merkel M (2011) Apolipoprotein A-V; a potent triglyceride reducer. *Atherosclerosis* 219: 15-21.
119. Gin P, Beigneux AP, Davies B, Young MF, Ryan RO, et al. (2007) Normal binding of lipoprotein lipase, chylomicrons, and apo-AV to GPIHBP1 containing a G56R amino acid substitution. *Biochim Biophys Acta* 1771: 1464-1468.
120. Alborn WE, Johnson MG, Prince MJ, Konrad RJ (2006) Definitive N-terminal protein sequence and further characterization of the novel apolipoprotein A5 in human serum. *Clin Chem* 52: 514-517.
121. Helleboid-Chapman A, Nowak M, Helleboid S, Moitrot E, Rommens C, et al. (2009) Apolipoprotein A-V modulates insulin secretion in pancreatic beta-cells through its interaction with midkine. *Cell Physiol Biochem* 24: 451-460.
122. Grosskopf I, Baroukh N, Lee SJ, Kamari Y, Harats D, et al. (2005) Apolipoprotein A-V deficiency results in marked hypertriglyceridemia attributable to decreased lipolysis of triglyceride-rich lipoproteins and removal of their remnants. *Arterioscler Thromb Vasc Biol* 25: 2573-2579.
123. Weinberg RB, Cook VR, Beckstead JA, Martin DD, Gallagher JW, et al. (2003) Structure and interfacial properties of human apolipoprotein A-V. *J Biol Chem* 278: 34438-34444.
124. Zhang Z, Peng B, Gong RR, Gao LB, Du J, et al. (2011) Apolipoprotein A5 polymorphisms and risk of coronary artery disease: a meta-analysis. *Biosci Trends* 5: 165-172.
125. Sarwar N, Sandhu MS, Ricketts SL, Butterworth AS, Di Angelantonio E, et al. (2010) Triglyceride-mediated pathways and coronary disease: collaborative analysis of 101 studies. *Lancet* 375: 1634-1639.
126. Kisfali P, Mohas M, Maasz A, Polgar N, Hadarits F, et al. (2009) Haplotype analysis of the apolipoprotein A5 gene in patients with the metabolic syndrome. *Nutr Metab Cardiovasc Dis* 20: 505-511.
127. Wang W, Gong G, Wang X, Wei-LaPierre L, Cheng H, et al. (2016) Mitochondrial Flash: Integrative Reactive Oxygen Species and pH Signals in Cell and Organelle Biology. *Antioxid Redox Signal* 25: 534-549.
128. Galloway CA, Yoon Y (2013) Mitochondrial morphology in metabolic diseases. *Antioxid Redox Signal* 19: 415-430.
129. Hogeboom GH, Schneider WC (1950) Cytochemical studies of mammalian tissues. III. Isocitric dehydrogenase and triphosphopyridine nucleotide-cytochrome c reductase of mouse liver. *J Biol Chem* 186: 417-427.
130. Sims NR (1990) Rapid isolation of metabolically active mitochondria from rat brain and subregions using Percoll density gradient centrifugation. *J Neurochem* 55: 698-707.

131. Papazisis KT, Geromichalos GD, Dimitriadis KA, Kortsaris AH (1997) Optimization of the sulforhodamine B colorimetric assay. *J Immunol Methods* 208: 151-158.
132. Barrett JC, Fry B, Maller J, Daly MJ (2005) Haploview: analysis and visualization of LD and haplotype maps. *Bioinformatics* 21: 263-265.
133. Tao H, Zhang Y, Zeng X, Shulman GI, Jin S (2014) Niclosamide ethanolamine-induced mild mitochondrial uncoupling improves diabetic symptoms in mice. *Nat Med* 20: 1263-1269.
134. Teshima Y, Takahashi N, Nishio S, Saito S, Kondo H, et al. (2014) Production of reactive oxygen species in the diabetic heart. Roles of mitochondria and NADPH oxidase. *Circ J* 78: 300-306.
135. Robinson KM, Janes MS, Beckman JS (2008) The selective detection of mitochondrial superoxide by live cell imaging. *Nat Protoc* 3: 941-947.
136. Ni R, Cao T, Xiong S, Ma J, Fan GC, et al. (2016) Therapeutic inhibition of mitochondrial reactive oxygen species with mito-TEMPO reduces diabetic cardiomyopathy. *Free Radic Biol Med* 90: 12-23.
137. Huang LS, Cobessi D, Tung EY, Berry EA (2005) Binding of the respiratory chain inhibitor antimycin to the mitochondrial bc1 complex: a new crystal structure reveals an altered intramolecular hydrogen-bonding pattern. *J Mol Biol* 351: 573-597.
138. Klegeris A, McGeer PL (2001) Inflammatory cytokine levels are influenced by interactions between THP-1 monocytic, U-373 MG astrocytic, and SH-SY5Y neuronal cell lines of human origin. *Neurosci Lett* 313: 41-44.
139. von Bernhardi R, Eugenin-von Bernhardi L, Eugenin J (2015) Microglial cell dysregulation in brain aging and neurodegeneration. *Front Aging Neurosci* 7: 124.
140. Brenner C, Galluzzi L, Kepp O, Kroemer G (2013) Decoding cell death signals in liver inflammation. *J Hepatol* 59: 583-594.
141. Fonai F, Priber JK, Jakus PB, Kalman N, Antus C, et al. (2015) Lack of cyclophilin D protects against the development of acute lung injury in endotoxemia. *Biochim Biophys Acta* 1852: 2563-2573.
142. Priber J, Fonai F, Jakus PB, Racz B, Chinopoulos C, et al. (2015) Cyclophilin D disruption attenuates lipopolysaccharide-induced inflammatory response in primary mouse macrophages. *Biochem Cell Biol* 93: 241-250.
143. Tucsek Z, Radnai B, Racz B, Debreceni B, Priber JK, et al. (2011) Suppressing LPS-induced early signal transduction in macrophages by a polyphenol degradation product: a critical role of MKP-1. *J Leukoc Biol* 89: 105-111.
144. Seeley EJ, Rosenberg P, Matthay MA (2013) Calcium flux and endothelial dysfunction during acute lung injury: a STIMulating target for therapy. *J Clin Invest* 123: 1015-1018.
145. Idelman G, Smith DL, Zucker SD (2015) Bilirubin inhibits the up-regulation of inducible nitric oxide synthase by scavenging reactive oxygen species generated by the toll-like receptor 4-dependent activation of NADPH oxidase. *Redox Biol* 5: 398-408.
146. Mohammad HA, Farghaly HS, Metwalley KA, Monazea EM, Abd El-Hafeez HA (2012) Predictors of glycemic control in children with Type 1 diabetes mellitus in Assiut-Egypt. *Indian J Endocrinol Metab* 16: 796-802.
147. Johannsen TH, Frikke-Schmidt R, Schou J, Nordestgaard BG, Tybjaerg-Hansen A (2012) Genetic Inhibition of CETP, Ischemic Vascular Disease and Mortality, and Possible Adverse Effects. *J Am Coll Cardiol* 60: 2041-2048.
148. Bal SS, Khurana D, Sharma A, Lal V, Bhansali A, et al. (2011) Association of metabolic syndrome with carotid atherosclerosis in the young North Indian population. *Diabetes Metab Syndr* 5: 153-157.
149. Cabrera MA, de Andrade SM, Mesas AE (2012) A prospective study of risk factors for cardiovascular events among the elderly. *Clin Interv Aging* 7: 463-468.

150. Martinelli N, Trabetti E, Bassi A, Girelli D, Friso S, et al. (2007) The -1131 T>C and S19W APOA5 gene polymorphisms are associated with high levels of triglycerides and apolipoprotein C-III, but not with coronary artery disease: an angiographic study. *Atherosclerosis* 191: 409-417.
151. Perez-Martinez P, Corella D, Shen J, Arnett DK, Yiannakouris N, et al. (2009) Association between glucokinase regulatory protein (GCKR) and apolipoprotein A5 (APOA5) gene polymorphisms and triacylglycerol concentrations in fasting, postprandial, and fenofibrate-treated states. *Am J Clin Nutr* 89: 391-399.
152. Hishida A, Morita E, Naito M, Okada R, Wakai K, et al. (2012) Associations of apolipoprotein A5 (APOA5), glucokinase (GCK) and glucokinase regulatory protein (GCKR) polymorphisms and lifestyle factors with the risk of dyslipidemia and dysglycemia in Japanese - a cross-sectional data from the J-MICC Study. *Endocr J* 59: 589-599.
153. Jorgensen AB, Frikke-Schmidt R, West AS, Grande P, Nordestgaard BG, et al. (2012) Genetically elevated non-fasting triglycerides and calculated remnant cholesterol as causal risk factors for myocardial infarction. *Eur Heart J*.
154. Dussallant C, Serrano V, Maiz A, Eyheramendy S, Cataldo LR, et al. (2012) APOA5 Q97X Mutation Identified through homozygosity mapping causes severe hypertriglyceridemia in a Chilean consanguineous family. *BMC Med Genet* 13: 106.
155. Rafiq S, Venkata KK, Gupta V, Guru VD, Spurgeon CJ, et al. (2012) Evaluation of seven common lipid associated loci in a large Indian sib pair study. *Lipids Health Dis* 11: 155.
156. Veiga-da-Cunha M, Delplanque J, Gillain A, Bonthron DT, Boutin P, et al. (2003) Mutations in the glucokinase regulatory protein gene in 2p23 in obese French caucasians. *Diabetologia* 46: 704-711.
157. Santoro N, Zhang CK, Zhao H, Pakstis AJ, Kim G, et al. (2012) Variant in the glucokinase regulatory protein (GCKR) gene is associated with fatty liver in obese children and adolescents. *Hepatology* 55: 781-789.
158. Pisciotta L, Favari E, Magnolo L, Simonelli S, Adorni MP, et al. (2012) Characterization of three kindreds with familial combined hypolipidemia caused by loss-of-function mutations of ANGPTL3. *Circ Cardiovasc Genet* 5: 42-50.
159. Liu Y, Zhou D, Zhang Z, Song Y, Zhang D, et al. (2010) Effects of genetic variants on lipid parameters and dyslipidemia in a Chinese population. *J Lipid Res* 52: 354-360.
160. Vrablik M, Hubacek JA, Dlouha D, Lanska V, Rynekrova J, et al. (2012) Impact of variants within seven candidate genes on statin treatment efficacy. *Physiol Res*.
161. Tai ES, Sim XL, Ong TH, Wong TY, Saw SM, et al. (2009) Polymorphisms at newly identified lipid-associated loci are associated with blood lipids and cardiovascular disease in an Asian Malay population. *J Lipid Res* 50: 514-520.
162. Flecha A (2013) Healthier lives for European minority groups: school and health care, lessons from the Roma. *Int J Environ Res Public Health* 10: 3089-3111.
163. Bogdanovic D, Nikic D, Petrovic B, Kocic B, Jovanovic J, et al. (2007) Mortality of Roma population in Serbia, 2002-2005. *Croat Med J* 48: 720-726.
164. Masseria C, Mladovsky P, Hernandez-Quevedo C (2010) The socio-economic determinants of the health status of Roma in comparison with non-Roma in Bulgaria, Hungary and Romania. *Eur J Public Health* 20: 549-554.
165. Albery R, Alberyova D, Ahlers I (2009) Distribution and correlations of non-high-density lipoprotein cholesterol in Roma and Caucasian children: the Slovak Lipid Community Study. *Coll Antropol* 33: 1015-1022.
166. Carrasco-Garrido P, Lopez de Andres A, Hernandez Barrera V, Jimenez-Trujillo I, Jimenez-Garcia R (2011) Health status of Roma women in Spain. *Eur J Public Health* 21: 793-798.
167. Gualdi-Russo E, Zironi A, Dallari GV, Toselli S (2009) Migration and health in Italy: a multiethnic adult sample. *J Travel Med* 16: 88-95.

168. Krajcovicova-Kudlackova M, Blazicek P, Spustova V, Valachovicova M, Ginter E (2004) Cardiovascular risk factors in young Gypsy population. *Bratisl Lek Listy* 105: 256-259.
169. Sipeky C, Weber A, Szabo M, Melegh BI, Janicsek I, et al. (2013) High prevalence of CYP2C19*2 allele in Roma samples: study on Roma and Hungarian population samples with review of the literature. *Mol Biol Rep* 40: 4727-4735.
170. Sipeky C, Csongei V, Jaromi L, Safrany E, Maasz A, et al. (2011) Genetic variability and haplotype profile of MDR1 (ABCB1) in Roma and Hungarian population samples with a review of the literature. *Drug Metab Pharmacokinet* 26: 206-215.
171. Sipeky C, Lakner L, Szabo M, Takacs I, Tamasi V, et al. (2009) Interethnic differences of CYP2C9 alleles in healthy Hungarian and Roma population samples: relationship to worldwide allelic frequencies. *Blood Cells Mol Dis* 43: 239-242.
172. Sipeky C, Csongei V, Jaromi L, Safrany E, Polgar N, et al. (2009) Vitamin K epoxide reductase complex 1 (VKORC1) haplotypes in healthy Hungarian and Roma population samples. *Pharmacogenomics* 10: 1025-1032.
173. Moorjani P, Patterson N, Loh PR, Lipson M, Kisfali P, et al. (2013) Reconstructing Roma history from genome-wide data. *PLoS One* 8: e58633.
174. Mendizabal I, Lao O, Marigorta UM, Wollstein A, Gusmao L, et al. (2012) Reconstructing the population history of European Romani from genome-wide data. *Curr Biol* 22: 2342-2349.
175. Evans D, Seedorf U, Beil FU (2005) Polymorphisms in the apolipoprotein A5 (APOA5) gene and type III hyperlipidemia. *Clin Genet* 68: 369-372.
176. Dallongeville J, Cottel D, Wagner A, Ducimetiere P, Ruidavets JB, et al. (2008) The APOA5 Trp19 allele is associated with metabolic syndrome via its association with plasma triglycerides. *BMC Med Genet* 9: 84.
177. Melegh BI, Duga B, Sumegi K, Kisfali P, Maasz A, et al. (2012) Mutations of the apolipoprotein A5 gene with inherited hypertriglyceridaemia: review of the current literature. *Curr Med Chem* 19: 6163-6170.
178. Yin RX, Li YY, Lai CQ (2011) Apolipoprotein A1/C3/A5 haplotypes and serum lipid levels. *Lipids Health Dis* 10: 140.
179. Furuya TK, Chen ES, Ota VK, Mazzotti DR, Ramos LR, et al. (2013) Association of APOA1 and APOA5 polymorphisms and haplotypes with lipid parameters in a Brazilian elderly cohort. *Genet Mol Res* 12: 3495-3499.
180. Sapa G, Tham YK, Cemerlang N, Matsumoto A, Kiriazis H, et al. (2014) The small-molecule BGP-15 protects against heart failure and atrial fibrillation in mice. *Nat Commun* 5: 5705.
181. Racz I, Tory K, Gallyas F, Jr., Berente Z, Osz E, et al. (2002) BGP-15 - a novel poly(ADP-ribose) polymerase inhibitor - protects against nephrotoxicity of cisplatin without compromising its antitumor activity. *Biochem Pharmacol* 63: 1099-1111.
182. Perry RJ, Kim T, Zhang XM, Lee HY, Pesta D, et al. (2013) Reversal of hypertriglyceridemia, fatty liver disease, and insulin resistance by a liver-targeted mitochondrial uncoupler. *Cell Metab* 18: 740-748.
183. Keipert S, Ost M, Johann K, Imber F, Jastroch M, et al. (2014) Skeletal muscle mitochondrial uncoupling drives endocrine cross-talk through the induction of FGF21 as a myokine. *Am J Physiol Endocrinol Metab* 306: E469-482.
184. Gao L, Laude K, Cai H (2008) Mitochondrial pathophysiology, reactive oxygen species, and cardiovascular diseases. *Vet Clin North Am Small Anim Pract* 38: 137-155, vi.
185. Jheng HF, Tsai PJ, Guo SM, Kuo LH, Chang CS, et al. (2012) Mitochondrial fission contributes to mitochondrial dysfunction and insulin resistance in skeletal muscle. *Mol Cell Biol* 32: 309-319.
186. Circu ML, Aw TY (2010) Reactive oxygen species, cellular redox systems, and apoptosis. *Free Radic Biol Med* 48: 749-762.

187. Babot M, Birch A, Labarbuta P, Galkin A (2014) Characterisation of the active/de-active transition of mitochondrial complex I. *Biochim Biophys Acta* 1837: 1083-1092.
188. Ray PD, Huang BW, Tsuji Y (2012) Reactive oxygen species (ROS) homeostasis and redox regulation in cellular signaling. *Cell Signal* 24: 981-990.
189. Matsuzawa A, Ichijo H (2008) Redox control of cell fate by MAP kinase: physiological roles of ASK1-MAP kinase pathway in stress signaling. *Biochim Biophys Acta* 1780: 1325-1336.
190. Matsuno K, Iwata K, Matsumoto M, Katsuyama M, Cui W, et al. (2012) NOX1/NADPH oxidase is involved in endotoxin-induced cardiomyocyte apoptosis. *Free Radic Biol Med* 53: 1718-1728.
191. Scott AJ, O'Dea KP, O'Callaghan D, Williams L, Dokpesi JO, et al. (2011) Reactive oxygen species and p38 mitogen-activated protein kinase mediate tumor necrosis factor alpha-converting enzyme (TACE/ADAM-17) activation in primary human monocytes. *J Biol Chem* 286: 35466-35476.
192. Korbecki J, Baranowska-Bosiacka I, Gutowska I, Chlubek D (2013) The effect of reactive oxygen species on the synthesis of prostanoids from arachidonic acid. *J Physiol Pharmacol* 64: 409-421.

9. Publications

9.1 Publications related to thesis:

1. Marked Differences of Haplotype Tagging SNP Distribution, Linkage, and Haplotype Profile of APOA5 Gene in Roma Population Samples.

Sumegi K, Duga B, Melegh BI, Banfai Z, Kovesdi E, Maasz A, Melegh B

PATHOLOGY AND ONCOLOGY RESEARCH &: p. &. (2017)

Impact factor: 1.94

2. BGP-15 Protects against Oxidative Stress- or Lipopolysaccharide-Induced Mitochondrial Destabilization and Reduces Mitochondrial Production of Reactive Oxygen Species.

Sumegi K, Fekete K, Antus C, Debreceni B, Hocsak E, Gallyas F Jr, Sumegi B, Szabo A

PLOS ONE 12:(1) Paper e0169372. 19 p. (2017)

Impact factor: 3.057

3. Functional Variants of Lipid Level Modifier MLXIPL, GCKR, GALNT2, CILP2, ANGPTL3 and TRIB1 Genes in Healthy Roma and Hungarian Populations

Katalin Sumegi, Luca Jaromi, Lili Magyari, Erzsebet Kovesdi, Balazs Duga, Renata Szalai, Anita Maasz, Petra Matyas, Ingrid Janicsek, Bela Melegh

PATHOLOGY AND ONCOLOGY RESEARCH 21:(3) pp. 743-749. (2015)

Impact factor: 1.94

Total impact factors related to thesis: 6.937

9.2 Publications non-related to thesis:

1. Activation of mitochondrial fusion provides a new treatment for mitochondria-related diseases

Szabo A, Sumegi K, Fekete K, Hocsak E, Debreceni B, Setalo Gy, Kovacs K, Deres L, Kengyel A, Kovacs D, Mandl J, Nyitrai M, Febbraio M, Gallyas F, Sumegi B

BIOCHEMICAL PHARMACOLOGY 150, 86-96 (2018)

Impact factor: 4.235

2. PARP inhibition protects mitochondria and reduces ROS production via PARP-1-ATF4-MKP-1-MAPK retrograde pathway.

Hocsak E, Szabo V, Kalman N, Antus C, Cseh A, **Sumegi K**, Eros K, Hegedus Z, Gallyas F Jr, Sumegi B, Racz B

FREE RADICAL BIOLOGY AND MEDICINE &: p. &. (2017)

Impact factor: 5.784

3. Significant interethnic differences in functional variants of PON1 and P2RY12 genes in Roma and Hungarian population samples.

Janicsek I, Sipeky C, Bene J, Duga B, Melegh B, **Sumegi K**, Jaromi L, Magyar L, Melegh B
MOLECULAR BIOLOGY REPORTS 42:(1) pp. 227-232. (2015)

Impact factor: 1.698

4. Ritka genomikai betegségek azonosítása array komparatív genomhibridizációs módszerrel – elsőként Magyarországon

Duga B, Czako M, Hadzsiev K, Komlosi K, **Sumegi K**, Kisfali P, Kosztolanyi G, Melegh B
ORVOSI HETILAP 155:(9) pp. 358-361. (2014)

Impact factor: 0

5. Deletion of 4q28.3-31.23 in the background of multiple malformations with pulmonary hypertension.

Duga B, Czako M, Komlosi K, Hadzsiev K, Torok K, **Sumegi K**, Kisfali P, Kosztolanyi G, Melegh B

MOLECULAR CYTOGENETICS 7: Paper 36. 6 p. (2014)

Impact factor: 2.140

6. Figyelemhiányos hiperaktivásban szenvedő beteg vizsgálata array komparatív genomhibridizációs módszerrel

Duga B, Czako M, Komlosi K, Hadzsiev K, **Sumegi K**, Kisfali P, Melegh M, Melegh B
ORVOSI HETILAP 155 (40 pp. 1598-1601. (2014)

Impact factor: 0

7. Erratum to: Significant interethnic differences in functional variants of PON1 and P2RY12 genes in Roma and Hungarian population samples.

Janicsek I, Sipeky C, Bene J, Duga B, Melegh BI, **Sumegi K**, Jaromi L, Magyari L, Melegh B
MOLECULAR BIOLOGY REPORTS 42 (1) p. 227-232 (2014)

Impact factor: 2.024

8. Interleukin and interleukin receptor gene polymorphisms in inflammatory bowel diseases susceptibility

Lili Magyari, Erzsebet Kovesdi, Patricia Sarlos, Andras Javorhazy, **Katalin Sumegi**, Bela Melegh

WORLD JOURNAL OF GASTROENTEROLOGY 20:(12) pp. 3208-3222. (2014)

Impact factor: 2.369

9. Interleukins and interleukin receptors in rheumatoid arthritis: Research, diagnostics and clinical implications

Lili Magyari, Dalma Varszegi, Erzsebet Kovesdi, Patricia Sarlos, Bernadett Farago, Andras Javorhazy, **Katalin Sumegi**, Zsolt Banfai, Bela Melegh

WORLD JOURNAL OF ORTHOPEDICS 18:(5) pp. 516-536. (2014)

Impact factor: 0

10. Admixture of beneficial and unfavourable variants of GLCCI1 and FCER2 in Roma samples can implicate different clinical response to corticosteroids.

Szalai R, Matyas P, Varszegi D, Melegh M, Magyari L, Jaromi L, **Sumegi K**, Duga B, Kovesdi E, Hadzsiev K, Melegh B

MOLECULAR BIOLOGY REPORTS 41:(11) pp. 7665-7669. (2014)

Impact factor: 2.024

11. Hodgkin Disease Therapy Induced Second Malignancy Susceptibility 6q21 Functional Variants in Roma and Hungarian Population Samples.

Varszegi D, Duga B, Melegh BI, **Sumegi K**, Kisfali P, Maasz A, Melegh B

PATHOLOGY AND ONCOLOGY RESEARCH 20:(3) pp. 529-533. (2014)

Impact factor: 1.855

12. PARP Inhibition Attenuates Acute Kidney Allograft Rejection by Suppressing Cell Death Pathways and Activating PI-3K-Akt Cascade.

Kalmar-Nagy K, Degrell P, Szabo A, **Sumegi K**, Wittmann I, Gallyas F Jr, Sumegi B

PLOS ONE 8:(12) Paper e81928. 10 p. (2013)

Impact factor: 3.534

13. Difference of interleukin-23 receptor gene haplotype variants in ulcerative colitis compared to Crohn's disease and psoriasis.

Safrany E, Szabo M, Szell M, Kemeny L, **Sumegi K**, Melegh BI, Magyari L, Matyas P, Figler M, Weber A, Tulassay Z, Melegh B

INFLAMMATION RESEARCH 62:(2) pp. 195-200. (2013)

Impact factor: 2.143

14. High prevalence of CYP2C19*2 allele in Roma samples: study on Roma and Hungarian population samples with review of the literature

Sipeky C, Weber A, Szabo M, Melegh BI, Janicsek I, Tarlos G, Szabo I, **Sumegi K**, Melegh B

MOLECULAR BIOLOGY REPORTS 40:(8) pp. 4727-4735. (2013)

Impact factor: 1.958

15. Mutations of the Apolipoprotein A5 Gene with Inherited Hypertriglyceridaemia: Review of the Current Literature

Melegh BI, Duga B, **Sumegi K**, Kisfali P, Maasz A, Komlosi K, Hadzsiev K, Komoly S, Kosztolanyi G, Melegh B

CURRENT MEDICINAL CHEMISTRY 19:(36) pp. 6163-6170. (2012)

Impact factor: 4.07

16. Investigation of JAK2, STAT3 and CCR6 polymorphisms and their gene-gene interactions in inflammatory bowel disease.

Polgar N, Csongei V, Szabo M, Zambo V, Melegh BI, **Sumegi K**, Nagy G, Tulassay Z, Melegh B

INTERNATIONAL JOURNAL OF IMMUNOGENETICS 39:(3) pp. 247-252. (2012)

Impact factor: 1.355

17. Stepwise Positive Association Between APOA5 Minor Allele Frequencies and Increasing Plasma Triglyceride Quartiles in Random Patients with Hypertriglyceridemia of Unclarified Origin

Hadarits F, Kisfali P, Mohas M, Maasz A, **Sumegi K**, Szabo M, Hetyesy K, Valasek A, Janicsek I, Wittmann I, Melegh B

PATHOLOGY AND ONCOLOGY RESEARCH 17:(1) pp. 39-44. (2011)

Impact factor: 1.366

18. Triglyceride Level Affecting Shared Susceptibility Genes in Metabolic Syndrome and Coronary Artery Disease

Kisfali P, Polgar N, Safrany E, **Sumegi K**, Melegh BI, Bene J, Wéber Á, Hetyesy K, Melegh B

CURRENT MEDICINAL CHEMISTRY 17:(30) pp. 3533-3541. (2010)

Impact factor: 4.63

19. GCKR gene functional variants in type 2 diabetes and metabolic syndrome: do the rare variants associate with increased carotid intima-media thickness?

Mohás M, Kisfali P, Jaromi L, Maász A, Fehér E, Csongei V, Polgár N, Safrany E, Cseh J, **Sümege K**, Hetyesy K, Wittmann I, Melegh B

CARDIOVASCULAR DIABETOLOGY 9:(1) Paper 79. 7 p. (2010)

Impact factor: 2.72

9.3. Book Chapters

1. Role of Functional Variants and Mutations of the Apolipoprotein A5 Gene in Human Pathology

Balázs Duga, Béla I. Melegh, **Katalin Sümege**, Anita Maász, Péter Kisfali, Katalin Komlósi, Béla Melegh B.

Apolipoproteins: Regulatory Functions, Health Effects and Role in Disease

New York: Nova Science Publishers Inc., 2012. pp. 75-92

(ISBN:978-1-62257-484-1)

2. Ischemic Stroke Susceptibility Gene Research: Lessons We Learned

Bela I. Melegh, Anita Maasz, Peter Kisfali, **Katalin Sumegi**, Balazs Duga, Gyorgy Kosztolanyi, Samuel Komoly, Bela Melegh

Ischemic Stroke: Symptoms, Prevention and Recovery

New York: Nova Science Publishers Inc., 2013. pp. 117-144.

(ISBN:978-1-62257-799-6)

3. Role of Triglyceride Modifier Genetic Variants in Development of Metabolic Syndrome

Anita Maasz, Peter Kisfali, Bela I. Melegh, Balazs Duga, **Katalin Sümegi**, Bela Melegh
Handbook on Metabolic Syndrome: Classification, Risk Factors and Health Impact
New York: Nova Science Publishers Inc., 2012. pp.95-119.
(ISBN: 978-1-62257-025-6)

9.4. Abstracts

1. Genetic relationship of European Roma people and eight ethnic groups from the Caucasus area which suggest Romas probably admixed with during their migration

Szabó, Z. Bánfai, B. Duga, R. Szalai, L. Magyar, P. Mátyás, E. Kövesdi, **K.Sümegi**, B. Melegh
Eur J Hum Genet, 2014:22(S2):320

2. Deletion of 4q28.3-31.23 in the background of multiple malformations

B. Duga, M. Czako, K. Komlosi, K. Hadzsiev, K. Torok, **K. Sumegi**, P. Kisfali,
G. Kosztolanyi, B. Melegh
Eur J Hum Genet, 2014:22(S2):444

3. Admixture of Turks, Hungarians and Romas in the Carpathian Basin

Z. Bánfai, A. Szabó, **K. Sümegi**, B. Duga, L. Magyar, E. Kövesdi, P. Mátyás,
R. Szalai, B. Melegh
Eur J Hum Genet, 2014:22(S2):509

4. Marked differences of haplotype tagging SNP distribution, linkage, and haplotype profile of APOA5 gene in Roma population samples

B. Duga, B.I. Melegh, L. Jaromi, **K. Sümegi**, Z. Bánfai, K. Komlósi, K. Hadzsiev, A. Szabo,
R. Szalai, E. Kövesdi, J. Bene, P. Kisfali, B. Melegh
Eur J Hum Genet, 2013:21(S2):556

5. Distribution of eight SNPs of lipid level modifier genes in healthy Roma and Hungarian population samples

J. Bene, **K. Sumegi**, L. Jaromi, L. Magyar, E. Kovesdi, B. Duga, R. Szalai, P. Matyas, A.
Szabo, Z. Banfai, B. Melegh
Eur J Hum Genet, 2013:21(S2):404

6. Phenotypic variability in a Hungarian family with a novel TSC1 mutation

E. Kovesdi, K. Hadzsiev, K. Komlosi, I. Janicsek, J. Bene, L. Magyari, L. Jaromi, B. Duga, **K. Sumegi**, A. Szabo, Z. Banfai, B. Melegh

Eur J Hum Genet, 2013;21(S2):566

Total Impact factors: 50,842

According to Google Scholar:

<i>Citations</i>	<i>271</i>
<i>h-index</i>	<i>9</i>
<i>i10-index</i>	<i>9</i>

10. Acknowledgements

I would like to express my gratitude to all of those who made my Ph.D thesis possible.

First of all, I would like to thank my supervisor Professor Béla Melegh for his continuous support, efforts and guidance. I am thankful for the Department of Medical Genetics for their support, especially to Dr. Anita Maász, Dr. Luca Járomi, Dr. Erzsébet Kövesdi, Zsolt Bánfai, Dr. Balázs Duga, Dr. Lili Magyar, Dr. András Szabó, Gyöngyi Halmai and Etelka Pöstyéni. I am thankful for all of them for providing me the opportunity and scientific background for my work.

I would also like to thank the entire Department of Biochemistry and Medical Chemistry for their support and guidance.

Furthermore, I would like to thank my family and friends for their emotional support, patience and understanding.

RESEARCH ARTICLE

BGP-15 Protects against Oxidative Stress- or Lipopolysaccharide-Induced Mitochondrial Destabilization and Reduces Mitochondrial Production of Reactive Oxygen Species

Katalin Sumegi¹, Katalin Fekete¹, Csenge Antus¹, Balazs Debreceni¹, Eniko Hocsak¹, Ferenc Gallyas, Jr.^{1,2,3}, Balazs Sumegi^{1,2,3}, Aliz Szabo^{1*}

1 Department of Biochemistry and Medical Chemistry, University of Pécs Medical School, Pécs, Hungary, **2** MTA-PTE Nuclear-Mitochondrial Interactions Research Group, University of Pécs Medical School, Pécs, Hungary, **3** Szentagotthai Research Centre, Pécs, Hungary

* aliz.szabo@aok.pte.hu



OPEN ACCESS

Citation: Sumegi K, Fekete K, Antus C, Debreceni B, Hocsak E, Gallyas F, Jr., et al. (2017) BGP-15 Protects against Oxidative Stress- or Lipopolysaccharide-Induced Mitochondrial Destabilization and Reduces Mitochondrial Production of Reactive Oxygen Species. *PLoS ONE* 12(1): e0169372. doi:10.1371/journal.pone.0169372

Editor: Aamir Ahmad, University of South Alabama Mitchell Cancer Institute, UNITED STATES

Received: September 5, 2016

Accepted: December 15, 2016

Published: January 3, 2017

Copyright: © 2017 Sumegi et al. This is an open access article distributed under the terms of the [Creative Commons Attribution License](https://creativecommons.org/licenses/by/4.0/), which permits unrestricted use, distribution, and reproduction in any medium, provided the original author and source are credited.

Data Availability Statement: All relevant data are within the paper.

Funding: This work was supported by Hungarian National Research Foundations OTKA K-104220 (BS) and OTKA NN-109841 (FG). The funder had no role in study design, data collection and analysis, decision to publish, or preparation of the manuscript.

Abstract

Reactive oxygen species (ROS) play a critical role in the progression of mitochondria-related diseases. A novel insulin sensitizer drug candidate, BGP-15, has been shown to have protective effects in several oxidative stress-related diseases in animal and human studies. In this study, we investigated whether the protective effects of BGP-15 are predominantly via preserving mitochondrial integrity and reducing mitochondrial ROS production. BGP-15 was found to accumulate in the mitochondria, protect against ROS-induced mitochondrial depolarization and attenuate ROS-induced mitochondrial ROS production in a cell culture model, and also reduced ROS production predominantly at the complex I-III system in isolated mitochondria. At physiologically relevant concentrations, BGP-15 protected against hydrogen peroxide-induced cell death by reducing both apoptosis and necrosis. Additionally, it attenuated bacterial lipopolysaccharide (LPS)-induced collapse of mitochondrial membrane potential and ROS production in LPS-sensitive U-251 glioma cells, suggesting that BGP-15 may have a protective role in inflammatory diseases. However, BGP-15 did not have any antioxidant effects as shown by *in vitro* chemical and cell culture systems. These data suggest that BGP-15 could be a novel mitochondrial drug candidate for the prevention of ROS-related and inflammatory disease progression.

Introduction

Mitochondria play a critical role in the progression of oxidative stress-related diseases, as excess mitochondrial metabolites cause mitochondrial hyperpolarization and production of reactive oxygen species (ROS) [1]. Extramitochondrial ROS can amplify mitochondrial ROS production leading to mitochondrial damage and cell death [2–4]. In addition, mutations in the mitochondrial genome can lead to excess ROS production, which promotes the development of several diseases, in addition to accelerated aging [5–8]. Mitochondrial membrane

Competing Interests: The authors have declared that no competing interests exist.

potential ($\Delta\Psi$) lowering agents such as uncouplers and ROS reducing agents (e.g. superoxide dismutase, N-acetylcysteine and lipoic acid) prevent the development of several diseases including hypertriglyceridemia, fatty liver disease, insulin resistance and sepsis [9–13]. However, antioxidant therapy has previously failed in human clinical studies despite the supporting cell culture and animal experiments [14,15]. This failure could be explained by the requirement for antioxidants to be present at millimolar concentrations in order to significantly decrease oxidative damage [16]. Furthermore, oxidative stress activates mitogen-activated protein kinase (MAPK) and tyrosine kinase signaling pathways [17,18], nuclear factor- κ B (NF- κ B), activator protein-1 (AP-1) and hypoxia-inducible factor-1 (HIF-1 α) transcription factors, cell cycle proteins [19] and ion channels [20,21]. Therefore, it may be more favorable to prevent those processes, which lead to disease-promoting alterations in the signaling pathways, rather than attempting to reduce ROS levels using antioxidants.

BGP-15 (O-[3-piperidino-2-hydroxy-1-propyl]-nicotinic amidoxime) has a wide range of cytoprotective effects [22–25], but up to now there is no information about its affecting a known receptor or specific binding protein. In disease model systems, it has been shown to protect cells against cell death [24,26] and increased heat shock protein (HSP) expression [22,27–29], in addition to inhibiting the nuclear translocation of apoptosis-inducing factor (AIF) from the mitochondria [24] and inhibits c-Jun N-terminal kinase (JNK) [23,29,30] and p38 MAPK [23] activation. It has also been shown that BGP-15 is an insulin sensitizer in an olanzapine-induced metabolic disorder in human phase II studies, and also in insulin-resistant patients [27,31,32]. This insulin sensitizing effect was suggested to be related to its HSP co-inducer effect [27,31,32], however, no molecular mechanism has been presented yet for the regulation of HSP expression by BGP-15.

Because of the importance of mitochondria in regulating cell death in ROS-related diseases [1,33], in this study, we investigated whether the protective effects of BGP-15 rely on the preservation of mitochondrial integrity and reduction of mitochondrial ROS production.

Materials and Methods

Materials

All chemicals for cell culture studies were purchased from PAA Laboratories (Cölbe, Germany) and Gibco/Invitrogen (Carlsbad, CA, USA). The fluorescent dyes JC-1, fluorescein-conjugated annexin V (annexin V-FITC), propidium iodide (PI), Hoechst 33342, rhodamine 123 (R123), dihydrorhodamine 123 (DHR123) and MitoSOX were obtained from Molecular Probes (Carlsbad, CA, USA). BGP-15 was a gift from N-Gene (New York, NY, USA). All remaining chemicals were purchased from Sigma Aldrich Co. (Budapest, Hungary). All reagents were of the highest purity commercially available.

Cell cultures

WRL-68 (HeLa derivative), H9c2 (rat heart myoblast) and U-251 MG (human malignant glioblastoma; formerly known as U-373) cells were purchased from the European Collection of Cell Cultures. The cell lines were grown in a humidified 5% CO₂ atmosphere at 37°C. WRL-68 cells were cultured in Eagle's minimum essential medium, and H9c2 and U-251 MG cells in Dulbecco's modified Eagle's medium. All media contained an antibiotic solution (1% penicillin and streptomycin mixture) and 10% bovine serum. Cells were passaged every 3 days. Cells were seeded at a starting density of 2×10^4 cells/well in a 96-well plate for the viability and ROS production assays, or at a density of 1×10^5 cells/well in a 6-well plate for fluorescent microscopy.

Animals

Wistar rats were purchased from Charles River Hungary Breeding Ltd. (Budapest, Hungary). The animals were kept under standard conditions and tap water and rat chow were provided *ad libitum*. The investigation conformed to the Guide for the Care and Use of Laboratory Animals, published by the US National Institutes of Health (NIH Publication no. 85–23, revised in 1996), and was approved by the Animal Research Review Committee of the University of Pécs, Hungary.

Isolation of rat liver mitochondria

Rats were sacrificed by decapitation under isoflurane (AbbVie Ltd., Budapest, Hungary) anesthesia and mitochondria were isolated from the liver by differential centrifugation, as described in a standard protocol [34]. All isolated mitochondria were purified by Percoll density gradient centrifugation [35], and mitochondrial protein concentrations were determined using the biuret method with bovine serum albumin as a standard.

Determination of membrane potential ($\Delta\Psi$) in isolated rat liver mitochondria

$\Delta\Psi$ was monitored by measuring R123 fluorescence upon its release from the mitochondria. Fluorescence was measured using a fluorescence spectrometer (LS-50B; Perkin-Elmer; gift from Alexander von Humboldt Foundation, Bonn, Germany) at an excitation wavelength of 494 nm and an emission wavelength of 525 nm. Briefly, 1 mg protein/mL mitochondria were preincubated in assay buffer (70 mM sucrose, 214 mM mannitol, 20 mM N-2-hydroxyethyl piperazine-N'-2-ethanesulfonic acid, 5 mM glutamate, 0.5 mM malate and 0.5 mM phosphate) containing 1 μM R123 for 60 seconds. Alterations in $\Delta\Psi$ were induced by the addition of BGP-15 at the indicated concentrations.

Mitochondrial uptake of BGP-15

Mitochondrial uptake of BGP-15 (50 μM) was determined in 5 mM Tris buffer (pH 7.5) containing 150 mM KCl, 1 mM EDTA and 2.5 mg mitochondrial protein in 800 μl volume, in addition to 10 μM glucose-6-phosphate as a standard in order to determine the void volume. Uncoupling was induced with 50 μM 2,4-dinitrophenol. After an incubation of 10 min, the mitochondria was centrifuged at 20000 g, was washed then lysed in 800 μl of ethanol-water 1:1 solution, and centrifuged at 20000 g. Aliquots of the clear supernatant were freeze-dried, and taken up in aqueous formic acid solution (0.1%).

HPLC-MS/MS analysis

Aliquots (5 μl) of the samples were injected into the HPLC-MS system (Dionex Ultimate 3000 UHPLC, Q-Exactive HRMS; Thermo Fisher Scientific, Bremen, Germany). Liquid chromatographic separation was carried out using a Kinetex (Gen-Lab Kft., Budapest, Hungary) 2.6 μm C18 100 \AA HPLC column (100 \times 2.1 mm), which was maintained at 30°C. The mobile phase used was (A) aqueous formic acid solution (0.1%) with (B) acetonitrilic formic acid solution (0.1%). The flow rate was set to 300 $\mu\text{l}/\text{minute}$. The initial gradient conditions were set to 5% B and held for 3 minutes, then B was increased linearly until it had reached 80% after 12 minutes. The initial conditions were reached after 2 minutes, then the column was equilibrated for 8 minutes. The mass spectrometer was equipped with a heated electrospray ion source which was operated in the negative ion mode. The spray voltage was set to 3.5 kV, the capillary temperature set to 300°C and the temperature of the probe heater was set to 50°C. The S-lens

RF level was set to 70. Mass range was set to m/z 150–1500. Data analysis was performed using the Thermo Xcalibur (version 2.2 SP1.48) software. Ion intensities were determined by matching them to a BGP-15 calibration curve.

Cell viability assay

The viability of WRL-68 cells after the different treatments were evaluated by sulforhodamine B (SRB) assay. The method is customarily used for cell density determination in cytotoxicity screening, based on the measurement of cellular protein content. The assay was performed according to the method described by Papazisis and colleagues [36], with some modifications. The culture medium was aspirated prior to fixation of the cells by the addition of 200 μL of cold 10% trichloroacetic acid. After a 20 minute incubation at 4°C, cells were washed twice with deionized water. Microplates were then left to dry at room temperature for at least 24 hours. When dried, the cells were stained with 200 μL of 0.1% SRB dissolved in 1% acetic acid for at least 20 minutes at room temperature, after which they were washed four times with 1% acetic acid to remove any unbound stain molecules. The plates were left to dry at room temperature. The bound SRB was solubilized with 200 μL of 10 mM unbuffered Tris-base solution and plates were left on a plate shaker for at least 10 minutes. Absorbance was measured using the GloMax Multi Detection System (Promega, USA) at 560 nm in addition to the background measurement at 620 nm. The optical density values were defined as the absorbance of each individual well minus the blank value (the mean optical density of the background control wells). All experiments were run in at least eight replicates and each measurement was repeated three times.

Determination of reactive oxygen species in cell culture

Intracellular ROS (peroxynitrite, $\bullet\text{OH}$ and iron + hydrogen peroxide (H_2O_2)) were determined by using two separate approaches, fluorescence microscopy and quantitative determination of ROS-evoked fluorescence intensities by a plate reader. WRL-68 or U-251 MG cells were seeded to glass coverslips and cultured at least overnight before the experiment. WRL-68 cells were transiently transfected with mitochondria directed enhanced red fluorescent protein (mERFP). The next day, cells were washed twice with phosphate buffered saline (PBS), and were treated as it is described in the Results and the figure legends. Then, the medium was replaced to a fresh one containing 1 μM of the oxidation-sensitive DHR123 fluorescent dye, and the incubation continued for an additional 15 minutes to allow for oxidation of DHR123 by the endogenous ROS.

The fluorescence of mERFP and the oxidized DHR123 was excited at 615 and 485 nm and the evoked emission was measured at >650 and 525 nm, respectively using a Nikon Eclipse Ti-U fluorescent microscope (Auro-Science Consulting Ltd., Budapest, Hungary) equipped with a Spot RT3 camera using a 60x objective lens. The nuclei of U-251 MG cells were labelled using Hoechst 33342 (1 $\mu\text{g}/\text{mL}$) dye, which were excited at 350 nm and read at 460 nm emission wavelengths. All experiments were repeated three times.

Alternatively, WRL-68, H9c2 or U-251 MG cells were seeded in 96-wells plates and kept in Krebs-Henseleit buffer containing 10% fetal bovine serum (FBS). The WRL-68 and H9c2 cells were treated with either H_2O_2 for 30 minutes alone or with increasing concentrations of BGP-15 in the absence or presence of 20 μM MitoTEMPO (Sigma Aldrich Co.) After 30 minutes, DHR123 (1 μM) was added to the medium and R123 formation was detected after 15 minutes with the GloMax Multi Detection System (excitation wavelength was 490 nm and emission wavelength was between 510–570 nm). The U-251 MG cells were treated with either LPS for 30 minutes alone or with 50 μM BGP-15 in the absence or presence of 20 μM MitoTEMPO

(Sigma Aldrich Co.). Superoxide anions were detected by the addition of MitoSOX (0.3 μM) fluorescent dye. Fluorescence of oxidized MitoSOX was excited at 365 nm and the evoked emission was measured at 410–460 nm by the GloMax Multi Detection System. All experiments were run in six replicates and each measurement was repeated three times.

Determination of mitochondrial production of reactive oxygen species

Mitochondria (100 $\mu\text{g}/\text{mL}$) were dissolved in a buffer solution containing 20 mM 3-(N-morpholino)propanesulfonic acid (MOPS) and 314 mM sucrose (pH 7.4), which also contained either malate (5 mM) and glutamate (5 mM) or succinate (5 mM). ROS production was determined by the oxidation of DHR123 (1 μM) to R123, as measured by a fluorescence spectrometer at an excitation wavelength of 494 and an emission wavelength of 525 nm, under continuous mixing at 30°C. ROS production was localized to respiratory complexes by either blocking the electron flow with antimycin A (10 μM) where glutamate (5 mM) and malate (5 mM) were used as substrates in order to localize ROS production to complex I, or by blocking electron flow with potassium cyanide (1 mM) where succinate was used as the substrate to localize ROS production to complex III. The antioxidant capacities of BGP-15 were determined by the chemical oxidation of DHR123 (1 μM ; excitation wavelength was 494 nm and emission wavelength was 525 nm) to R123. In these systems, we used either 500 μM H_2O_2 or 50 μM H_2O_2 plus 1 μM Fe^{2+} -EDTA.

Construction of mitochondria directed enhanced red fluorescent protein (mERFP; MitoRed)

The mERFP-expressing plasmid was constructed by firstly amplifying the mitochondrial targeting sequence by polymerase chain reaction from the cytochrome c oxidase subunit VIIIa (COX8A) gene (RZPD). The amplified sequence was then inserted into pDsRed-Monomer-N1 mammalian expression plasmid (Clontech-Takara Bio Europe; Saint-Germain-en-Laye, France) between the XhoI and HindIII restriction sites.

JC-1 assay for fluorescent microscopy

$\Delta\Psi$ was measured using the $\Delta\Psi$ specific fluorescent probe, JC-1. WRL-68 or U-251 MG cells were seeded to glass coverslips and cultured at least overnight before the experiment. After the indicated treatment, cells were washed twice in ice-cold PBS, then incubated for 15 minutes at 37°C in modified Krebs-Henseleit solution containing 100 ng/mL of JC-1. When excited at 490 nm, the dye emits either green fluorescence at a low $\Delta\Psi$ or red fluorescence at a high $\Delta\Psi$. Following incubation, the cells were washed once with modified Krebs-Henseleit solution, then visualized by a Nikon Eclipse Ti-U fluorescent microscope which was equipped with a Spot RT3 camera, using a 40x objective lens with epifluorescent illumination. All experiments were repeated three times.

Tetramethylrhodamine methyl ester (TMRM) assay

WRL-68 cells were seeded in 96-wells plates, kept in Krebs-Henseleit buffer containing 10% fetal bovine serum (FBS), then treated with either H_2O_2 alone or with BGP-15 for 3 hours. In a separate experiment, U-251 MG cells were treated with either LPS for 60 minutes alone or with 50 μM BGP-15. Then, the medium was replaced with Krebs-Henseleit solution containing TMRM (50 nM), a cationic, cell-permeant, red fluorescent dye. After 15 minutes incubation, excess dye was washed off and the fluorescence was measured by the GloMax Multi Detection System (excitation wavelength was 525 nm and emission wavelength was between

580–640 nm). To assess aspecific adsorption of the dye, the fluorescence signal was remeasured after addition of 1 μM carbonyl cyanide 4-(trifluoromethoxy)phenylhydrazone (FCCP) a mitochondrial uncoupling agent. $\Delta\Psi$ was calculated as the difference of fluorescence signal before and after FCCP-treatment. All experiments were run in six replicates and the measurement was repeated three times.

Identification of the type of cell death by annexin V/PI staining

Cell death was detected by the GloMax Multi Detection System after annexin V-FITC/PI double staining. WRL-68 cells were seeded at 2×10^4 cells/well in a 96-well, then cultured at least overnight before the experiment. After subjecting the cells to the indicated treatment, cells were washed once in PBS and then incubated in modified Krebs-Henseleit solution containing FITC-conjugated annexin V and PI, according to the manufacturer's protocol. Following incubation, the cells were washed once with modified Krebs-Henseleit solution. Then green fluorescence signal (annexin V-FITC) was detected with the GloMax Multi Detection System (excitation wavelength was 490 nm and emission wavelength was 518 nm). The red fluorescence signal (PI) was excited at 525 nm and the evoked emission was measured at 617 nm. All experiments were run in six replicates and each measurement was repeated three times.

Statistical analyses

All data were expressed as the mean \pm standard error of mean (SEM) of the replicate measurements. Differences between treatment groups were determined by ANOVA with a post-hoc test. A Student's t-test was used to compare the mean values from the two groups. Differences were regarded as significant when the P-value was < 0.05 .

Results

Mitochondrial uptake of BGP-15

BGP-15 possesses a delocalized positive charge, therefore, it is suitable for determining membrane potential-dependent uptake. Accordingly, we measured BGP-15 uptake in both energized and uncoupled mitochondria. The void volume was determined using glucose-6-phosphate, a substance that cannot permeate the mitochondrial inner membrane. When incubated in the presence of 50 μM BGP-15 for 10 minutes, the energized mitochondria took up more than 85% of the drug (Fig 1A), suggesting that the majority of BGP-15 was taken up in a membrane potential-dependent manner. Complete uncoupling by dinitrophenol significantly decreased BGP-15 uptake (Fig 1A). However, even the uncoupled mitochondria were found to bind more BGP-15 than the amount corresponding to the void volume, indicating that BGP-15 interacted with the mitochondrial proteins and/or lipids. Extrapolating this finding to physiological conditions, it is likely that more than 90% of BGP-15 had accumulated in the mitochondria, which raises the possibility that BGP-15 may protect cells via mitochondrial mechanisms.

Effect of BGP-15 on mitochondrial membrane potential ($\Delta\Psi$)

Since mild uncoupling of the mitochondria could be beneficial in insulin resistance [37], we tested the effect of BGP-15, an insulin sensitizer [27,31,32] on $\Delta\Psi$ by using a $\Delta\Psi$ -sensitive dye (R123) in isolated rat liver mitochondria. Treatment with BGP-15 alone resulted in a concentration-dependent decrease in $\Delta\Psi$ at millimolar concentrations (Fig 1B). The effect on $\Delta\Psi$ of submillimolar concentrations of BGP-15 was below the detection limit (Fig 1B) suggesting

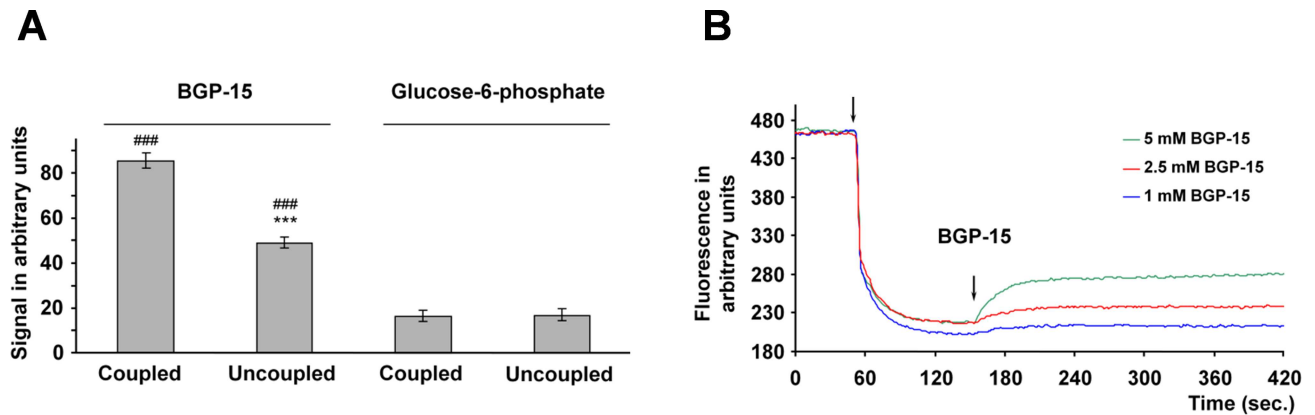


Fig 1. BGP-15 is enriched in mitochondria and reduces membrane potential ($\Delta\Psi$) in isolated mitochondria. (A) Membrane potential enhanced the mitochondrial uptake of BGP-15 (50 μM) in isolated rat liver mitochondria. Uncoupling was found to occur with 50 μM 2,4-dinitrophenol. Data are presented as the mean \pm SEM of three independent experiments. *** $P < 0.001$ compared to coupled mitochondria, ### $P < 0.001$ compared to the glucose-6-phosphate signal. (B) Mitochondrial membrane potential was monitored by measuring the fluorescence intensity of R123, a cationic fluorescent dye. Isolated rat liver mitochondria, represented by the first arrow, took up the dye in a voltage-dependent manner, resulting in fluorescent quenching. At the second arrow either 1 mM, 2.5 mM or 5 mM BGP-15 was added. A representative plot of three independent concurrent experiments is presented.

doi:10.1371/journal.pone.0169372.g001

that at the 50 μM concentration we have used throughout the study the drug could hardly cause any mitochondrial depolarization.

Under cell culture conditions, we analyzed the effect of BGP-15 on $\Delta\Psi$ using JC-1, a cell-permeable voltage-sensitive fluorescent mitochondrial dye. JC-1 emits red fluorescence in highly energized mitochondria (aggregated dye), while depolarized mitochondria emit green fluorescence (monomer dye). WRL-68 cells were incubated in the presence of 50 μM H_2O_2 , either alone or together with 50 μM BGP-15, for 3 hours before loading with 100 ng/mL JC-1 dye for 15 minutes, after which fluorescent microscopy was performed. In the control and BGP-15-treated cells, fluorescence microscopy showed strong red fluorescence and weak green fluorescence, which indicates a high $\Delta\Psi$ in mitochondria (Fig 2A and 2B). The addition of H_2O_2 to cells facilitates the depolarization of mitochondria, resulting in weaker red fluorescence and stronger green fluorescence (Fig 2A and 2B). When H_2O_2 was added to cells in addition to BGP-15, the depolarization of mitochondria was found to be weaker, as shown by a smaller decrease in red fluorescence and weaker increase in green fluorescence (Fig 2A and 2B). This was also demonstrated by the accurate (mitochondrial) labelling of red fluorescence in the cells treated with both H_2O_2 and BGP-15, and in cells treated with H_2O_2 only (Fig 2A). The quantitative assessment revealed that BGP-15 did not affect the $\Delta\Psi$ at a concentration of 50 μM (Fig 2B); however, it was found to reduce the H_2O_2 -induced depolarization of the mitochondrial membrane (Fig 2B), suggesting that even at this concentration it protected the $\Delta\Psi$ against oxidative stress. We have obtained identical results when we assessed $\Delta\Psi$ by using TMRM, another membrane potential sensitive fluorescent dye and a quantitative, plate reader-based method (Fig 2C).

BGP-15 attenuates mitochondrial production of reactive oxygen species

Destabilization of the mitochondrial membrane systems has previously been reported to contribute to mitochondrial ROS production [38]. As BGP-15 was shown to protect the mitochondrial membrane system under oxidative stress (Fig 2A, 2B and 2C), we assumed that it could also affect mitochondrial ROS production. To investigate this possibility, WRL-68 cells were transfected with mERFP to label the mitochondria, and then incubated in the presence or absence of 50 μM H_2O_2 for 30 minutes. Fresh medium containing DHR123 was added, and

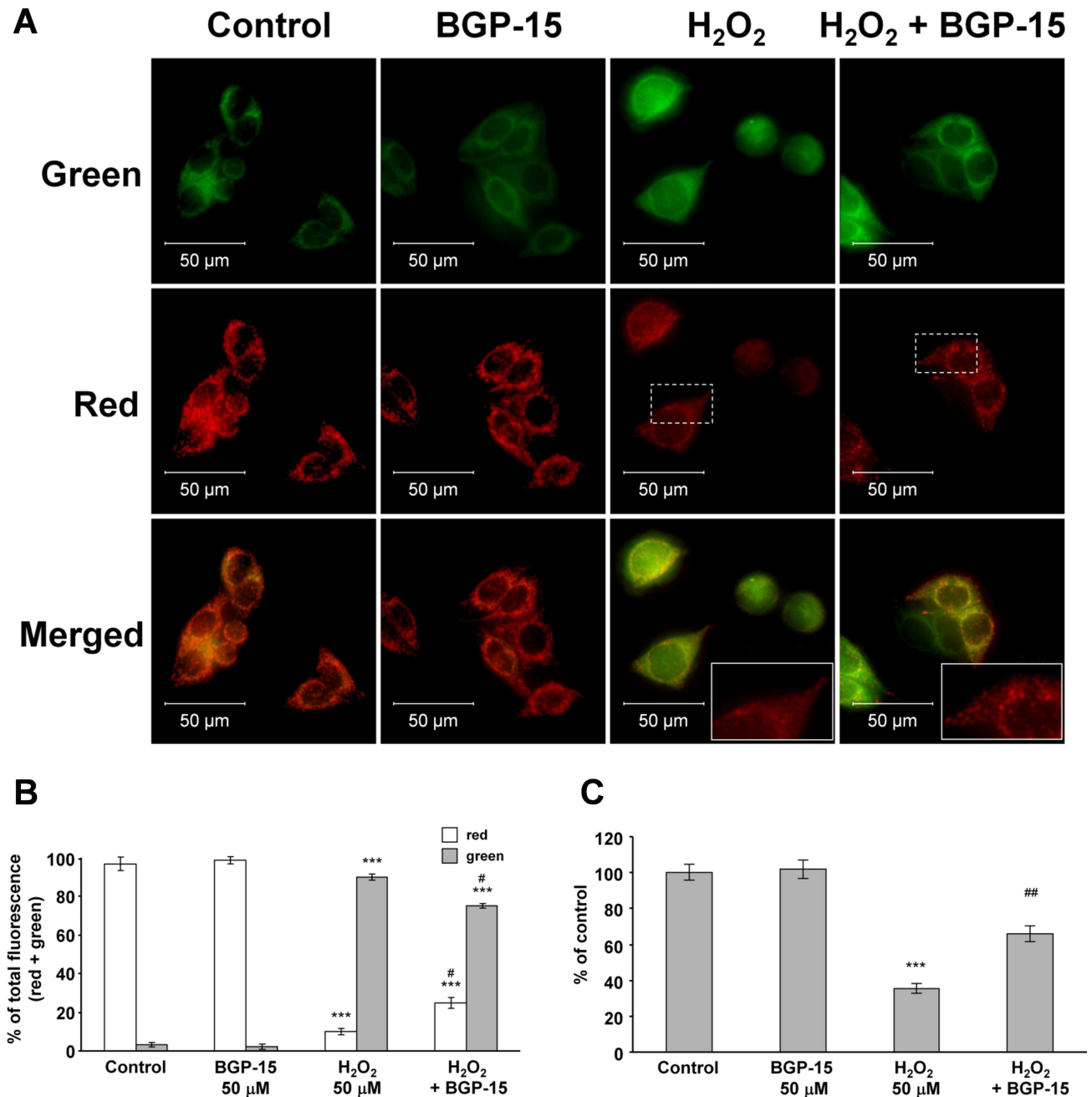


Fig 2. BGP-15 protects against reactive oxygen species-induced depolarization of mitochondria in WRL-68 cells, as determined by JC-1 and TMRM. (A) Effect of BGP-15 on H₂O₂-induced mitochondrial membrane depolarization in WRL-68 cells. Cells were exposed to 50 μM H₂O₂ in the absence or presence of 50 μM BGP-15 for 3 hours, then stained with 100 ng/mL of JC-1, a membrane potential-sensitive fluorescent dye. The dye was loaded, and after a 15 minute incubation fluorescent microscopic images were taken using both the red and green channels. The inserts show the homogenous red fluorescence in H₂O₂-treated cells, and the dotted labelling represents the H₂O₂ + BGP-15 treated cells, showing that BGP-15 protected the mitochondrial integrity in the presence of H₂O₂. Inserts are expanded from the area indicated by dashed rectangles. Representative merged images of three independent experiments are presented. (B) Quantitative analysis of mitochondrial depolarization induced by H₂O₂ (50 μM) and its reduction by BGP-15 (50 μM) in WRL-68 cells. Results are presented as the mean ± SEM. ***P < 0.001 compared to control cells, #P < 0.05 compared to H₂O₂-treated cells. (C) Effect of BGP-15 on H₂O₂-induced mitochondrial membrane depolarization in WRL-68 cells. Cells were treated with 50 μM H₂O₂ in the absence or presence of 50 μM BGP-15 for 3 hours, then stained with 50 ng/mL of TMRM, a cationic, cell-permeant, red fluorescent dye. After a 15 minutes incubation fluorescent signal was measured by the GloMax Multi Detection System, then remeasured after the application of 1 μM FCCP ΔΨ was calculated as the difference of fluorescence signal before and after FCCP-treatment. Data are presented as the mean ± SEM of three independent experiments. **P < 0.01, ***P < 0.001 compared to control cells; ##P < 0.01 compared to H₂O₂-treated cells.

doi:10.1371/journal.pone.0169372.g002

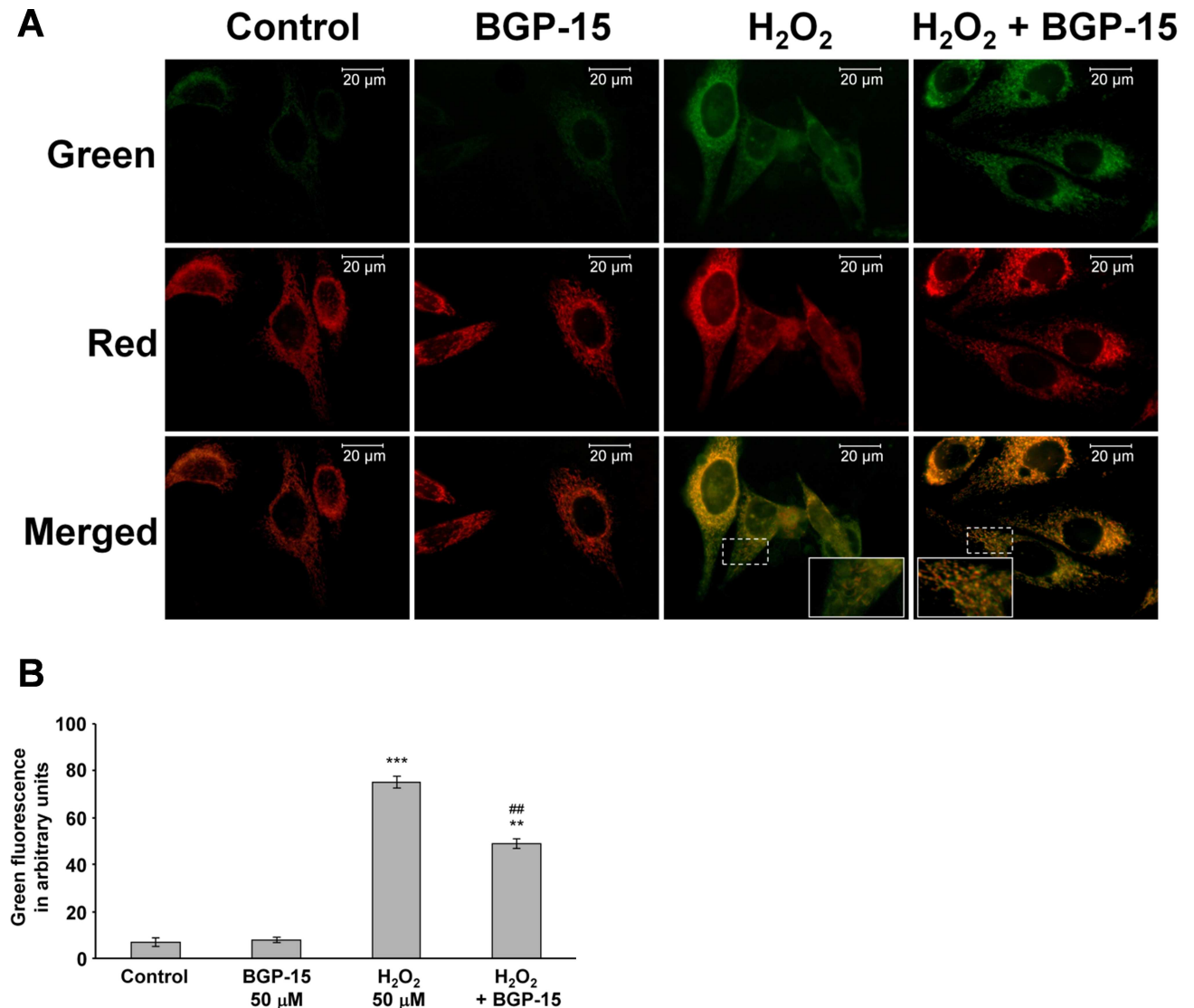


Fig 3. BGP-15 attenuates hydrogen peroxide-induced mitochondrial reactive oxygen species production in WRL-68 cells. (A) Effect of hydrogen peroxide and BGP-15 pretreatment (for 30 minutes) on mitochondrial ROS production, as determined by the oxidation of the mitochondrial enriched dye from DHR123 to R123 in WRL-68 cells that had been labelled with mitochondrial directed red fluorescent protein. High magnification fluorescent microscopic images show the different localization of the produced R123. Inserts are expanded from the area indicated by dashed rectangles. (B) Quantification of R123 production. Data are presented as the mean \pm SEM of three independent experiments. ** $P < 0.01$ and *** $P < 0.001$ compared to control cells; ## $P < 0.01$ compared to H₂O₂-treated cells.

doi:10.1371/journal.pone.0169372.g003

after 15 minutes the amount of green R123 fluorescence, as a result of oxidation from non-fluorescent DHR123, was measured by fluorescence microscopy. BGP-15 at a concentration of 50 μ M did not affect the weak green fluorescence of mitochondrial localization (Fig 3A). However, its addition did reduce the substantial increase in green fluorescence induced by the H₂O₂ treatment (Fig 3A and 3B). Furthermore, oxidative stress-induced green fluorescence was diffuse in the absence of BGP-15, whereas it was predominantly localized to the mitochondria in the presence of BGP-15 (Fig 3A inserts). Although the R123 fluorescence could result from cytosolically produced R123 taken up to the mitochondria and DHR123 oxidized by mitochondrial ROS, we think that R123 fluorescence reflected mitochondrial ROS production, as it was predominantly localized to the mitochondria when $\Delta\psi$ was not compromised.

As found previously (N-Gene Inc., personal communication), BGP-15 serum concentration does not exceed 25 nmoles/mL. Therefore, we analyzed the effect of BGP-15 on ROS-induced ROS production at concentrations ranging between 1–50 μM under cell culture conditions using a quantitative, plate-reader based method instead of microscopy. BGP-15 had a concentration-dependent inhibitory effect on the ROS-induced ROS production in WRL-68 cells, which was significant even at the 1 μM concentration (Fig 4A). In order to show that these observations apply to other cell lines too, we analyzed the effect of BGP-15 on H_2O_2 -induced ROS production in H9c2 cardiomyocytes using the same system. Fig 4B shows that BGP-15 decreased the ROS-induced ROS production in H9c2 cardiomyocytes in a concentration-dependent manner (1–50 μM range).

In order to study whether the observed antioxidant effect of BGP-15 have resulted from scavenging property of the drug, we determined its effect on 500 μM H_2O_2 - (Fig 4C) and H_2O_2 and Fe^{2+} -EDTA (Fenton reaction, Fig 4D)-induced DHR123 oxidation in cell-free systems. Since BGP-15 did not affect DHR123 oxidation in any of these systems (Fig 4C and 4D) its antioxidant effect could not result from scavenging property of the drug. DHR123 can be oxidized predominantly by peroxynitrite and hydroxyl radicals that are formed in the Fenton reaction; however, it cannot detect superoxide. Therefore, we wanted to investigate whether BGP-15 could reduce the production of mitochondrial superoxide. To this end, we determined H_2O_2 -induced ROS production in WRL-68 (Fig 4E) and H9c2 (Fig 4F) cells using the mitochondria-targeted redox fluorescent dye MitoSOX [39] instead of DHR123. Essentially, the results were comparable to those we obtained with DHR123 (Fig 4A and 4B vs. 4E and 4F). Furthermore, we repeated these experiments in the presence of the mitochondria-targeted antioxidant MitoTEMPO [40]. MitoTEMPO abolished H_2O_2 -induced ROS production in all groups (Fig 4E and 4F) indicating mitochondrial localization of the BGP-sensitive ROS production. These data provide evidence that BGP-15 reduced mitochondrial superoxide production in both WRL-68 cells (Fig 4E) and H9c2 cardiomyocytes (Fig 4F).

Effect of BGP-15 on mitochondrial reactive oxygen species production in isolated mitochondria

In order to provide unequivocal evidence for the mitochondrial mechanism underlying the inhibitory effect of BGP-15 on ROS-induced ROS production, we used Percoll gradient-purified mitochondria. We determined the effect of BGP-15 on the oxidation of DHR123 in the presence of glutamate and malate as substrates, with antimycin A for complex III inhibition, and showed the production of ROS in complex I and the complex III cytochrome b region of the respiratory chain. We found that the addition of BGP-15 at concentrations of 10 to 50 μM had a ~50% inhibitory effect on mitochondrial ROS production (Fig 4G). These results suggest that the target of BGP-15 was between complex I and the complex III cytochrome b region of the respiratory chain [41].

BGP-15 was also shown to reduce mitochondrial ROS production in the presence of succinate as a substrate and CN^- as the cytochrome oxidase inhibitor (Fig 4H), however, to a much smaller extent. This suggests that BGP-15 affected ROS production mainly via complex I and the cytochrome b part of complex III. These data show that BGP-15 has a specific inhibitory effect on mitochondrial ROS production at the complex I and complex III cytochrome b region of the respiratory chain, which is not an antioxidant effect.

Effect of BGP-15 on reactive oxygen species-induced cell death

As BGP-15 was shown to protect against H_2O_2 -induced mitochondrial damage in addition to reducing mitochondrial ROS production, we analyzed its effects on H_2O_2 -induced cell death.

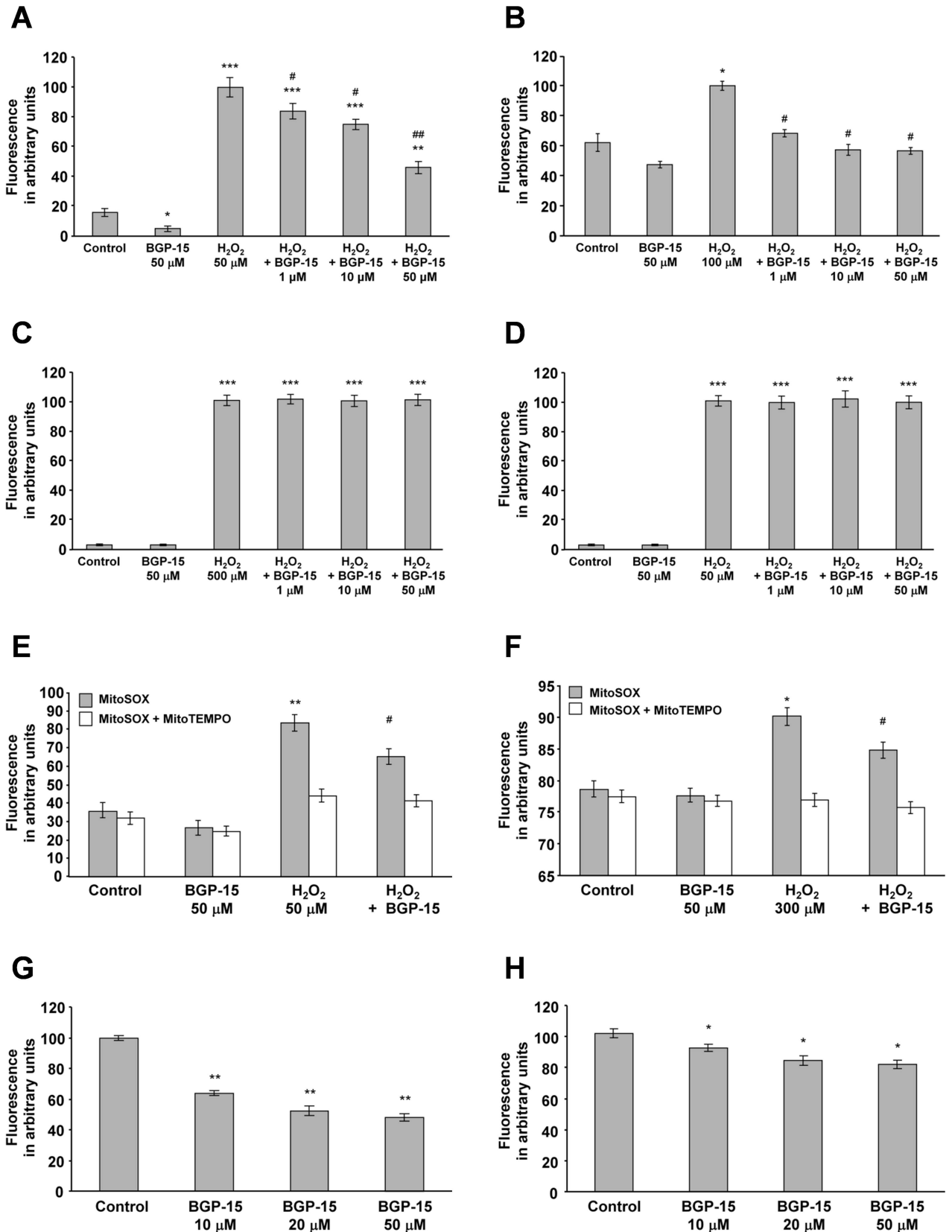


Fig 4. BGP-15 attenuates oxidative stress-induced DHR123 oxidation and superoxide formation in complexes I-III in WRL-68 and H9c2 cells. (A) Effect of BGP-15 on oxidative stress-induced DHR123 oxidation in WRL-68 cells. Data are presented as the mean ± SEM of three independent experiments. *P < 0.05, **P < 0.01 and ***P < 0.001 compared to control cells; #P < 0.05 and ##P < 0.01 compared to H₂O₂-treated cells. (B) Effect of BGP-15 on oxidative stress-induced DHR123 oxidation in H9c2 cardiomyocytes. Results are presented as the mean ± SEM of three independent experiments. *P < 0.05 compared to control cells, #P < 0.05 compared to H₂O₂-treated cells. (C) BGP-15 in chemical reactions does not inhibit DHR123 oxidation induced by H₂O₂ (500 μM). Data are presented as the mean ± SEM of three independent experiments. ***P < 0.001 compared to control group. (D) BGP-15 in chemical reactions does not inhibit DHR123 oxidation induced by H₂O₂ (50 μM) and Fe(II)-EDTA (66 μM) (Fenton reaction system). Results are presented as the mean ± SEM of three independent experiments. ***P < 0.001 compared to the control group. (E) Effect of BGP-15 on oxidative stress-induced superoxide production in WRL-68 cells in the absence or presence of 20 μM MitoTEMPO as determined by MitoSOX (0.3 μM). Data are presented as the mean ± SEM of three independent experiments. *P < 0.05, **P < 0.01 compared to control cells, #P < 0.05 compared to H₂O₂-treated cells. (F) Effect of BGP-15 on the oxidative stress-induced superoxide production in H9c2 cardiomyocytes in the absence or presence of 20 μM MitoTEMPO as determined by MitoSOX (0.3 μM). Results are presented as the mean ± SEM of three independent experiments. *P < 0.05 compared to control cells, #P < 0.05 compared to H₂O₂-treated cells. (G) Effect of BGP-15 on mitochondrial DHR123 oxidation using glutamate-malate as substrate and with complex III inhibited by antimycin A. Data are presented as the mean ± SEM of three independent experiments. **P < 0.01 compared to the control group. (H) Effect of BGP-15 on mitochondrial DHR123 oxidation using succinate as substrate and with complex IV inhibited by CN⁻. Results are presented as the mean ± SEM of three independent experiments. *P < 0.05 compared to the control group.

doi:10.1371/journal.pone.0169372.g004

We treated WRL-68 cells with 50 μM H₂O₂ in the presence of 0–50 μM BGP-15 for 24 hours, then determined cell survival using the SRB method. We found that, consistent with its aforementioned protective effects (Figs 2–4), BGP-15 increased cell survival in a concentration-dependent manner (Fig 5A). To further investigate the underlying mechanism behind the cytoprotective effect of BGP-15, we determined the proportion of apoptosis and necrosis using annexin V-conjugated fluorescein-isothiocyanate and PI staining, which was performed after exposing the cells to 50 μM H₂O₂ in the presence or absence of 50 μM BGP-15 for 24 hours, which was then measured by the GloMax Multi Detection System. We found that under these conditions, H₂O₂-induced cell death was predominantly necrotic and only approximately 10% of the cells died by apoptosis (Fig 5B). BGP-15 significantly reduced both apoptotic and necrotic cell death, which was likely to be a result of mitochondrial protection.

BGP-15 protects against LPS-induced mitochondrial depolarization

It has been shown that the U-251 MG human malignant glioblastoma cell line contains components of the LPS signaling pathway [42], and LPS-induced signaling has been shown to be

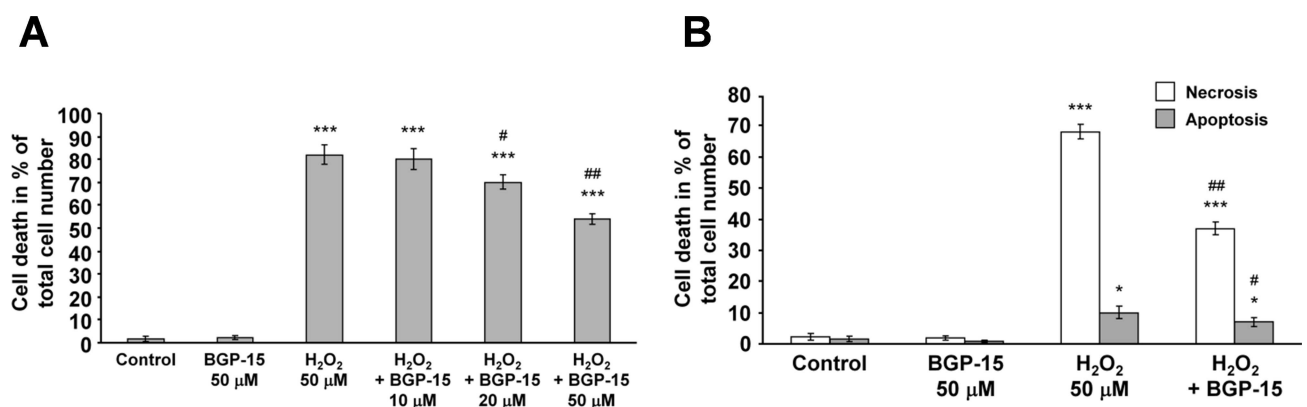


Fig 5. BGP-15 attenuates reactive oxygen species-induced apoptotic and necrotic cell death in WRL-68 cells. (A) BGP-15 protects against H₂O₂-induced cell death (sulforhodamine B assay). Data are presented as the mean ± SEM of eight independent experiments. ***P < 0.001 compared to control cells; #P < 0.05 and ##P < 0.01 compared to H₂O₂-treated cells. (B) Determination of the effect of BGP-15 on H₂O₂-induced apoptosis (fluorescein-labelled annexin V) and necrosis (propidium iodide) pathways. Data are presented as the mean ± SEM of three independent experiments. *P < 0.05 and ***P < 0.001 compared to control cells; #P < 0.05 and ##P < 0.01 compared to H₂O₂-treated cells.

doi:10.1371/journal.pone.0169372.g005

important in neurodegenerative, liver and several other diseases [43,44]. Additionally, mitochondria have been reported to play an important role in LPS signaling [43–47]. Therefore, we analyzed the effect of BGP-15 on LPS-induced mitochondrial depolarization in the U-251 MG cell line. This system is much more complex than the ROS-induced depolarization because LPS induces toll-like receptor 4 (TLR4)-dependent signaling and NADPH oxidase (NOX)-dependent ROS production, thereby increasing intracellular Ca^{2+} levels [48,49]. Mitochondrial depolarization was found to be induced by the addition of 1 $\mu\text{g}/\text{mL}$ LPS for 1 hour, as determined by JC-1 staining and fluorescent microscopy (Fig 6A and 6B). We found that the addition of BGP-15 alone did not affect $\Delta\psi$, but significantly attenuated LPS-induced mitochondrial depolarization in the U-251 MG human malignant glioblastoma cells (Fig 6A and 6B). We have obtained identical results when we assessed $\Delta\Psi$ by using TMRM, another membrane potential sensitive fluorescent dye and a quantitative, plate reader-based method (Fig 6C). These data suggest that BGP-15 may play a role in inflammatory processes by a novel mitochondrial mechanism.

BGP-15 protects against LPS-induced production of reactive oxygen species

Due to the association between mitochondrial depolarization and ROS production [38], we measured LPS-induced ROS production in the U-251 MG cells. We exposed the cells to 1 $\mu\text{g}/\text{mL}$ LPS in the presence or absence of 50 μM BGP-15 for 1 hour, and then measured the fluorescence of R123 which had been oxidized from non-fluorescent DHR123 by the ROS (Fig 6D and 6E). Very low fluorescence intensities were detected in the untreated and BGP-15-treated cells, however, the addition of LPS was found to greatly induce ROS production (Fig 6D and 6E). BGP-15 reduced the LPS-induced ROS production almost to control levels (Fig 6D and 6E). Similarly to the H_2O_2 -induced ROS production, we wanted to determine the intracellular localization of the LPS-induced ROS. To this end, we repeated the previous experiment using MitoSOX instead of DHR123 and a plate-reader instead of microscopy. Essentially, the results were comparable to those we obtained with DHR123 (Fig 6D and 6E vs. 6F). Furthermore, we repeated the experiment in the presence of MitoTEMPO. MitoTEMPO abolished LPS-induced ROS production (Fig 6F) indicating mitochondrial localization of the BGP-sensitive ROS production. These data provide evidence that BGP-15 reduced LPS-induced mitochondrial superoxide production in.

Discussion

BGP-15 has been shown to have a protective effect in several disease models, including ischemic heart disease [30], Duchenne muscular dystrophy [22], neuropathy [25], cisplatin-induced kidney disease [26], glivec-induced cardiac disease [23] and paracetamol-induced liver disease [24], in addition to insulin resistance, as investigated in both animal and human studies [27, 31,32]. For all these diseases, oxidative stress and inflammatory processes play an important role in disease progression, and in several cases, mitochondrial damage is pivotal. Therefore, we studied the effect of BGP-15 on ROS- or inflammatory response-induced mitochondrial damage in cell culture models. We focused on the effects of BGP-15 on mitochondrial membrane stability and ROS production, which are critical for mitochondrial-induced signaling, energy metabolism and mitochondrial cell death pathways. Recently, it has been shown that mild mitochondrial uncoupling can be protective in several disease models, including insulin resistance [37], hypertriglyceridemia and fatty liver disease [9], and can have a regulatory role in endocrine cross-talk via the induction of fibroblast growth factor 21 and the growth hormone/insulin-like growth factor I axis [10]. However, as we found, BGP-15 exerted a mild uncoupling effect only

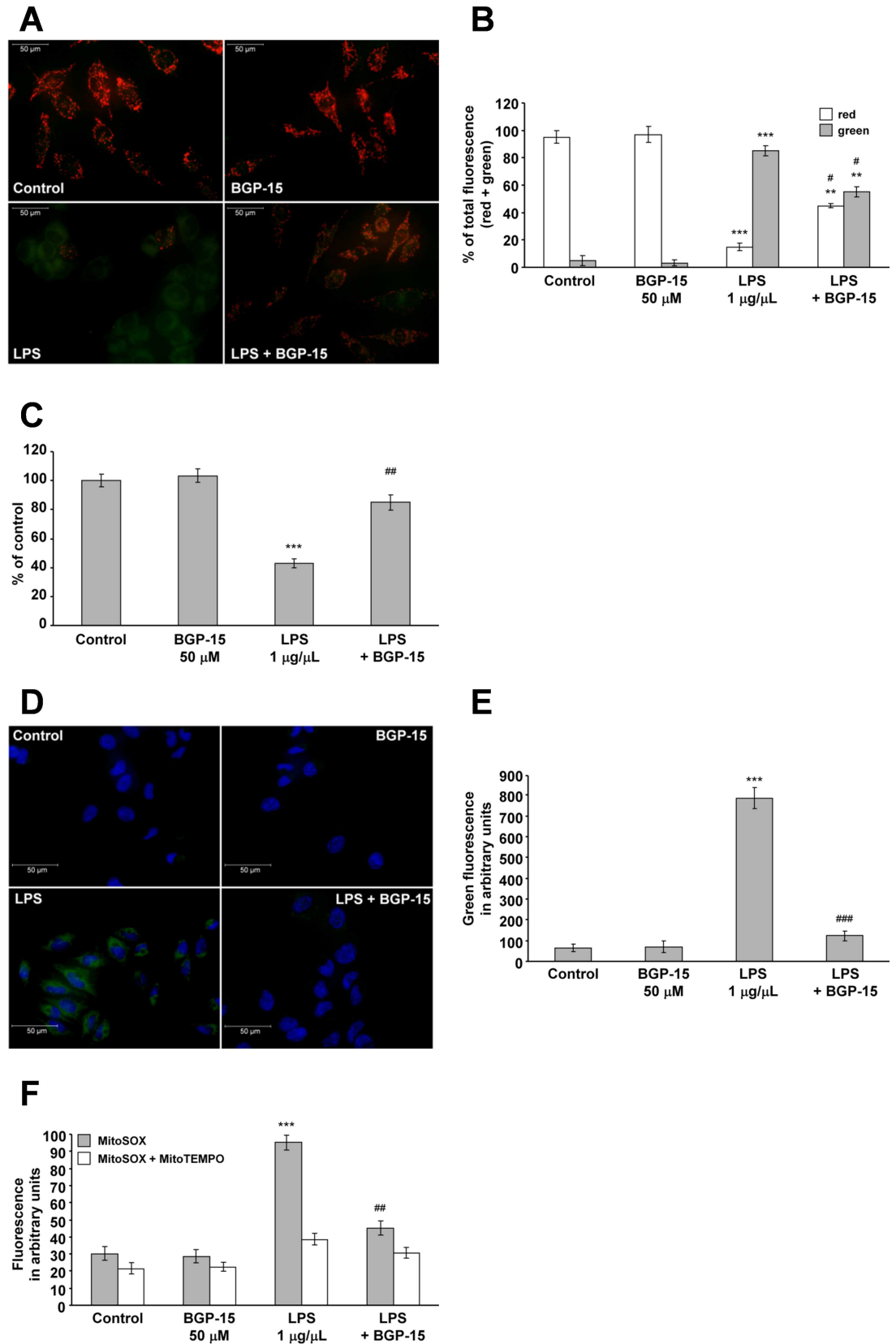


Fig 6. BGP-15 attenuates lipopolysaccharide-induced mitochondrial depolarization and production of reactive oxygen species. (A) Effect of BGP-15 on LPS-induced mitochondrial membrane depolarization in U-251 MG cells. Cells were exposed to 1 $\mu\text{g}/\text{mL}$ LPS in the absence or presence of 50 μM BGP-15 for 1 hour, then stained with 100 ng/mL of JC-1. Fluorescent microscopic images were taken using both the red and green channels. Representative merged images of three independent experiments are presented. (B) Quantitative analysis of LPS-induced (1 $\mu\text{g}/\text{mL}$) mitochondrial depolarization and its reduction by BGP-15 (50 μM) in U-251 MG cells. Results are presented as the mean \pm SEM. $^{**}P < 0.01$ and $^{***}P < 0.001$ compared to control cells; $^{\#}P < 0.05$ compared to LPS-treated cells. (C) Effect of BGP-15 on LPS-induced mitochondrial membrane depolarization in U-251 MG cells. Cells were treated with 1 $\mu\text{g}/\text{mL}$ LPS in the absence or presence of 50 μM BGP-15 for 1 hour, then stained with 50 nM of TMRM. After a 15 minutes incubation fluorescent signal was measured by the GloMax Multi Detection System, then remeasured after the application of 1 μM FCCP. $\Delta\Psi$ was calculated as the difference of fluorescence signal before and after FCCP-treatment. Data are presented as the mean \pm SEM of three independent experiments. $^{*}P < 0.05$, $^{***}P < 0.001$ compared to control cells; $^{\#}P < 0.01$ compared to LPS-treated cells. (D) Effect of BGP-15 on the LPS-induced ROS production in U-251 MG cells (containing the TLR4 receptor). Cells were treated with 1 mg/mL LPS in the presence or absence of 50 μM BGP-15 for 30 minutes. LPS-induced ROS production was determined by the oxidation of DHR123 (1 μM) to R123, measured with fluorescent microscopy. Cell nuclei were labelled using Hoechst 33342. Representative merged images of three independent experiments are presented. (E) Quantitative analysis of LPS-induced (1 $\mu\text{g}/\text{mL}$) ROS production and the protective effect of BGP-15 (50 μM). Data are presented as the mean \pm SEM of three independent experiments. $^{***}P < 0.001$ compared to control cells; $^{\#\#}P < 0.001$ compared to LPS-treated cells. (F) Effect of BGP-15 on oxidative stress-induced superoxide production in U-251 MG cells in the absence or presence of 20 μM MitoTEMPO as determined by MitoSOX (0.3 μM). Data are presented as the mean \pm SEM of three independent experiments. $^{*}P < 0.05$, $^{***}P < 0.001$ compared to control cells, $^{\#\#}P < 0.01$ compared to LPS-treated cells.

doi:10.1371/journal.pone.0169372.g006

in millimolar concentrations. Since we have used BGP-15 at a 50 μM concentration, it is unlikely that its uncoupling effect played a significant role in its mitochondria- and cytoprotecting effects. On the other hand, BGP-15 reduced the oxidative stress-induced mitochondrial depolarization as we revealed by using two membrane potential sensitive dyes. ROS-induced mitochondrial depolarization could result in decreased ATP synthesis, increased superoxide production by the electron-transport chain, release of proapoptotic proteins from the intermembrane space, decreased mitochondrial fusion and increased fission [33,50–52]. All of these processes cause disturbance of cellular energy metabolism and a shift toward proapoptotic signaling eventually resulting in death of the cell [33,50–52]. Therefore, the membrane potential stabilizing effect of BGP-15 likely contributed to its protective effect in the aforementioned diseases.

BGP-15 was also found to be critical in the reduction of ROS- and LPS-induced ROS production (Figs 3A and 6D), which can play a significant role in the progression of several diseases. However, it is difficult to localize the site of ROS production by using conventional mitochondria-targeted redox dyes since oxidation of the dye by extramitochondrial or mitochondrial ROS results in identical fluorescence localized to the mitochondria. Therefore, we used MitoSOX [39] at a concentration of 0.3 μM excited at 365 nm. Under these conditions, the resulting 440 nm fluorescence is believed to result from oxidation of the dye by mitochondrially produced superoxide (Fig 4E and 4F). Furthermore, we have quenched mitochondrial ROS by the mitochondria-targeted antioxidant MitoTEMPO [40]. All the results supported that BGP-15 reduced mitochondrial ROS production. This effect could not result from antioxidant property of the molecule as it was revealed by our experiments on various cell-free ROS-generating systems (Fig 4C and 4D). Even, we believe that we localized the most important target of BGP-15, complex I-III, which is critical for ROS production by the respiratory chain. It can generate significant amounts of ROS under conditions of hypoxia, mitochondrial hyperpolarization, inhibition of respiratory complexes and in several other conditions [53]. The significant ROS-reducing effect of BGP-15 may be important in regulating ROS-dependent processes including cell death, MAPK and poly(ADP-ribose) polymerase (PARP) pathways, in addition to transcription factor activation (NF- κ B, AP-1, NRF2, etc.) [54]. The high enrichment of BGP-15 in the mitochondria, combined with the significant reduction in mitochondrial ROS production

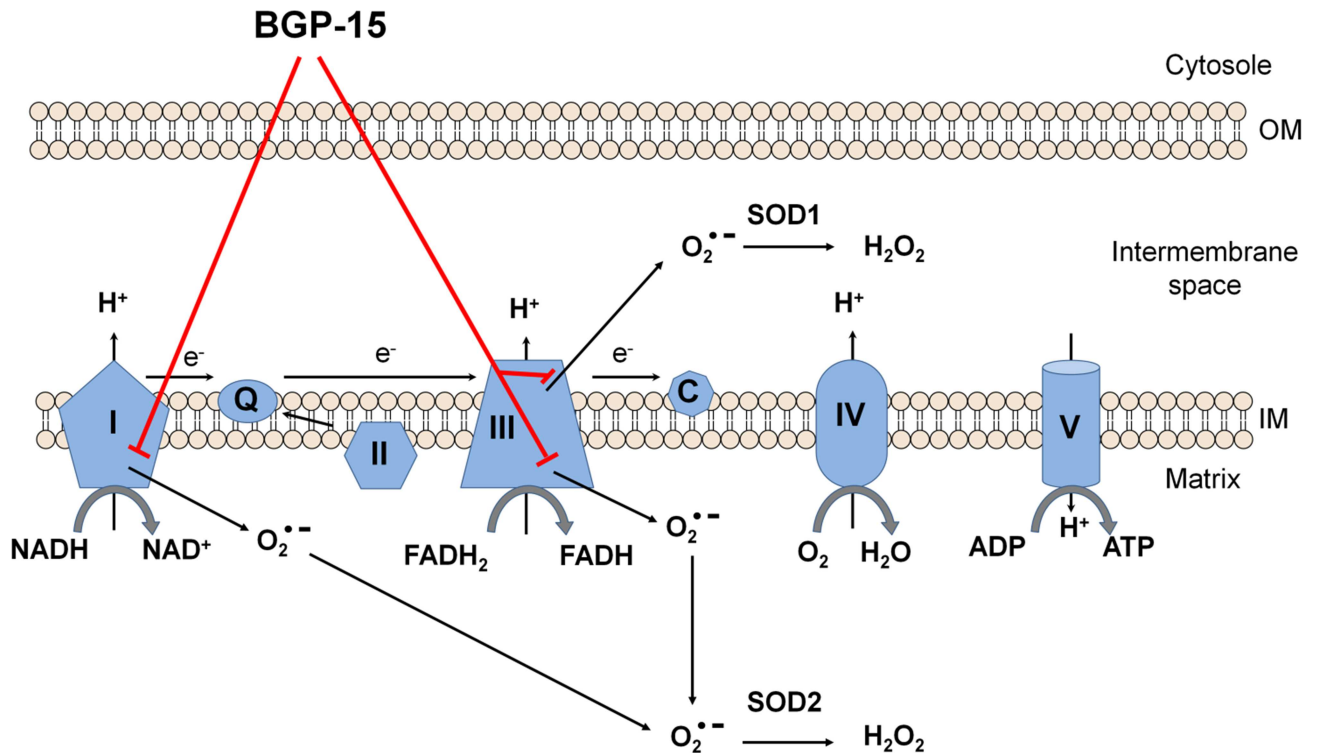


Fig 7. Possible mitochondrial molecular mechanism of BGP-15 cytoprotective action. BGP-15 reduces mitochondrial ROS production at complex I and at complex III, and so reduces ROS induced mitochondrial damage, as well as cell death.

doi:10.1371/journal.pone.0169372.g007

at complex I by BGP-15, suggests that the protective effect of BGP-15 observed in different disease models is likely to be mediated by the aforementioned mitochondrial mechanisms. Our results also suggest that the effect of BGP-15 on signaling pathways, such as BGP-15-induced reduction in JNK and p38 MAPK activation [55] or BGP-15-induced Akt activation [56], could also potentially be related to reduced ROS production. LPS induces a complex stress pattern in sensitive cells, including ROS production by NADPH oxidases, an increase in cytoplasmic free calcium level and activation of mitochondria damaging signaling pathways [57,58]. In a separate study on cyclophilin D (CypD) knockout mice, we reported that LPS-induced mitochondrial ROS production was substantially reduced in CypD deficient cells and tissues, accompanied by reduced MAPK activation [45,46]. This stabilized the mitochondrial membrane systems by preventing high calcium-induced mitochondrial permeability transition, resulting in attenuated ROS production and benign intracellular signaling. Therefore, we assumed that, similar to the oxidative stress situation, BGP-15 would protect against LPS-induced mitochondrial damage. Indeed, we found that BGP-15 prevented LPS-induced mitochondrial depolarization and ROS production (Fig 6), demonstrating that BGP-15 can protect mitochondria against complex inflammatory damage as well as against ROS-induced damage. These results suggest the potential of BGP-15 as an experimental drug, not only in ROS-related diseases, but also in inflammatory diseases.

In conclusion, the critical mechanism underlying the protective effect of BGP-15 on the mitochondria appear to be due to reduced ROS production, predominantly at the first and third respiratory complexes (Fig 7). By this mechanism, it may regulate several pathways that play critical roles in the progression of ROS-related and inflammatory diseases.

Author Contributions

Conceptualization: KS AS FG BS.

Formal analysis: KS AS FG BS.

Investigation: KS AS KF CA BD EH FG BS.

References

1. Wang W, Gong G, Wang X, Wei-LaPierre L, Cheng H, Dirksen R, et al. (2016) Mitochondrial Flash: Integrative Reactive Oxygen Species and pH Signals in Cell and Organelle Biology. *Antioxid Redox Signal* 25: 534–549. doi: [10.1089/ars.2016.6739](https://doi.org/10.1089/ars.2016.6739) PMID: [27245241](https://pubmed.ncbi.nlm.nih.gov/27245241/)
2. Daiber A, Di Lisa F, Oelze M, Kroller-Schon S, Steven S, Schulz E, et al. (2015) Crosstalk of mitochondria with NADPH oxidase via reactive oxygen and nitrogen species signalling and its role for vascular function. *Br J Pharmacol*.
3. Dan Dunn J, Alvarez LA, Zhang X, Soldati T (2015) Reactive oxygen species and mitochondria: A nexus of cellular homeostasis. *Redox Biol* 6: 472–485. doi: [10.1016/j.redox.2015.09.005](https://doi.org/10.1016/j.redox.2015.09.005) PMID: [26432659](https://pubmed.ncbi.nlm.nih.gov/26432659/)
4. Tajeddine N (2016) How do reactive oxygen species and calcium trigger mitochondrial membrane permeabilisation? *Biochim Biophys Acta* 1860: 1079–1088. doi: [10.1016/j.bbagen.2016.02.013](https://doi.org/10.1016/j.bbagen.2016.02.013) PMID: [26922832](https://pubmed.ncbi.nlm.nih.gov/26922832/)
5. Baines HL, Turnbull DM, Greaves LC (2014) Human stem cell aging: do mitochondrial DNA mutations have a causal role? *Aging Cell* 13: 201–205. doi: [10.1111/ace1.12199](https://doi.org/10.1111/ace1.12199) PMID: [24382254](https://pubmed.ncbi.nlm.nih.gov/24382254/)
6. Szczepanowska K, Trifunovic A (2015) Different faces of mitochondrial DNA mutators. *Biochim Biophys Acta* 1847: 1362–1372. doi: [10.1016/j.bbabi.2015.05.016](https://doi.org/10.1016/j.bbabi.2015.05.016) PMID: [26014346](https://pubmed.ncbi.nlm.nih.gov/26014346/)
7. Mazzaccara C, Iafusco D, Liguori R, Ferrigno M, Galderisi A, Vitale D, et al. (2012) Mitochondrial diabetes in children: seek and you will find it. *PLoS One* 7: e34956. doi: [10.1371/journal.pone.0034956](https://doi.org/10.1371/journal.pone.0034956) PMID: [22536343](https://pubmed.ncbi.nlm.nih.gov/22536343/)
8. Schapira AH (2012) Mitochondrial diseases. *Lancet* 379: 1825–1834. doi: [10.1016/S0140-6736\(11\)61305-6](https://doi.org/10.1016/S0140-6736(11)61305-6) PMID: [22482939](https://pubmed.ncbi.nlm.nih.gov/22482939/)
9. Perry RJ, Kim T, Zhang XM, Lee HY, Pesta D, Popov VB, et al. (2013) Reversal of hypertriglyceridemia, fatty liver disease, and insulin resistance by a liver-targeted mitochondrial uncoupler. *Cell Metab* 18: 740–748. doi: [10.1016/j.cmet.2013.10.004](https://doi.org/10.1016/j.cmet.2013.10.004) PMID: [24206666](https://pubmed.ncbi.nlm.nih.gov/24206666/)
10. Keipert S, Ost M, Johann K, Imber F, Jastroch M, van Schothorst EM, et al. (2014) Skeletal muscle mitochondrial uncoupling drives endocrine cross-talk through the induction of FGF21 as a myokine. *Am J Physiol Endocrinol Metab* 306: E469–482. doi: [10.1152/ajpendo.00330.2013](https://doi.org/10.1152/ajpendo.00330.2013) PMID: [24347058](https://pubmed.ncbi.nlm.nih.gov/24347058/)
11. Bavarsad Shahripour R, Harrigan MR, Alexandrov AV (2014) N-acetylcysteine (NAC) in neurological disorders: mechanisms of action and therapeutic opportunities. *Brain Behav* 4: 108–122. doi: [10.1002/brb3.208](https://doi.org/10.1002/brb3.208) PMID: [24683506](https://pubmed.ncbi.nlm.nih.gov/24683506/)
12. Jegatheeswaran S, Siriwardena AK (2011) Experimental and clinical evidence for modification of hepatic ischaemia-reperfusion injury by N-acetylcysteine during major liver surgery. *HPB (Oxford)* 13: 71–78.
13. Newsholme P, Gaudel C, Krause M (2012) Mitochondria and diabetes. An intriguing pathogenetic role. *Adv Exp Med Biol* 942: 235–247. doi: [10.1007/978-94-007-2869-1_10](https://doi.org/10.1007/978-94-007-2869-1_10) PMID: [22399425](https://pubmed.ncbi.nlm.nih.gov/22399425/)
14. Coyle LC, Rodriguez A, Jeschke RE, Simon-Lee A, Abbott KC, Taylor AJ (2006) Acetylcysteine In Diabetes (AID): a randomized study of acetylcysteine for the prevention of contrast nephropathy in diabetics. *Am Heart J* 151: 1032 e1039–1012.
15. Jaffery Z, Verma A, White CJ, Grant AG, Collins TJ, Grise MA, et al. (2012) A randomized trial of intravenous n-acetylcysteine to prevent contrast induced nephropathy in acute coronary syndromes. *Cather Cardiovasc Interv* 79: 921–926. doi: [10.1002/ccd.23157](https://doi.org/10.1002/ccd.23157) PMID: [21542122](https://pubmed.ncbi.nlm.nih.gov/21542122/)
16. Drummond GR, Selemidis S, Griending KK, Sobey CG (2011) Combating oxidative stress in vascular disease: NADPH oxidases as therapeutic targets. *Nat Rev Drug Discov* 10: 453–471. doi: [10.1038/nrd3403](https://doi.org/10.1038/nrd3403) PMID: [21629295](https://pubmed.ncbi.nlm.nih.gov/21629295/)
17. Gao YJ, Ji RR (2010) Chemokines, neuronal-glia interactions, and central processing of neuropathic pain. *Pharmacol Ther* 126: 56–68. doi: [10.1016/j.pharmthera.2010.01.002](https://doi.org/10.1016/j.pharmthera.2010.01.002) PMID: [20117131](https://pubmed.ncbi.nlm.nih.gov/20117131/)
18. Yuzefovych L, Wilson G, Rachek L (2010) Different effects of oleate vs. palmitate on mitochondrial function, apoptosis, and insulin signaling in L6 skeletal muscle cells: role of oxidative stress. *Am J Physiol Endocrinol Metab* 299: E1096–1105. doi: [10.1152/ajpendo.00238.2010](https://doi.org/10.1152/ajpendo.00238.2010) PMID: [20876761](https://pubmed.ncbi.nlm.nih.gov/20876761/)

19. Diaz-Vivancos P, de Simone A, Kiddle G, Foyer CH (2015) Glutathione—linking cell proliferation to oxidative stress. *Free Radic Biol Med* 89: 1154–1164. doi: [10.1016/j.freeradbiomed.2015.09.023](https://doi.org/10.1016/j.freeradbiomed.2015.09.023) PMID: [26546102](https://pubmed.ncbi.nlm.nih.gov/26546102/)
20. Marionneau C, Abriel H (2015) Regulation of the cardiac Na⁺ channel NaV1.5 by post-translational modifications. *J Mol Cell Cardiol* 82: 36–47. doi: [10.1016/j.yjmcc.2015.02.013](https://doi.org/10.1016/j.yjmcc.2015.02.013) PMID: [25748040](https://pubmed.ncbi.nlm.nih.gov/25748040/)
21. Zsurka G, Kunz WS (2015) Mitochondrial dysfunction and seizures: the neuronal energy crisis. *Lancet Neurol* 14: 956–966. doi: [10.1016/S1474-4422\(15\)00148-9](https://doi.org/10.1016/S1474-4422(15)00148-9) PMID: [26293567](https://pubmed.ncbi.nlm.nih.gov/26293567/)
22. Gehrig SM, van der Poel C, Sayer TA, Schertzer JD, Henstridge DC, Church JE, et al. (2012) Hsp72 preserves muscle function and slows progression of severe muscular dystrophy. *Nature* 484: 394–398. doi: [10.1038/nature10980](https://doi.org/10.1038/nature10980) PMID: [22495301](https://pubmed.ncbi.nlm.nih.gov/22495301/)
23. Sarszegi Z, Bogнар E, Gaszner B, Konyi A, Gallyas F Jr., Sumeги B, et al. (2012) BGP-15, a PARP-inhibitor, prevents imatinib-induced cardiotoxicity by activating Akt and suppressing JNK and p38 MAP kinases. *Mol Cell Biochem* 365: 129–137. doi: [10.1007/s11010-012-1252-8](https://doi.org/10.1007/s11010-012-1252-8) PMID: [22350755](https://pubmed.ncbi.nlm.nih.gov/22350755/)
24. Nagy G, Szarka A, Lotz G, Doczi J, Wunderlich L, Kiss A, et al. (2010) BGP-15 inhibits caspase-independent programmed cell death in acetaminophen-induced liver injury. *Toxicol Appl Pharmacol* 243: 96–103. doi: [10.1016/j.taap.2009.11.017](https://doi.org/10.1016/j.taap.2009.11.017) PMID: [19931551](https://pubmed.ncbi.nlm.nih.gov/19931551/)
25. Bardos G, Moricz K, Jaszlits L, Rablóczyk G, Tory K, Racz I, et al. (2003) BGP-15, a hydroxamic acid derivative, protects against cisplatin- or taxol-induced peripheral neuropathy in rats. *Toxicol Appl Pharmacol* 190: 9–16. PMID: [12831778](https://pubmed.ncbi.nlm.nih.gov/12831778/)
26. Racz I, Tory K, Gallyas F Jr., Berente Z, Osz E, Jaszlits L, et al. (2002) BGP-15—a novel poly(ADP-ribose) polymerase inhibitor—protects against nephrotoxicity of cisplatin without compromising its anti-tumor activity. *Biochem Pharmacol* 63: 1099–1111. PMID: [11931842](https://pubmed.ncbi.nlm.nih.gov/11931842/)
27. Literati-Nagy Z, Tory K, Literati-Nagy B, Kolonics A, Torok Z, Gombos I, et al. (2012) The HSP co-inducer BGP-15 can prevent the metabolic side effects of the atypical antipsychotics. *Cell Stress Chaperones* 17: 517–521. doi: [10.1007/s12192-012-0327-5](https://doi.org/10.1007/s12192-012-0327-5) PMID: [22322357](https://pubmed.ncbi.nlm.nih.gov/22322357/)
28. Gombos I, Crul T, Piotto S, Gungor B, Torok Z, Balogh G, et al. (2011) Membrane-lipid therapy in operation: the HSP co-inducer BGP-15 activates stress signal transduction pathways by remodeling plasma membrane rafts. *PLoS One* 6: e28818. doi: [10.1371/journal.pone.0028818](https://doi.org/10.1371/journal.pone.0028818) PMID: [22174906](https://pubmed.ncbi.nlm.nih.gov/22174906/)
29. Chung J, Nguyen AK, Henstridge DC, Holmes AG, Chan MH, Mesa JL, et al. (2008) HSP72 protects against obesity-induced insulin resistance. *Proc Natl Acad Sci U S A* 105: 1739–1744. doi: [10.1073/pnas.0705799105](https://doi.org/10.1073/pnas.0705799105) PMID: [18223156](https://pubmed.ncbi.nlm.nih.gov/18223156/)
30. Sapra G, Tham YK, Cemerlang N, Matsumoto A, Kiriazis H, Bernardo BC, et al. (2014) The small-molecule BGP-15 protects against heart failure and atrial fibrillation in mice. *Nat Commun* 5: 5705. doi: [10.1038/ncomms6705](https://doi.org/10.1038/ncomms6705) PMID: [25489988](https://pubmed.ncbi.nlm.nih.gov/25489988/)
31. Literati-Nagy B, Peterfai E, Kulcsar E, Literati-Nagy Z, Buday B, Tory K, et al. (2010) Beneficial effect of the insulin sensitizer (HSP inducer) BGP-15 on olanzapine-induced metabolic disorders. *Brain Res Bull* 83: 340–344. doi: [10.1016/j.brainresbull.2010.09.005](https://doi.org/10.1016/j.brainresbull.2010.09.005) PMID: [20849938](https://pubmed.ncbi.nlm.nih.gov/20849938/)
32. Literati-Nagy Z, Tory K, Literati-Nagy B, Kolonics A, Vigh L Jr., Vigh L, et al. (2012) A novel insulin sensitizer drug candidate-BGP-15-can prevent metabolic side effects of atypical antipsychotics. *Pathol Oncol Res* 18: 1071–1076. doi: [10.1007/s12253-012-9546-4](https://doi.org/10.1007/s12253-012-9546-4) PMID: [22743983](https://pubmed.ncbi.nlm.nih.gov/22743983/)
33. Galloway CA, Yoon Y (2013) Mitochondrial morphology in metabolic diseases. *Antioxid Redox Signal* 19: 415–430. doi: [10.1089/ars.2012.4779](https://doi.org/10.1089/ars.2012.4779) PMID: [22793999](https://pubmed.ncbi.nlm.nih.gov/22793999/)
34. Hogeboom GH, Schneider WC (1950) Cytochemical studies of mammalian tissues. III. Isocitric dehydrogenase and triphosphopyridine nucleotide-cytochrome c reductase of mouse liver. *J Biol Chem* 186: 417–427. PMID: [14794638](https://pubmed.ncbi.nlm.nih.gov/14794638/)
35. Sims NR (1990) Rapid isolation of metabolically active mitochondria from rat brain and subregions using Percoll density gradient centrifugation. *J Neurochem* 55: 698–707. PMID: [2164576](https://pubmed.ncbi.nlm.nih.gov/2164576/)
36. Papazisis KT, Geromichalos GD, Dimitriadis KA, Kortsaris AH (1997) Optimization of the sulforhodamine B colorimetric assay. *J Immunol Methods* 208: 151–158. PMID: [9433470](https://pubmed.ncbi.nlm.nih.gov/9433470/)
37. Tao H, Zhang Y, Zeng X, Shulman GI, Jin S (2014) Niclosamide ethanolamine-induced mild mitochondrial uncoupling improves diabetic symptoms in mice. *Nat Med* 20: 1263–1269. doi: [10.1038/nm.3699](https://doi.org/10.1038/nm.3699) PMID: [25282357](https://pubmed.ncbi.nlm.nih.gov/25282357/)
38. Teshima Y, Takahashi N, Nishio S, Saito S, Kondo H, Fukui A, et al. (2014) Production of reactive oxygen species in the diabetic heart. Roles of mitochondria and NADPH oxidase. *Circ J* 78: 300–306. PMID: [24334638](https://pubmed.ncbi.nlm.nih.gov/24334638/)
39. Robinson KM, Janes MS, Beckman JS (2008) The selective detection of mitochondrial superoxide by live cell imaging. *Nat Protoc* 3: 941–947. doi: [10.1038/nprot.2008.56](https://doi.org/10.1038/nprot.2008.56) PMID: [18536642](https://pubmed.ncbi.nlm.nih.gov/18536642/)

40. Ni R, Cao T, Xiong S, Ma J, Fan GC, Laceyfield JC, et al. (2016) Therapeutic inhibition of mitochondrial reactive oxygen species with mito-TEMPO reduces diabetic cardiomyopathy. *Free Radic Biol Med* 90: 12–23. doi: [10.1016/j.freeradbiomed.2015.11.013](https://doi.org/10.1016/j.freeradbiomed.2015.11.013) PMID: [26577173](https://pubmed.ncbi.nlm.nih.gov/26577173/)
41. Huang LS, Cobessi D, Tung EY, Berry EA (2005) Binding of the respiratory chain inhibitor antimycin to the mitochondrial bc1 complex: a new crystal structure reveals an altered intramolecular hydrogen-bonding pattern. *J Mol Biol* 351: 573–597. doi: [10.1016/j.jmb.2005.05.053](https://doi.org/10.1016/j.jmb.2005.05.053) PMID: [16024040](https://pubmed.ncbi.nlm.nih.gov/16024040/)
42. Klegeris A, McGeer PL (2001) Inflammatory cytokine levels are influenced by interactions between THP-1 monocytic, U-373 MG astrocytic, and SH-SY5Y neuronal cell lines of human origin. *Neurosci Lett* 313: 41–44. PMID: [11684335](https://pubmed.ncbi.nlm.nih.gov/11684335/)
43. von Bernhardt R, Eugenin-von Bernhardt L, Eugenin J (2015) Microglial cell dysregulation in brain aging and neurodegeneration. *Front Aging Neurosci* 7: 124. doi: [10.3389/fnagi.2015.00124](https://doi.org/10.3389/fnagi.2015.00124) PMID: [26257642](https://pubmed.ncbi.nlm.nih.gov/26257642/)
44. Brenner C, Galluzzi L, Kepp O, Kroemer G (2013) Decoding cell death signals in liver inflammation. *J Hepatol* 59: 583–594. doi: [10.1016/j.jhep.2013.03.033](https://doi.org/10.1016/j.jhep.2013.03.033) PMID: [23567086](https://pubmed.ncbi.nlm.nih.gov/23567086/)
45. Fonai F, Priber JK, Jakus PB, Kalman N, Antus C, Pollak E, et al. (2015) Lack of cyclophilin D protects against the development of acute lung injury in endotoxemia. *Biochim Biophys Acta* 1852: 2563–2573. doi: [10.1016/j.bbadis.2015.09.004](https://doi.org/10.1016/j.bbadis.2015.09.004) PMID: [26385159](https://pubmed.ncbi.nlm.nih.gov/26385159/)
46. Priber J, Fonai F, Jakus PB, Racz B, Chinopoulos C, Tretter L, et al. (2015) Cyclophilin D disruption attenuates lipopolysaccharide-induced inflammatory response in primary mouse macrophages. *Biochem Cell Biol* 93: 241–250. doi: [10.1139/bcb-2014-0120](https://doi.org/10.1139/bcb-2014-0120) PMID: [25728038](https://pubmed.ncbi.nlm.nih.gov/25728038/)
47. Tucsek Z, Radnai B, Racz B, Debreceni B, Priber JK, Dolowschik T, et al. (2011) Suppressing LPS-induced early signal transduction in macrophages by a polyphenol degradation product: a critical role of MKP-1. *J Leukoc Biol* 89: 105–111. doi: [10.1189/jlb.0610355](https://doi.org/10.1189/jlb.0610355) PMID: [20884647](https://pubmed.ncbi.nlm.nih.gov/20884647/)
48. Seeley EJ, Rosenberg P, Matthay MA (2013) Calcium flux and endothelial dysfunction during acute lung injury: a STIMulating target for therapy. *J Clin Invest* 123: 1015–1018. doi: [10.1172/JCI68093](https://doi.org/10.1172/JCI68093) PMID: [23434597](https://pubmed.ncbi.nlm.nih.gov/23434597/)
49. Idelman G, Smith DL, Zucker SD (2015) Bilirubin inhibits the up-regulation of inducible nitric oxide synthase by scavenging reactive oxygen species generated by the toll-like receptor 4-dependent activation of NADPH oxidase. *Redox Biol* 5: 398–408. doi: [10.1016/j.redox.2015.06.008](https://doi.org/10.1016/j.redox.2015.06.008) PMID: [26163808](https://pubmed.ncbi.nlm.nih.gov/26163808/)
50. Gao L, Laude K, Cai H (2008) Mitochondrial pathophysiology, reactive oxygen species, and cardiovascular diseases. *Vet Clin North Am Small Anim Pract* 38: 137–155, vi. doi: [10.1016/j.cvsm.2007.10.004](https://doi.org/10.1016/j.cvsm.2007.10.004) PMID: [18249246](https://pubmed.ncbi.nlm.nih.gov/18249246/)
51. Jheng HF, Tsai PJ, Guo SM, Kuo LH, Chang CS, Su IJ, et al. (2012) Mitochondrial fission contributes to mitochondrial dysfunction and insulin resistance in skeletal muscle. *Mol Cell Biol* 32: 309–319. doi: [10.1128/MCB.05603-11](https://doi.org/10.1128/MCB.05603-11) PMID: [22083962](https://pubmed.ncbi.nlm.nih.gov/22083962/)
52. Circu ML, Aw TY (2010) Reactive oxygen species, cellular redox systems, and apoptosis. *Free Radic Biol Med* 48: 749–762. doi: [10.1016/j.freeradbiomed.2009.12.022](https://doi.org/10.1016/j.freeradbiomed.2009.12.022) PMID: [20045723](https://pubmed.ncbi.nlm.nih.gov/20045723/)
53. Babot M, Birch A, Labarbuta P, Galkin A (2014) Characterisation of the active/de-active transition of mitochondrial complex I. *Biochim Biophys Acta* 1837: 1083–1092. doi: [10.1016/j.bbabi.2014.02.018](https://doi.org/10.1016/j.bbabi.2014.02.018) PMID: [24569053](https://pubmed.ncbi.nlm.nih.gov/24569053/)
54. Ray PD, Huang BW, Tsuji Y (2012) Reactive oxygen species (ROS) homeostasis and redox regulation in cellular signaling. *Cell Signal* 24: 981–990. doi: [10.1016/j.cellsig.2012.01.008](https://doi.org/10.1016/j.cellsig.2012.01.008) PMID: [22286106](https://pubmed.ncbi.nlm.nih.gov/22286106/)
55. Matsuzawa A, Ichijo H (2008) Redox control of cell fate by MAP kinase: physiological roles of ASK1-MAP kinase pathway in stress signaling. *Biochim Biophys Acta* 1780: 1325–1336. doi: [10.1016/j.bbagen.2007.12.011](https://doi.org/10.1016/j.bbagen.2007.12.011) PMID: [18206122](https://pubmed.ncbi.nlm.nih.gov/18206122/)
56. Matsuno K, Iwata K, Matsumoto M, Katsuyama M, Cui W, Murata A, et al. (2012) NOX1/NADPH oxidase is involved in endotoxin-induced cardiomyocyte apoptosis. *Free Radic Biol Med* 53: 1718–1728. doi: [10.1016/j.freeradbiomed.2012.08.590](https://doi.org/10.1016/j.freeradbiomed.2012.08.590) PMID: [22982050](https://pubmed.ncbi.nlm.nih.gov/22982050/)
57. Scott AJ, O’Dea KP, O’Callaghan D, Williams L, Dokpesi JO, Tatton L, et al. (2011) Reactive oxygen species and p38 mitogen-activated protein kinase mediate tumor necrosis factor alpha-converting enzyme (TACE/ADAM-17) activation in primary human monocytes. *J Biol Chem* 286: 35466–35476. doi: [10.1074/jbc.M111.277434](https://doi.org/10.1074/jbc.M111.277434) PMID: [21865167](https://pubmed.ncbi.nlm.nih.gov/21865167/)
58. Korbecki J, Baranowska-Bosiacka I, Gutowska I, Chlubek D (2013) The effect of reactive oxygen species on the synthesis of prostanoids from arachidonic acid. *J Physiol Pharmacol* 64: 409–421. PMID: [24101387](https://pubmed.ncbi.nlm.nih.gov/24101387/)

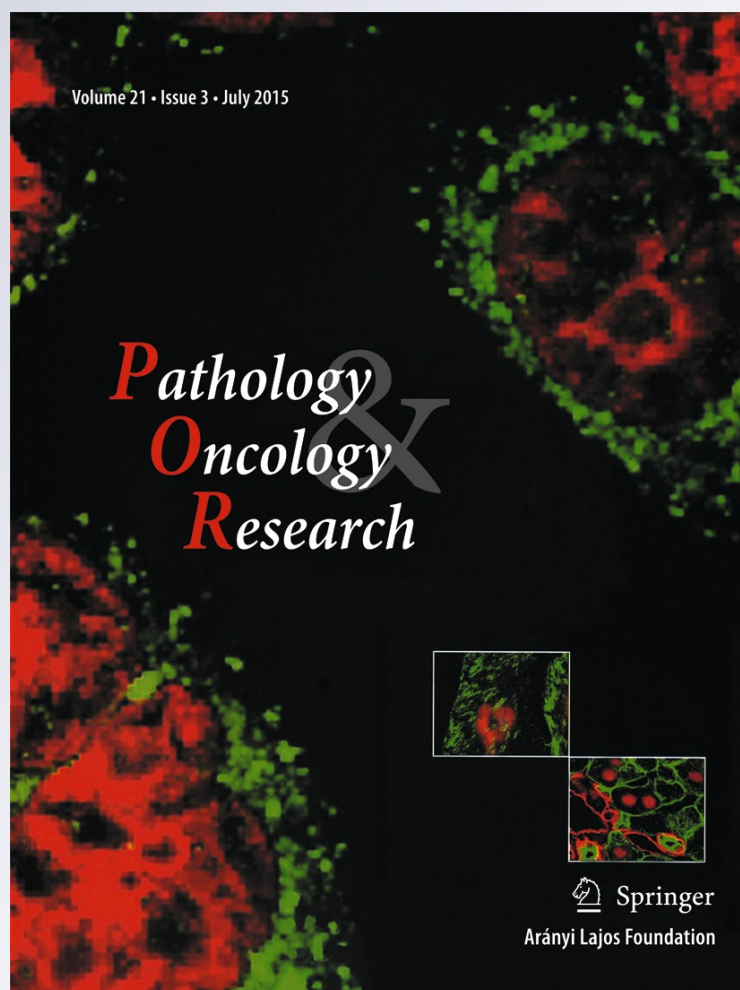
*Functional Variants of Lipid Level Modifier
MLXIPL, GCKR, GALNT2, CILP2,
ANGPTL3 and TRIB1 Genes in Healthy
Roma and Hungarian Populations*

**Katalin Sumegi, Luca Jaromi, Lili
Magyari, Erzsebet Kovesdi, Balazs
Duga, Renata Szalai, Anita Maasz, Petra
Matyas, Ingrid Janicsek, et al.**

Pathology & Oncology Research
Official Journal of the Arányi Lajos
Foundation

ISSN 1219-4956
Volume 21
Number 3

Pathol. Oncol. Res. (2015) 21:743-749
DOI 10.1007/s12253-014-9884-5



Your article is protected by copyright and all rights are held exclusively by Arányi Lajos Foundation. This e-offprint is for personal use only and shall not be self-archived in electronic repositories. If you wish to self-archive your article, please use the accepted manuscript version for posting on your own website. You may further deposit the accepted manuscript version in any repository, provided it is only made publicly available 12 months after official publication or later and provided acknowledgement is given to the original source of publication and a link is inserted to the published article on Springer's website. The link must be accompanied by the following text: "The final publication is available at link.springer.com".

Functional Variants of Lipid Level Modifier MLXIPL, GCKR, GALNT2, CILP2, ANGPTL3 and TRIB1 Genes in Healthy Roma and Hungarian Populations

Katalin Sumegi · Luca Jaromi · Lili Magyari ·
Erzsebet Kovetsdi · Balazs Duga · Renata Szalai ·
Anita Maasz · Petra Matyas · Ingrid Janicsek ·
Bela Melegh

Received: 14 March 2014 / Accepted: 22 December 2014 / Published online: 9 January 2015
© Arányi Lajos Foundation 2015

Abstract The role of triglyceride metabolism in different diseases, such as cardiovascular or cerebrovascular diseases is still under extensive investigations. In genome-wide studies several polymorphisms have been reported, which are highly associated with plasma lipid level changes. Our goal was to examine eight variants: rs12130333 at the ANGPTL3,

rs16996148 at the CILP2, rs17321515 at the TRIB1, rs17145738 and rs3812316 of the MLXIPL, rs4846914 at GALNT2, rs1260326 and rs780094 residing at the GCKR loci. A total of 399 Roma (Gypsy) and 404 Hungarian population samples were genotyped using PCR-RFLP method. Significant differences were found between Roma and Hungarian population samples in both MLXIPL variants (C allele frequency of rs17145738: 94.1% vs. 85.6%, C allele frequency of rs3812316: 94.2% vs. 86.8% in Romas vs. in Hungarians, $p < 0.05$), in ANGPTL3 (T allele frequency of rs12130333: 12.2% vs. 18.5% in Romas vs. Hungarians, $p < 0.05$) and GALNT2 (G allele frequency of rs4846914: 46.6% vs. 54.5% Romas vs. in Hungarians, $p < 0.05$), while no differences over SNPs could be verified and the known minor alleles showed no correlation with triglyceride levels in any population samples. The current study revealed fundamental differences of known triglyceride modifying SNPs in Roma population. Failure of finding evidence for affected triglyceride metabolism shows that these susceptibility genes are much less effective compared for example to the apolipoprotein A5 gene.

K. Sumegi · L. Jaromi · L. Magyari · E. Kovetsdi · B. Duga ·
R. Szalai · A. Maasz · P. Matyas · I. Janicsek · B. Melegh (✉)
Department of Medical Genetics, Clinical Centre, University of Pecs,
Szigeti u. 12, Pecs H-7624, Hungary
e-mail: melegh.bela@pte.hu

K. Sumegi
e-mail: sumegi.katalin@pte.hu

L. Jaromi
e-mail: jaromi.luca@pte.hu

L. Magyari
e-mail: magyari.lili@pte.hu

E. Kovetsdi
e-mail: kovetsdi.erzsebet@pte.hu

B. Duga
e-mail: duga.balazs@pte.hu

R. Szalai
e-mail: szalai.renata@pte.hu

A. Maasz
e-mail: maasz.anita@pte.hu

P. Matyas
e-mail: matyas.petra@pte.hu

I. Janicsek
e-mail: ingrid.janicsek@aok.pte.hu

K. Sumegi · L. Jaromi · L. Magyari · E. Kovetsdi · B. Duga ·
B. Melegh
Szentágothai Research Centre, University of Pecs, Ifjusag u. 20,
Pecs H-7624, Hungary

Keywords Polymorphisms · Triglyceride · Roma · Hungarian

Introduction

The recent genome-wide association studies (GWAS) revealed genetic polymorphisms associated with blood lipid level changes. Nowadays, special attention gained on

metabolic consequences, including triglyceride level increases, confirming risk for cardiovascular diseases, metabolic syndrome or for cerebrovascular diseases, especially stroke events [1–19]. The National Cholesterol Education Program (NCEP) in 2001 ascertained several markers which are in strong association with coronary risk, stratified as risk factors related to lifestyle, such as physical inactivity, obesity, atherogenic diet; and emerging risk factors, as lipoprotein profile, homocysteine level, changed fasting glycaemia and evidence of subclinical atherosclerosis. Approach to lipoprotein management in 2001 National Cholesterol Guidelines [20].

As a prominent example, the functional role of *APOA5* polymorphisms had already been widely investigated [1–7]. Several of them are associated with elevated triglyceride levels and higher risks for ischemic stroke and cardio- or cerebrovascular diseases or for metabolic syndrome [4, 5, 8–11, 21, 22]. Recently, other triglyceride modifying polymorphisms came into focus, which may also have role in development of different diseases [2, 12, 15, 16, 19, 23–25]. Some variants of these are mentioned in connection with increased, while others with decreased triglyceride levels [16, 23, 24, 26, 27]. The elevated levels of certain triglycerides may have a higher risk for several vascular diseases, moreover significant associations between triglyceride level-elevating and polymorphisms were confirmed [1, 2, 4, 5, 12–15, 17, 28, 26, 29–32, 25].

Romani people, who are often neglected, strongly differ from other nations [33]. In this work, our goal was to investigate the possible relationship of functional polymorphisms of *GCKR*, *MLXIPL*, *ANGPTL3*, *CILP2*, *GALNT2* and *TRIB1* gene loci with altering triglyceride levels in Roma and in Hungarian population samples.

Materials and Methods

Patients

The DNA samples were from the central Biobank managed by the University of Pecs, belonging to the National Biobank Network of Hungary (<http://www.biobanks.hu>); clinical features are shown in Table 1. The molecular investigations were carried out on genomic DNA, which was isolated from

Table 1 Major clinical and laboratory data of Roma and Hungarian population samples

	Roma (399)	Hungarians (404)
Males/females	179/221	141/263
Age (years)	55.7±0.94	61.5±0.79
Plasma triglyceride (mmol/l)	1.61±0.04	1.44±0.02
Total cholesterol (mmol/l)	4.70±0.06	5.58±0.06

peripheral EDTA-anticoagulated blood leukocytes, by a standard desalting method [34]. The maintenance, management and governance principles of the Biobank had been endorsed by the national Scientific Research Ethics Committee, Budapest (ETT TUKEB). During the collection and use of DNA samples and the consorting clinical and personal data were in complete compliance with the guidelines of the 1975 Helsinki Declaration and the currently operative national laws and regulations.

Here we studied eight polymorphisms reportedly associated with triglyceride-level changes: rs17145738 and rs3812316 of the *MLXIPL* locus, rs1260326 and rs780094 of the *GCKR* gene, rs4846914 variant of *GALNT2* gene, rs1699614 of *CILP2*, rs1213033 of *ANGPTL3* gene locus and rs17321515 of *TRIB1* gene locus in biobanked samples in Roma and Hungarian populations. Sample size determination was based on our preliminary analyses of the prevalence of these SNPs. Based on the important significant difference in frequencies of the genetic alterations between Roma and Hungarian samples; we calculated how many samples we would need per group to be adequately small and large enough to detect a statistically significant difference and to exclude Type I and Type II errors ($\alpha=0.05$ and $\beta<0.03$, two tailed). Thus, a total of 399 Roma samples compared with 404 Hungarians, rs4846914 variant of *GALNT2* gene, rs1699614 of *CILP2*, rs1213033 of *ANGPTL3*, rs17321515 of *TRIB1*, rs17145738 and rs3812316 of the *MLXIPL* locus, rs1260326 and rs780094 of the *GCKR* gene were enrolled in this study.

Molecular Biology Methods

The allele specific amplification was performed by synthetic oligonucleotide primers, using standard polymerase chain reaction technique. After the PCR reaction, restriction fragment length polymorphisms procedures were used to get the genetic pattern. All the methods were designed to involve an obligate cleavage site on the amplicon in the amplified DNA sequence thus enabling us to verify the efficacy of the digestion. The position of the analyzed gene loci, the sequences of the primers, the restriction enzymes and cleavage sites and patterns were shown in Table 2.

Statistical Analysis

All clinical data were represented as means±SEM where appropriate. For continuous variables the Mann–Whitney *U* test and for discrete variables the Chi-square tests were applied to compute the differences between the clinical parameters in Roma population and in Hungarian participants. The value of $p<0.05$ was considered as statistically significant. SPSS 20.0 package for Windows (SPSS Inc., Chicago, IL, USA) was employed for all statistical analyses.

Table 2 Primer sequences and PCR-RFLP conditions

Gene	Functional variants	Forward primer	Reverse primer	Melting temperature (°C)	PCR product size (bp)	Restriction endonuclease	Ancestral genotype fragments (bp)	Heterozygous genotype fragments (bp)	Minor allele genotype fragments (bp)
<i>GCKR</i>	C1337T	TGCAGACTAAGTGGAGCCG	CATCACATGGCCACTGCTTT	60	231	<i>HpaII</i>	18, 63, 150	18, 63, 150, 213	18, 213
	rs1260326								
<i>MLXIPL</i>	rs780094	AATTGTCAGGCAACCTGGTA	CCCGGCCTCAACAAATGTAT	60	273	<i>PseI</i>	63, 210	33, 63, 177, 210	33, 63, 177
	rs17145738	ATGGTCCAGGAGTCTGCC	AGGCATCGTGCCTAGTAAA	60	615	<i>TaqI</i>	49, 113, 253	49, 113, 253, 366	49, 366
<i>ANGPTL3</i>	rs3812316	CCATCCCAGCCATCCCT	TTCTCCAGTGTGGTCCCGT	60	239	<i>BspLI</i>	16, 17, 203	16, 17, 26, 177, 203	16, 17, 26, 177
	rs12130333	TTTCTAAAACCTTGGTATCTT	CATTTTCATGGTTGCTTTGT	58	372	<i>DraI</i>	79, 294	26, 79, 268, 294	26, 79, 268
<i>CILP2</i>	rs16996148	TCTCATCAATCACCCATCCA	AATGTGTGTTCTCCCAAGCC	58	466	<i>HinIII</i>	184, 283	47, 184, 235, 283	47, 184, 235
<i>GALNT2</i>	rs4846914	CTGTGCCCTCTGGGACTGCTA	AGTGAGGAAGGACTAAGA	57	200	<i>HpyF3I</i>	19, 74, 107	19, 74, 107, 126	74, 126
<i>TRIB1</i>	rs17321515	AAGGAAGGTTAGGTAGACC	GACACCAGCTGTAGAGAA	57	596	<i>FspBI</i>	56, 90, 450	56, 90, 450, 541	56, 541

Results

All allele distribution and allele frequencies of polymorphisms summarized in Table 3 and Table 4 were in Hardy–Weinberg equilibrium both in Roma and in Hungarian individuals. In allele frequencies significant differences were found for *MLXIPL* both variants, *GALNT2* rs4846914 and *ANGPTL3* rs1213033 polymorphisms comparing Roma participants to the Hungarians. The C alleles in rs17145738 and rs3812316 variants of *MLXIPL* occurred more frequently in Roma population than in Hungarians. Contrary to this, variants rs1213033 of *ANGPTL3* and rs4846914 of *GALNT2* genes exhibited a significantly lower allele frequency in Romas than in Hungarians.

Serum triglyceride and total cholesterol levels in two examined populations with different genotypes are summarized in Table 5 and Table 6. We found no association between serum triglyceride levels and carrying minor alleles analyzed compared with the non-carriers in Roma and Hungarian population samples.

Discussion

Worldwide, the role of serum triglycerides and total cholesterol in relation to development of several diseases, especially cardio-and cerebrovascular diseases, metabolic syndrome and diabetes mellitus is extensively investigated [4, 10, 11, 30, 35–38]. In the past few years, several studies described new genetic polymorphisms which have an effect on triglyceride level alteration, like *GCKR* and *APOA5* variants [11, 30, 35–38]. The mechanism of glucokinase enzyme of the liver is under control by glucokinase regulatory protein (GCKR), which enzyme has a dominant glucose phosphorylase role of

Table 3 Allele distribution of polymorphisms of GCKR and MLXIPL gene loci

	Roma (399)		Hungarians (404)	
GCKR rs1260326	CC (n=119)	CT+TT (n=205+75)	CC (n=102)	CT+TT (n=208+94)
T allele frequency	44.5%		49.0%	
GCKR rs780094	GG (n=119)	GA+AA (n=180+100)	GG (n=99)	GA+AA (n=218+87)
A allele frequency	47.6%		48.5%	
MLXIPL rs17145738	TT (n=2)	TC+CC (n=43+354)	TT (n=9)	TC+CC (n=98+297)
C allele frequency	94.1%*		85.6%	
MLXIPL rs3812316	GG (n=5)	GC+CC (n=36+358)	GG (n=9)	GC+CC (n=89+306)
C allele frequency	94.2%*		86.8%	

*p<0.025 vs. Hungarians

Table 4 Allele distribution of polymorphisms of CILP2, GALNT2, ANGPTL3 and TRIB1 gene loci

	Roma (394)		Hungarians (400)	
	GG (n=333)	GT+TT (n=60+1)	GG (n=342)	GT+TT (n=56+2)
CILP2 rs1699614				
T allele frequency	7.86%		7.50%	
GALNT2 rs4846914	AA (n=90)	AG+GG (n=243+63)	AA (n=91)	AG+GG (n=182+127)
G allele frequency	46.6%*		54.5%	
ANGPTL3 rs1213033	CC (n=309)	CT+TT (n=81+8)	CC (n=270)	CT+TT (n=112+18)
T allele frequency	12.2%*		18.5%	
TRIB1 rs17321515	AA (n=103)	GA+GG (n=203+93)	AA (n=107)	GA+GG (n=186+107)
G allele frequency	48.8%		50.0%	

**p*<0.025 vs. Hungarians

the liver and of the pancreatic β-cells in the glucose homeostasis of the blood [39–41]. In genome-wide association studies the possible effect of functional variants in *GCKR* gene in association with hypertriglyceridemia was analyzed [15, 42]. The intronic rs780094 and the exonic rs1260326 variants are the most investigated, the last variant causes a Leu/Pro change at 446 amino acid position, which indirectly affects triglyceride levels alteration, has a role in impaired fasting glycaemia, and is a possible risk for type II diabetes mellitus, as Veiga-da Cunha observed [43]. Santoro et al. examined 455 obese children and adolescents (181 Caucasians, 139 African Americans, and 135 Hispanics) for rs1260326 of *GCKR* gene. The

variant showed an association with hepatic fat accumulation along with large VLDL and triglyceride levels. Two genes, as *GCKR* and *PNPLA3* act together and have a susceptible effect for manifestation of fatty liver in obese young people [44].

Several studies confirmed the fact, that Angiopoietin-like protein 3 (ANGPTL3) has an effect on lipid metabolism; the protein indirectly inhibits the activity of lipoprotein and other endothelial lipases. The loss-of-function mutations of *ANGPTL3* gene causes total ANGPTL3 absence, which shows a high association rate with recessive hypolipidemia. This type of hypolipidemia is characteristic for decrease of apolipoprotein B and apolipoprotein A-I-enclosing lipoproteins, which leads to altering levels of high-density lipoprotein. By contrast, the incomplete scarcity of ANGPTL3 is related to attenuation of low-density lipoprotein. Pisciotta et al. investigated *ANGPTL3* gene in 4 persons with low levels of LDL cholesterol and HDL cholesterol, and they found homozygous, compound heterozygous for *ANGPTL3* loss-of-function mutations (p.I19LfsX22/p.N147X, p.G400VfsX52) associated with the deficiency of ANGPTL3 in plasma. Decreased plasma levels of triglyceride-containing lipoproteins and of HDL particles were observed, moreover, the heterozygous carriers showed normal level of plasma high-density lipoprotein cholesterol, but low plasma level of ANGPTL3 and attenuated level of low-density lipoprotein cholesterol [45].

A Max-like-interacting-protein-like (*MLXIPL*; or carbohydrate response element binding protein, *ChREBP*) gene is located in the WBSR14 deletion region at chromosome 7q11.23. Recently, in genome-wide association studies between the plasma triglyceride-level alterations and *MLXIPL*

Table 5 The effect on lipid parameters of polymorphisms of GCKR and MLXIPL gene loci

	Roma (399)		Hungarians (404)	
	CC (n=119)	CT+TT (n=205+75)	CC (n=102)	CT+TT (n=208+94)
GCKR rs1260326				
Plasma triglyceride (mmol/l)	1.47±0.06	1.66±0.05	1.58±0.06	1.52±0.03
Serum cholesterol (mmol/l)	4.57±0.11	4.76±0.07	5.66±0.10	5.54±0.07
GCKR rs780094	GG (n=119)	GA+AA (n=180+100)	GG (n=99)	GA+AA (n=218+87)
Plasma triglyceride (mmol/l)	1.50±0.06	1.65±0.05	1.51±0.05	1.54±0.03
Serum cholesterol (mmol/l)	4.57±0.10	4.76±0.07	5.69±0.10	5.54±0.07
MLXIPL rs17145738	TT (n=2)	TC+CC (n=43+354)	TT (n=9)	TC+CC (n=98+297)
Plasma triglyceride (mmol/l)	1.22±0.12	1.61±0.04	1.44±0.09	1.54±0.03
Serum cholesterol (mmol/l)	4.75±0.15	4.70±0.06	6.23±0.53	5.56±0.06
MLXIPL rs3812316	GG (n=5)	GC+CC (n=36+358)	GG (n=9)	GC+CC (n=89+306)
Plasma triglyceride (mmol/l)	1.51±0.25	1.61±0.04	1.41±0.09	1.54±0.03
Serum cholesterol (mmol/l)	4.88±0.30	4.7±0.06	5.90±0.52	5.57±0.06

Values are means ± SEM. Triglycerides and serum total cholesterol levels are mmol/l

Table 6 The effect on lipid parameters of polymorphisms of *CILP2*, *GALNT2*, *ANGPTL3* and *TRIB1* gene loci

	Roma (394)		Hungarians (400)	
<i>CILP2</i> rs1699614	GG (n=333)	GT+TT (n=60+1)	GG (n=342)	GT+TT (n=56+2)
Plasma triglyceride (mmol/l)	1.60±0.04	1.62±0.10	1.54±0.03	1.52±0.05
Serum cholesterol (mmol/l)	4.71±0.06	4.69±0.14	5.59±0.06	5.53±0.16
<i>GALNT2</i> rs4846914	AA (n=90)	AG+GG (n=243+63)	AA (n=91)	AG+GG (n=182+127)
Plasma triglyceride (mmol/l)	1.65±0.09	1.59±0.04	1.57±0.05	1.53±0.03
Serum cholesterol (mmol/l)	4.72±0.11	4.70±0.07	5.66±0.11	5.56±0.07
<i>ANGPTL3</i> rs1213033	CC (n=309)	CT+TT (n=81+8)	CC (n=270)	CT+TT (n=112+18)
Plasma triglyceride (mmol/l)	1.61±0.04	1.61±0.08	1.52±0.03	1.58±0.04
Serum cholesterol (mmol/l)	4.67±0.06	4.81±0.12	5.57±0.07	5.60±0.10
<i>TRIB1</i> rs17321515	AA (n=103)	GA+GG (n=203+93)	AA (n=107)	GA+GG (n=186+107)
Plasma triglyceride (mmol/l)	1.71±0.07	1.57±0.04	1.51±0.04	1.55±0.03
Serum cholesterol (mmol/l)	4.76±0.11	4.69±0.06	5.59±0.11	5.57±0.07

Values are means ± SEM. Triglycerides and serum total cholesterol levels are mmol/l

locus correlations were found. Moreover, the influence of triglyceride level increase of the major alleles of the rs17145738 and rs3812316 variants in *MLXIPL* locus were observed [15, 16].

In recent GWAS studies, the minor G-allele of the rs4846914 intronic variant of the *GALNT2* (UDP-N-acetyl-alpha-D-galactosamine: polypeptide-N-acetyl-galactose-aminotransferase 2) gene associated with increased triglyceride concentrations of the plasma. In a case-control study, which was performed on Han Chinese population analyzing 4192 individuals for type 2 diabetes, the association between elevated triglyceride levels and genotypes for *MLXIPL* rs17145738 variant and for *GCKR* rs780094 was confirmed, but not for *GALNT2* rs4846914 polymorphism [46].

In the last years an association has been detected between dyslipidemia and the rs16996148 (near *CILP2*), rs17321515 (near *TRIB1*), rs12130333 (near *ANGPTL3*) variants [16]. Moreover, these loci were correlated with the manifestation of cardiovascular diseases [15].

The *CILP2* gene the proteins' relation to lipid metabolism is not well studied yet. In a genome-wide association study, a triglyceride level reducing role of the rs16996148 variant was confirmed analyzing Caucasian individuals [23]. Vrablík et al. investigated 895 Czech patients with primary dyslipidemia comparing with 672 healthy controls. There was no significant effect of the polymorphisms *CILP2* on lipid levels after receiving statin treatment [47].

The human tribbles-1 (*TRIB1*) facilitates the proteasome-dependent protein degradation. In an Asian Malay population, the variant adjacent to the *TRIB1* locus (rs17321515) showed a significant correlation with increased total cholesterol and

LDL-cholesterol, moreover higher risk for coronary heart disease and cardiovascular disease was described [48].

Conclusion

Our findings could verify earlier results [15], in allele frequencies showed significant differences in both variants of *MLXIPL*, *GALNT2* rs4846914 and *ANGPTL3* rs1213033 polymorphisms comparing Roma individuals to Hungarians. Analyzing Roma and Hungarian population samples we could not confirm any associations between altering levels of triglycerides and minor allele carriers compared with the non-carriers. This shows a much weaker triglyceride influencing activity for all these genotypes compared with the apolipoprotein A5 gene, which had been showed to influence the triglycerides using almost the same biobanks and populations as we used the current study [4, 5, 49].

Acknowledgments Study was supported by the grant of Hungarian Science Foundation OTKA K103983 and T73430.

Conflict of Interests The authors declare that they have no conflict of interests related to this manuscript.

References

1. Szalai C, Keszei M, Duba J, Prohaszka Z, Kozma GT, Csaszar A, Balogh S, Almasy Z, Fust G, Czinner A (2004) Polymorphism in the promoter region of the apolipoprotein A5 gene is associated with an

- increased susceptibility for coronary artery disease. *Atherosclerosis* 173(1):109–114
2. Vaessen SF, Schaap FG, Kuivenhoven JA, Groen AK, Hutten BA, Boekholdt SM, Hattori H, Sandhu MS, Bingham SA, Luben R, Palmen JA, Wareham NJ, Humphries SE, Kastelein JJ, Talmud PJ, Khaw KT (2006) Apolipoprotein A-V, triglycerides and risk of coronary artery disease: the prospective Epic-Norfolk Population Study. *J Lipid Res* 47(9):2064–2070
 3. Martinelli N, Girelli D, Ferraresi P, Olivieri O, Lunghi B, Manzato F, Corrocher R, Bernardi F (2007) Increased factor VIII coagulant activity levels in male carriers of the factor V R2 polymorphism. *Blood Coagul Fibrinolysis* 18(2):125–129
 4. Maasz A, Kisfalvi P, Jaromi L, Horvatovich K, Szolnoki Z, Csongei V, Safrany E, Sipeky C, Hadarits F, Melegh B (2008) Apolipoprotein A5 gene IVS3+G476A allelic variant confers susceptibility for development of ischemic stroke. *Circ J* 72(7):1065–1070
 5. Maasz A, Kisfalvi P, Szolnoki Z, Hadarits F, Melegh B (2008) Apolipoprotein A5 gene C56G variant confers risk for the development of large-vessel associated ischemic stroke. *J Neurol* 255(5):649–654
 6. Feitosa MF, An P, Ordovas JM, Ketkar S, Hopkins PN, Straka RJ, Arnett DK, Borecki IB (2011) Association of gene variants with lipid levels in response to fenofibrate is influenced by metabolic syndrome status. *Atherosclerosis* 215(2):435–439
 7. Garelnabi M, Lor K, Jin J, Chai F, Santanam N (2012) The paradox of ApoA5 modulation of triglycerides: Evidence from clinical and basic research. *Clin Biochem*
 8. Mohas M, Kisfalvi P, Jaromi L, Maasz A, Feher E, Csongei V, Polgar N, Safrany E, Cseh J, Sumegi K, Hetyesy K, Wittmann I, Melegh B (2010) GCKR gene functional variants in type 2 diabetes and metabolic syndrome: do the rare variants associate with increased carotid intima-media thickness? *Cardiovasc Diabetol* 9:79
 9. Jaromi L, Csongei V, Polgar N, Szolnoki Z, Maasz A, Horvatovich K, Farago B, Sipeky C, Safrany E, Magyari L, Kisfalvi P, Mohas M, Janicsek I, Lakner L, Melegh B (2010) Functional variants of glucokinase regulatory protein and apolipoprotein A5 genes in ischemic stroke. *J Mol Neurosci* 41(1):121–128
 10. Jaromi L, Csongei V, Polgar N, Rappai G, Szolnoki Z, Maasz A, Horvatovich K, Safrany E, Sipeky C, Magyari L, Melegh B (2011) Triglyceride level-influencing functional variants of the ANGPTL3, CILP2, and TRIB1 loci in ischemic stroke. *Neuromolecular Med* 13(3):179–186
 11. Johansen CT, Hegele RA (2012) Allelic and phenotypic spectrum of plasma triglycerides. *Biochim Biophys Acta* 1821(5):833–842
 12. Sovereign OW, Jukema JW, Boekholdt SM, Zwinderman AH, Tanck MW (2005) Polymorphisms in APOA1 and LPL genes are statistically independently associated with fasting TG in men with CAD. *Eur J Hum Genet* 13(4):445–451
 13. Havasi V, Szolnoki Z, Talian G, Bene J, Komlosi K, Maasz A, Somogyvari F, Kondacs A, Szabo M, Fodor L, Bodor A, Melegh B (2006) Apolipoprotein A5 gene promoter region T-1131C polymorphism associates with elevated circulating triglyceride levels and confers susceptibility for development of ischemic stroke. *J Mol Neurosci* 29(2):177–183
 14. Freiberg JJ, Tybjaerg-Hansen A, Jensen JS, Nordestgaard BG (2008) Nonfasting triglycerides and risk of ischemic stroke in the general population. *JAMA* 300(18):2142–2152
 15. Willer CJ, Sanna S, Jackson AU, Scuteri A, Bonnycastle LL, Clarke R, Heath SC, Timpson NJ, Najjar SS, Stringham HM, Strait J, Duren WL, Maschio A, Busonero F, Mulas A, Albai G, Swift AJ, Morken MA, Narisu N, Bennett D, Parish S, Shen H, Galan P, Meneton P, Hercberg S, Zelenika D, Chen WM, Li Y, Scott LJ, Scheet PA, Sundvall J, Watanabe RM, Nagaraja R, Ebrahim S, Lawlor DA, Ben-Shlomo Y, Davey-Smith G, Shuldiner AR, Collins R, Bergman RN, Uda M, Tuomilehto J, Cao A, Collins FS, Lakatta E, Lathrop GM, Boehnke M, Schlessinger D, Mohlke KL, Abecasis GR (2008) Newly identified loci that influence lipid concentrations and risk of coronary artery disease. *Nat Genet* 40(2):161–169
 16. Kathiresan S, Willer CJ, Peloso GM, Demissie S, Musunuru K, Schadt EE, Kaplan L, Bennett D, Li Y, Tanaka T, Voight BF, Bonnycastle LL, Jackson AU, Crawford G, Surti A, Guiducci C, Burt NP, Parish S, Clarke R, Zelenika D, Kubalanza KA, Morken MA, Scott LJ, Stringham HM, Galan P, Swift AJ, Kuusisto J, Bergman RN, Sundvall J, Laakso M, Ferrucci L, Scheet P, Sanna S, Uda M, Yang Q, Lunetta KL, Dupuis J, de Bakker PI, O'Donnell CJ, Chambers JC, Kooner JS, Hercberg S, Meneton P, Lakatta EG, Scuteri A, Schlessinger D, Tuomilehto J, Collins FS, Groop L, Altshuler D, Collins R, Lathrop GM, Melander O, Salomaa V, Peltonen L, Orho-Melander M, Ordovas JM, Boehnke M, Abecasis GR, Mohlke KL, Cupples LA (2009) Common variants at 30 loci contribute to polygenic dyslipidemia. *Nat Genet* 41(1):56–65
 17. Labreuche J, Touboul PJ, Amarenco P (2009) Plasma triglyceride levels and risk of stroke and carotid atherosclerosis: a systematic review of the epidemiological studies. *Atherosclerosis* 203(2):331–345
 18. Perez-Martinez P, Garcia-Rios A, Delgado-Lista J, Perez-Jimenez F, Lopez-Miranda J (2011) Nutrigenetics of the postprandial lipoprotein metabolism: evidences from human intervention studies. *Curr Vasc Pharmacol* 9(3):287–291
 19. Aslibekyan S, Goodarzi MO, Frazier-Wood AC, Yan X, Irvin MR, Kim E, Tiwari HK, Guo X, Straka RJ, Taylor KD, Tsai MY, Hopkins PN, Korenman SG, Borecki IB, Chen YD, Ordovas JM, Rotter JL, Arnett DK (2012) Variants identified in a GWAS meta-analysis for blood lipids are associated with the lipid response to fenofibrate. *PLoS One* 7(10):e48663
 20. Grundy SM (2002) Approach to lipoprotein management in 2001 National Cholesterol Guidelines. *Am J Cardiol* 90(8A):11i–21i
 21. Brautbar A, Covarrubias D, Belmont J, Lara-Garduno F, Virani SS, Jones PH, Leal SM, Ballantyne CM (2011) Variants in the APOA5 gene region and the response to combination therapy with statins and fenofibric acid in a randomized clinical trial of individuals with mixed dyslipidemia. *Atherosclerosis* 219(2):737–742
 22. Kisfalvi P, Mohas M, Maasz A, Hadarits F, Marko L, Horvatovich K, Oroszlan T, Bagosi Z, Bujtor Z, Gasztonyi B, Wittmann I, Melegh B (2008) Apolipoprotein A5 IVS3+476A allelic variant associates with increased triglyceride levels and confers risk for development of metabolic syndrome in Hungarians. *Circ J* 72(1):40–43
 23. Kathiresan S, Melander O, Guiducci C, Surti A, Burt NP, Rieder MJ, Cooper GM, Roos C, Voight BF, Havulinna AS, Wahlstrand B, Hedner T, Corella D, Tai ES, Ordovas JM, Berglund G, Vartiainen E, Jousilahti P, Hedblad B, Taskinen MR, Newton-Cheh C, Salomaa V, Peltonen L, Groop L, Altshuler DM, Orho-Melander M (2008) Six new loci associated with blood low-density lipoprotein cholesterol, high-density lipoprotein cholesterol or triglycerides in humans. *Nat Genet* 40(2):189–197
 24. Shimizugawa T, Ono M, Shimamura M, Yoshida K, Ando Y, Koishi R, Ueda K, Inaba T, Minekura H, Kohama T, Furukawa H (2002) ANGPTL3 decreases very low density lipoprotein triglyceride clearance by inhibition of lipoprotein lipase. *J Biol Chem* 277(37):33742–33748
 25. Seidelmann SB, Li L, Shen GQ, Topol EJ, Wang QK (2008) Identification of a novel locus for triglyceride on chromosome 1p31-32 in families with premature CAD and MI. *J Lipid Res* 49(5):1034–1038
 26. Izar MC, Fonseca FA, Ihara SS, Kasinski N, Sang WH, Lopes IE, Pinto Ldo E, Relvas WG, Lourenco D, Tufik S, de Paola AA, Carvalho AC (2003) Risk factors, biochemical markers, and genetic polymorphisms in early coronary artery disease. *Arq Bras Cardiol* 80(4):379–395
 27. Thomsen SB, Rathcke CN, Skaaby T, Linneberg A, Vestergaard H (2012) The association between genetic variations of CH3L1, levels

- of the encoded glycoprotein YKL-40 and the lipid profile in a Danish population. *PLoS One* 7(10):e47094
28. Baroni MG, Berni A, Romeo S, Arca M, Tesorio T, Sorropago G, Di Mario U, Galton DJ (2003) Genetic study of common variants at the Apo E, Apo AI, Apo CIII, Apo B, lipoprotein lipase (LPL) and hepatic lipase (LIPC) genes and coronary artery disease (CAD): variation in LIPC gene associates with clinical outcomes in patients with established CAD. *BMC Med Genet* 4:8
 29. Meigs JB, Nathan DM, D'Agostino RB Sr, Wilson PW (2002) Fasting and postchallenge glycemia and cardiovascular disease risk: the Framingham offspring study. *Diabetes Care* 25(10):1845–1850
 30. Pennacchio LA, Rubin EM (2003) Apolipoprotein A5, a newly identified gene that affects plasma triglyceride levels in humans and mice. *Arterioscler Thromb Vasc Biol* 23(4):529–534
 31. Ma X, Bacci S, Mlynarski W, Gottardo L, Soccio T, Menzaghi C, Iori E, Lager RA, Shroff AR, Gervino EV, Nesto RW, Johnstone MT, Abumrad NA, Avogaro A, Trischitta V, Doria A (2004) A common haplotype at the CD36 locus is associated with high free fatty acid levels and increased cardiovascular risk in Caucasians. *Hum Mol Genet* 13(19):2197–2205
 32. Saidi S, Slamia LB, Ammou SB, Mahjoub T, Almawi WY (2007) Association of apolipoprotein E gene polymorphism with ischemic stroke involving large-vessel disease and its relation to serum lipid levels. *J Stroke Cerebrovasc Dis* 16(4):160–166
 33. Moorjani P, Patterson N, Loh P, Lipson M, Kiszfalvi P, Melegh B, Bonin M, Kádaši L, Rieβ O, Berger B, Reich D, Melegh B (2013) Reconstructing Roma history from genome-wide data. *American Journal of Human Genetics*
 34. Miller SA, Dykes DD, Polesky HF (1988) A simple salting out procedure for extracting DNA from human nucleated cells. *Nucleic Acids Res* 16(3):1215
 35. Martinelli N, Trabetti E, Bassi A, Girelli D, Friso S, Pizzolo F, Sandri M, Malerba G, Pignatti PF, Corrocher R, Olivieri O (2007) The -1131 T>C and S19W APOA5 gene polymorphisms are associated with high levels of triglycerides and apolipoprotein C-III, but not with coronary artery disease: an angiographic study. *Atherosclerosis* 191(2):409–417
 36. Vaxillaire M, Cavalcanti-Proenca C, Dechaume A, Tichet J, Marre M, Balkau B, Froguel P (2008) The common P446L polymorphism in GCKR inversely modulates fasting glucose and triglyceride levels and reduces type 2 diabetes risk in the DESIR prospective general French population. *Diabetes* 57(8):2253–2257
 37. Hishida A, Morita E, Naito M, Okada R, Wakai K, Matsuo K, Nakamura K, Takashima N, Suzuki S, Takezaki T, Mikami H, Ohnaka K, Watanabe Y, Uemura H, Kubo M, Tanaka H, Hamajima N (2012) Associations of apolipoprotein A5 (APOA5), glucokinase (GCK) and glucokinase regulatory protein (GCKR) polymorphisms and lifestyle factors with the risk of dyslipidemia and dysglycemia in Japanese—a cross-sectional data from the J-MICC Study. *Endocr J* 59(7):589–599
 38. Dussaillant C, Serrano V, Maiz A, Eyheramendy S, Cataldo LR, Chavez M, Smalley SV, Fuentes M, Rigotti A, Rubio L, Lagos CF, Martinez JA, Santos JL (2012) APOA5 Q97X mutation identified through homozygosity mapping causes severe hypertriglyceridemia in a Chilean consanguineous family. *BMC Med Genet* 13:106
 39. Warner JP, Leek JP, Intody S, Markham AF, Bonthron DT (1995) Human glucokinase regulatory protein (GCKR): cDNA and genomic cloning, complete primary structure, and chromosomal localization. *Mamm Genome* 6(8):532–536
 40. Hayward BE, Dunlop N, Intody S, Leek JP, Markham AF, Warner JP, Bonthron DT (1998) Organization of the human glucokinase regulator gene GCKR. *Genomics* 49(1):137–142
 41. Orho-Melander M, Melander O, Guiducci C, Perez-Martinez P, Corella D, Roos C, Tewhey R, Rieder MJ, Hall J, Abecasis G, Tai ES, Welch C, Arnett DK, Lyssenko V, Lindholm E, Saxena R, de Bakker PI, Burt N, Voight BF, Hirschhorn JN, Tucker KL, Hedner T, Tuomi T, Isomaa B, Eriksson KF, Taskinen MR, Wahlstrand B, Hughes TE, Parnell LD, Lai CQ, Berglund G, Peltonen L, Vartiainen E, Jousilahti P, Havulinna AS, Salomaa V, Nilsson P, Groop L, Altshuler D, Ordovas JM, Kathiresan S (2008) Common missense variant in the glucokinase regulatory protein gene is associated with increased plasma triglyceride and C-reactive protein but lower fasting glucose concentrations. *Diabetes* 57(11):3112–3121
 42. Rafiq S, Venkata KK, Gupta V, Guru VD, Spurgeon CJ, Parameshwaran S, Madana SN, Kinra S, Bowen L, Timpson NJ, Smith GD, Dudbridge F, Prabhakaran D, Ben-Shlomo Y, Reddy KS, Ebrahim S, Chandak GR (2012) Evaluation of seven common lipid associated loci in a large Indian sib pair study. *Lipids Health Dis* 11(1):155
 43. Veiga-da-Cunha M, Delplanque J, Gillain A, Bonthron DT, Boutin P, Van Schaftingen E, Froguel P (2003) Mutations in the glucokinase regulatory protein gene in 2p23 in obese French caucasians. *Diabetologia* 46(5):704–711
 44. Santoro N, Zhang CK, Zhao H, Pakstis AJ, Kim G, Kursawe R, Dykas DJ, Bale AE, Giannini C, Pierpont B, Shaw MM, Groop L, Caprio S (2012) Variant in the glucokinase regulatory protein (GCKR) gene is associated with fatty liver in obese children and adolescents. *Hepatology* 55(3):781–789
 45. Pisciotto L, Favari E, Magnolo L, Simonelli S, Adorni MP, Sallo R, Fancello T, Zavaroni I, Ardigo D, Bernini F, Calabresi L, Franceschini G, Tarugi P, Calandra S, Bertolini S (2012) Characterization of three kindreds with familial combined hypolipidemia caused by loss-of-function mutations of ANGPTL3. *Circ Cardiovasc Genet* 5(1):42–50
 46. Liu Y, Zhou D, Zhang Z, Song Y, Zhang D, Zhao T, Chen Z, Sun Y, Yang Y, Xing Q, Zhao X, Xu H, He L (2010) Effects of genetic variants on lipid parameters and dyslipidemia in a Chinese population. *J Lipid Res* 52(2):354–360
 47. Vrablik M, Hubacek JA, Dlouha D, Lanska V, Rynekrova J, Zlatohlavek L, Prusikova M, Ceska R, Adamkova V (2012) Impact of variants within seven candidate genes on statin treatment efficacy. *Physiol Res*
 48. Tai ES, Sim XL, Ong TH, Wong TY, Saw SM, Aung T, Kathiresan S, Orho-Melander M, Ordovas JM, Tan JT, Seielstad M (2009) Polymorphisms at newly identified lipid-associated loci are associated with blood lipids and cardiovascular disease in an Asian Malay population. *J Lipid Res* 50(3):514–520
 49. Maasz A, Kiszfalvi P, Horvatovich K, Mohas M, Marko L, Csonge V, Farago B, Jaromi L, Magyari L, Safrany E, Sipeky C, Wittmann I, Melegh B (2007) Apolipoprotein A5 T-1131C variant confers risk for metabolic syndrome. *Pathol Oncol Res* 13(3):243–247

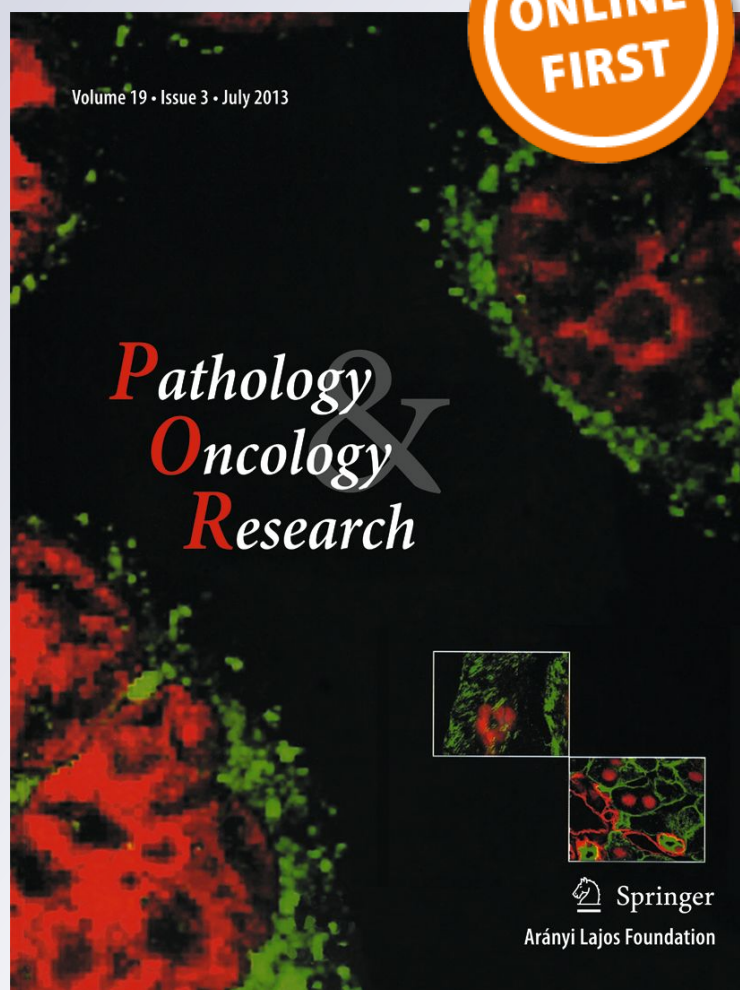
Marked Differences of Haplotype Tagging SNP Distribution, Linkage, and Haplotype Profile of APOA5 Gene in Roma Population Samples

Katalin Sumegi, Balazs Duga, Bela I. Melegh, Zsolt Banfai, Erzsebet Kovesdi, Anita Maasz & Bela Melegh

Pathology & Oncology Research
Official Journal of the Arányi Lajos
Foundation

ISSN 1219-4956

Pathol. Oncol. Res.
DOI 10.1007/s12253-017-0197-3



Your article is protected by copyright and all rights are held exclusively by Arányi Lajos Foundation. This e-offprint is for personal use only and shall not be self-archived in electronic repositories. If you wish to self-archive your article, please use the accepted manuscript version for posting on your own website. You may further deposit the accepted manuscript version in any repository, provided it is only made publicly available 12 months after official publication or later and provided acknowledgement is given to the original source of publication and a link is inserted to the published article on Springer's website. The link must be accompanied by the following text: "The final publication is available at link.springer.com".

Marked Differences of Haplotype Tagging SNP Distribution, Linkage, and Haplotype Profile of APOA5 Gene in Roma Population Samples

Katalin Sumegi^{1,2} · Balazs Duga^{1,2} · Bela I. Melegh^{1,2} · Zsolt Banfai^{1,2} ·
Erzsebet Kovsdi^{1,2} · Anita Maasz¹ · Bela Melegh^{1,2}

Received: 4 April 2016 / Accepted: 10 January 2017
© Arányi Lajos Foundation 2017

Abstract Roma people are underprivileged, neglected population worldwide, with severe healthcare problems. They have significantly increased prevalence of cardiovascular morbidity, presumably related to their poor social status, alcohol consumption and smoking habits. Assuming that genetic background also plays a role in their susceptibility for cardiovascular diseases, we hypothesized that APOA5 gene polymorphisms, an important role-player in lipid metabolism and in the development of metabolic syndrome and cardio/cerebrovascular events, may also be involved. We examined four APOA5 polymorphisms in 363 Roma and 404 Hungarian DNA samples. For rs662799, rs2266788,

rs207560 and rs3135506 we found elevated plasma triglyceride levels in the risk allele carriers compared to non-carriers in both populations. At least a two-fold significant increase was detected in minor allele frequencies in Roma when compared to Hungarians, except the rs2266788 variant. Haplotype analysis revealed significant increase of APOA5*2, APOA5*4 in Roma, as opposed to the higher levels of APOA5*5 found in Hungarians. Different linkage disequilibrium was found between rs207560 and rs3135506 variants in Roma compared to Hungarians. The profound differences observed in almost all APOA5 polymorphisms in Roma require special attention, since these variants are known to associate with cardio/cerebrovascular susceptibility.

Keywords APOA5 · Triglyceride · Haplotype · Linkage disequilibrium · Roma

✉ Bela Melegh
melegh.bela@pte.hu

Katalin Sumegi
sumegi.katalin@pte.hu

Balazs Duga
duga.balazs@pte.hu

Bela I. Melegh
bela.melegh@gmail.com

Zsolt Banfai
banfai.zsolt@pte.hu

Erzsebet Kovsdi
kovsdi.erszsebet@pte.hu

Anita Maasz
maasz.anita@pte.hu

¹ Department of Medical Genetics, Clinical Center, University of Pecs, Hungary, Szegeti Street 12, Pecs H-7624, Hungary

² Human Genetic and Pharmacogenomic Research Group, Janos Szentagothai Research Centre, Pecs, Hungary, Ifjusag Street 20, Pecs 7624, Hungary

Background

Cardiovascular diseases (CVD) are the major cause of death worldwide. However, their exact prevalence is unknown [1, 2]. Several studies have established that elevated triglyceride (TG) levels are independent risk factors for vascular occlusions [3, 4]. Thus, research of the TG level modifier factors, especially genetic susceptibility variants, may have clinical importance. One of these factors is the APOA5 gene. Apolipoprotein AV (apoAV) protein is the latest identified member of the apolipoprotein family, which was discovered more than a decade ago [5, 6]. ApoA5 has been shown to play an important role in lipid metabolism via interacting with lipoprotein lipase (LPL) and the anchoring molecules [7–10]. This interaction accelerates the hydrolysis of triglyceride-rich lipoproteins by affecting LPL or promotes a receptor mediated endocytosis of lipoprotein [11, 12]. The presence of naturally existing polymorphisms of the

APOA5 gene modifies the effect of the protein on lipid metabolism, resulting in increased TG levels [5, 13, 14] as confirmed in several populations worldwide. The APOA5 polymorphisms may trigger the development of several diseases like metabolic syndrome, stroke and CVD [15–19].

In the past decade, several polymorphisms were identified in the protein encoding gene. Among these, the most extensively studied four single nucleotide polymorphisms (SNPs) are the following: rs662799, rs2266788, rs207560 and rs3135506. Epidemiological and clinical studies show that some of these SNPs are independent risk factors for CVD, metabolic syndrome and stroke [3, 20]. The most extensively studied rs662799 polymorphism has been associated with coronary artery disease in almost all populations [21]. Pennacchio et al. confirmed that the most common SNPs in the APOA5 gene are in strong linkage disequilibrium and constitute haplotype variants [13]. One of these haplotypes, APOA5*2, was found to be strongly associated with increased TG levels and confers susceptibility for metabolic and vascular events [18, 22].

Historical, linguistic and genetic studies suggest that the Roma people originate from South Asia, mainly Northwest India [23, 24]. The estimated size of the Roma population is 12–15 million globally. Most of them - approximately 10–12 million - live in Europe, with the highest population (70%) in Central and South-Eastern Europe [25]. Careful review of the available literature revealed that the Roma in Central-Eastern Europe often have a higher rate of cardiovascular events and morbidity than other European populations [26, 27]. This is related to the Roma population's poor socioeconomic status, social exclusion, and other risk factors like disturbed lipid metabolism, hypertension, obesity, drinking and smoking habits [28]. However, little information is available about the effects of genetic variants. Moreover, it is also known, that the Roma population has high prevalence of increased TG levels [28]. These considerations prompted us to examine TG level modifier APOA5 polymorphisms in Roma samples as susceptibility factor.

Methods

Study Populations

DNA samples used in this study were selected from the Biobank of the Department of Medical Genetics at the University of Pécs, which is a member of the National Biobank Network of Hungary and Biomolecular Resources Research Infrastructure (BBMRI). The collection and analysis of the DNA samples were conducted according to the regulations of the Declaration of Helsinki Declaration in 1975 and the currently operative National regulations were followed. The study protocol was reviewed and approved by the Hungarian Scientific and Research Ethics Committee of the Medical Research Council (ETT TUKÉB). Informed written

consents were obtained from all subjects prior to study. During the sample collection samples were deposited from Roma minority who self-reported at least three past generations of Roma ancestry. Care was also taken during the selection of the already biobanked samples to minimize biased results coming from possible sampling errors; like exclusion of the known family members, selection from different living areas. The same also applied for the average Hungarians as well; none of them self-reported to belong to any known ethnic groups living in Hungary, they were apparently healthy and free from any known disease.

Sample size determination was based on our preliminary analyses of the prevalence of APOA5 SNPs. Based on the important significant difference in frequencies of the genetic alterations between Roma and Hungarian samples; we calculated how many samples we would need per group to be adequately small and large enough to detect a statistically significant difference and to exclude Type I and Type II errors ($\alpha = 0.05$ and $\beta < 0.03$, two tailed). Thus, a total of 363 (gender: 162 male, 201 female; age: 55.86 ± 0.99) Roma and 404 (gender: 141 male, 263 female; age: 61.51 ± 0.79) Hungarian samples. The fasting serum TG and total cholesterol levels of the subjects were measured right after taking blood samples, which was carried out morning up between 8:00 and 9:00 in the morning.

Genotyping

The genomic DNA was obtained from peripheral blood leukocytes. PCR-RFLP method was used for genotyping. GenBank reference sequence NM_001166598.1 and NG_015894.1 of APOA5 were used and variants were described in accordance with Human Genome Variation Society (HGVS) nomenclature guidelines. The APOA5 variants in this manuscript have been submitted to the Leiden Open Variation Database (<http://databases.lovd.nl/shared/genes/APOA5>, LOVD v.3.0, Screening ID: 000165133, Individual ID: 0016581, Variant ID: 0000036378). The APOA5 rs662799 variant was determined with the following primers: forward primer: 5'-CCCCAGGAACTGGAGCGACCTT-3', reverse primer: 5'-TTCAAGCAGAGGGAAGCCTGTA 3'. PCR conditions were the following: 2 min of predenaturation at 96 °C then 35 cycles of denaturation at 96 °C for 30 s, annealing at 55 °C for 30 s and extension at 72 °C for 30 s followed by a final elongation period at 72 °C for 5 min. After amplification, the PCR products were digested by 1 U of *TruI* restriction enzyme (Fermentas, Burlington, ON, Canada). The digestion resulted in 109 and 289 bp long fragments in GG homozygous samples, 22, 109, 267 bp long fragments in AA homozygous samples, and 22, 109, 267, 289 bp long fragments in heterozygous samples. DNA fragments were

separated by agarose electrophoresis and visualized by ethidium bromide staining and UV illumination.

For genotyping the rs207560 variant the following primers were used: forward primer: 5'-CTCAAGGCTGTCTTCAG-3', reverse primer: 5'-CCTTTGATTCTGGGGACTGG-3'. For amplification we used the following PCR conditions: 2 min of predenaturation at 96 °C then 35 cycles of denaturation at 96 °C for 30 s, annealing at 62 °C for 30 s and extension at 72 °C for 30 s followed by a final elongation period at 72 °C for 5 min. PCR products were digested with *MnlI* enzyme (Fermentas, Burlington, ON, Canada) resulting in 25, 41, 73, 141 bp long fragments in TT homozygous samples; 25, 114, 141 bp long fragments in CC homozygous samples and 25, 41, 73, 114, 141 bp long fragments if the sample was heterozygous for this variant. Separation and visualization were performed as written above.

For the rs2266788 polymorphism we used the following primers to amplify the region of interest: forward primer: 5'-TCAGTCCTTGAAAGTGGCCT-3', reverse primer: 5'-ATGTAGTGGCACAGGCTTCC-3'. PCR conditions were the following: 2 min of predenaturation at 96 °C then 35 cycles of denaturation at 96 °C for 30 s, annealing at 62 °C for 30 s and extension at 72 °C for 30 s followed by a final elongation period at 72 °C for 5 min. After amplification, the PCR products were digested by 1 U of *BseGI* restriction enzyme (Fermentas, Burlington, ON, Canada). The digestion resulted in 35, 87 and 165 bp long fragments in GG homozygous samples, 122, 165 bp long fragments in AA homozygotes, and 35, 87, 122, 165 bp long fragments in the case of heterozygous samples. DNA fragments were separated by electrophoresis and visualized by ethidium bromide staining and UV illumination.

For genotyping the rs3135506 variant we used the following primers: forward primer: 5'-AGAGCTAGCACCGC TCCTTT, reverse primer: 5'-TAGTCCCTCTCCAC AGCGTT-3'. For amplification we used the following PCR conditions: 2 min of predenaturation at 96 °C then 35 cycles of denaturation at 96 °C for 30 s, annealing at 62 °C for 30 s and extension at 72 °C for 30 s followed by a final elongation period at 72 °C for 5 min. PCR products were digested with *Cfr13I* enzyme (Fermentas, Burlington, ON, Canada) resulting 26, 79 and 151 bp long fragments in GG homozygous samples 79 and 177 bp long fragments in CC homozygous samples and 26, 79, 151 and 177 bp long fragments if the sample was heterozygous for this variant. Separation and visualization were performed as described above.

Statistical Analyses

All clinical data are represented as mean \pm SEM. The variables showed non-normal distribution therefore we used non-parametric tests to assess the differences between the study groups. The χ^2 tests were used for discrete variables like sex of the participants, genotype- and allele count. Mann-Whitney

tests were used for continuous variables like age and lipid levels. Linear regression analysis was used to identify any correlation between APOA5 variants and lipid levels. Variables were log-transformed to obtain approximate normal distribution for performing the analysis. Correlation coefficients (crude r) were derived from the analysis of lipid levels (dependent variable) and carriers of APOA5 risk alleles (independent variable) at 95% confidence intervals (CI). The regression models were adjusted for age and total cholesterol levels, which variables were significantly different between the study groups (adjusted r). Haploview 4.2 was used to study the linkage disequilibrium (LD) patterns. We required the minor allele frequency at each locus to be >0.05 , with an r^2 value of <0.8 between pairs of loci, based on the default settings in Haploview [29]. We used HAPSTAT 3.0 (<http://www.bios.unc.edu/wlin/hapstat/>) for haplotype assignment. The value of $p \leq 0.05$ was considered as statistically significant. For statistical analysis of the data we used PASW statistics 20 software package (SPSS Inc., Chicago IL).

Results

All of the alleles and genotype frequencies of the studied APOA5 alterations are reported in Table 1. The allele and genotype frequencies were in Hardy-Weinberg equilibrium in all study groups. The number of alleles and genotypes of Roma subjects were compared to Hungarians and four other populations derived from two databases. For rs662799 APOA5 polymorphism we found that the frequency of the G allele was almost three times higher in the Roma population compared to Hungarian samples ($p = 0.0001$) and almost two times higher than in European population (1000Genomes; $p = 0.006$). There was also a significantly large difference in allele frequency between Roma and HapMap European population ($p = 0.0001$). The G allele was at least two-fold more frequent in Asian (1000Genomes) and HapMap Chinese population than in Roma subjects ($p = 0.002$; 0.001). Homozygous carriers of G allele were more frequent in Roma population than in Hungarians ($p = 0.037$) and in Europeans (1000Genomes; $p = 0.010$); however, it was less frequent in Romas than in Asian (1000Genomes; $p = 0.027$) population. There was no significant difference in GG genotype frequencies between Roma and HapMap Chinese populations. Results of rs207560 show the frequency of the T allele in Roma samples was almost double than in those of the Hungarian population ($p = 0.018$). The T allele was significantly frequent in Asian (1000Genomes; $p = 0.0001$) population than in Romas. There was no difference between Roma and European populations (1000Genomes; $p = 0.185$). Homozygous carriers of T allele were more frequent in Asian population (1000Genomes) than in Roma subjects ($p = 0.0001$); however, the frequency of TT genotypes was

Table 1 Genotype and allele frequencies of APOA5 gene variants

APOA5 variant	Population	N	Alleles N	Risk allele frequency (%)	p-value ^a	Genotypes N (%)	p-value ^b
g.116792991G > <u>A</u>			<u>A</u> G G			AA AG GG	
	Roma from Hungary (this study)	363	628 98	13.50		278 (76.58) 72 (19.84) 13 (3.58)	
	non-Roma from Hungary (this study)	404	765 43	5.32	0.0001	366 (90.60) 33 (8.17) 5 (1.24)	0.037
	Asian (1000Genomes)	504	718 290	28.80	0.002	251 (49.80) 216 (42.86) 37 (7.34)	0.027
	European (1000Genomes)	503	922 84	8.35	0.006	424 (84.30) 74 (14.71) 5 (0.99)	0.010
	HapMap Chinese	45	66 24	26.70	0.001	23 (51.11) 20 (44.44) 2 (4.44)	0.780
g.116791110 T > <u>C</u>			<u>C</u> T T			CC CT TT	
	Roma from Hungary (this study)	363	680 46	6.34		318 (87.60) 44 (12.12) 1 (0.28)	
	non-Roma from Hungary (this study)	404	779 29	3.59	0.018	376 (93.07) 27 (6.68) 1 (0.25)	0.940
	Asian (1000Genomes)	504	768 240	23.81	0.0001	290 (57.54) 188 (37.3) 26 (5.16)	0.0001
	European (1000Genomes)	503	924 82	8.15	0.185	426 (84.70) 72 (14.31) 5 (0.99)	0.211
	g.116791691G > <u>C</u>			<u>C</u> G G			CC CG GG
Roma from Hungary (this study)		363	658 68	9.37		300 (82.64) 58 (15.98) 5 (1.38)	
non-Roma from Hungary (this study)		404	770 38	4.70	0.001	367 (90.84) 36 (8.91) 1 (0.25)	0.079
Asian (1000Genomes)		504	1008 0	0	-	504 (100) 0 0	-
European (1000Genomes)		503	938 68	6.76	0.066	438 (87.08) 62 (12.33) 3 (0.59)	0.240
g.116789970G > <u>A</u>			<u>A</u> G G			AA AG GG	
	Roma from Hungary (this study)	363	679 47	6.47		317 (87.33) 45 (12.40) 1 (0.27)	
	non-Roma from Hungary (this study)	404	747 61	7.55	0.473	344 (85.15) 59 (14.60) 1 (0.25)	0.940
	Asian (1000Genomes)	504	768 240	23.81	0.0001	290 (57.54) 188 (37.30) 26 (5.16)	0.0001
	European (1000Genomes)	503	914 92	9.15	0.062	416 (82.70) 82 (16.30) 5 (0.99)	0.211
	HapMap Chinese	45	68 22	24.40	0.0001	24 (53.33) 20 (44.44) 1 (2.22)	0.082
HapMap European	59	113 5	4.24	0.375	54 (91.53) 5 (8.47) 0	-	

Ancestral alleles are underlined

^a indicates significance of the differences between Roma and other population risk alleles

^b indicates significance of the differences between Roma and other population homozygous carriers

similar in Hungarians and in Europeans (1000 Genomes; $p = 0.940$; 0.211). Data of rs3135506 show that the G allele frequency in Roma's was more than two times higher compared to the Hungarian population ($p = 0.001$); however, it does not differ significantly from the European population (1000Genomes; $p = 0.066$). There was no significant difference in the frequency of GG genotype of Hungarians and of Europeans (1000 Genomes; $p = 0.079$; 0.240) compared to Roma subjects. Allele- and genotype frequency data of rs207560 and rs3135506 in European and Chinese populations are not available in HapMap database, thus the analyses were not executed in these cases. We also analyzed the rs2266788 variant, where we did not find any difference between G allele frequencies of Hungarian and European populations (1000Genomes, HapMap) compared to Roma subjects ($p = 0.473$; 0.062 ; 0.375). We found the frequency of the G allele was more than three times higher in Asian populations (1000Genomes and HapMap Chinese) compared to Roma samples ($p = 0.0001$). The frequency of GG genotype was significantly different only in Asian population (1000Genomes) compared to Roma ($p = 0.0001$). Cases with $n = 0$ were not analyzed statistically.

Table 2. summarizes the lipid parameters of the populations according to genotypes. The plasma triglyceride levels were significantly elevated in the carriers of the risk alleles when compared to non-carriers for all SNPs in both populations. Significantly higher triglyceride levels were found in heterozygous carriers of rs207560, rs3135506 and rs2266788 variants

compared to non-carriers in both study groups. Homozygous carriers of rs662799 variant have higher triglyceride levels than non-carriers in Roma subjects. In Hungarians, we did not find any difference in triglyceride levels between homo- or heterozygous carriers and non-carriers. Comparison of the cholesterol levels did not show any difference.

We analyzed associations among the four APOA5 variants in both study groups. (Table 3) Strong correlations were found among rs662799, rs207560 and rs2266788 variants. However, rs3135506 variant did not show significant correlation with other APOA5 variants in Roma samples as well as in Hungarians. The same associations were detected after inclusion of the adjustment parameters like age and total cholesterol levels.

The associations between APOA5 variants and triglyceride/cholesterol levels are summarized in Table 4. Significant correlations were found between all of the APOA5 variants and triglycerides in both populations. After inclusion of the adjustment parameters, such as age and total cholesterol levels, the association became even stronger. We did not observe any significant correlation between allelic variants and cholesterol levels in both populations (data not shown).

Furthermore, we examined the linkage disequilibrium among the APOA5 major polymorphisms in both populations. We found moderate association between the rs2266788 and the rs3135506 variants ($r^2 = 0.56$), likewise between rs207560 and rs3135506 ($r^2 = 0.42$) in Hungarian population. In Roma population we found strong association between the rs207560 and the rs3135506 variants ($r^2 = 0.97$).

Table 2 Lipid parameters (mmol/l) of the Roma and Hungarian population samples according to APOA5 gene variants

APOA5 variant	Parameter	Roma				Hungarian			
rs662799	Triglyceride	AA 1.59 ± 0.04	AG 1.72 ± 0.10	GG 2.00 ± 0.16	AG + GG 1.76 ± 0.08	AA 1.51 ± 0.02	AG 1.79 ± 0.13	GG 1.88 ± 0.31	AG + GG 1.81 ± 0.12
	Cholesterol	4.66 ± 0.07	4.77 ± 0.13 <i>p</i> = 0.245	4.91 ± 0.39 <i>p</i> = 0.009	4.79 ± 0.12 <i>p</i> = 0.049	5.57 ± 0.06	5.43 ± 0.22 <i>p</i> = 0.060	6.14 ± 1.16 <i>p</i> = 0.133	5.52 ± 0.24 <i>p</i> = 0.024
rs207560	Triglyceride	CC 1.59 ± 0.04	CT 1.92 ± 0.12	TT 1.27 ± 0	CT + TT 1.91 ± 0.12	CC 1.51 ± 0.02	CT 1.84 ± 0.13	TT 1.60 ± 0	CT + TT 1.84 ± 0.12
	Cholesterol	4.67 ± 0.06	4.85 ± 0.19 <i>p</i> = 0.009	3.90 ± 0 <i>p</i> = 0.668	4.83 ± 0.19 <i>p</i> = 0.011	5.57 ± 0.06	5.50 ± 0.29 <i>p</i> = 0.009	4.70 ± 0 <i>p</i> = 0.602	5.47 ± 0.28 <i>p</i> = 0.008
rs3135506	Triglyceride	CC 1.59 ± 0.04	CG 1.81 ± 0.10	GG 1.96 ± 0.50	CG + GG 1.82 ± 0.10	CC 1.52 ± 0.03	CG 1.71 ± 0.07	GG 1.50 ± 0	CG + GG 1.71 ± 0.06
	Cholesterol	4.67 ± 0.06	4.88 ± 0.14 <i>p</i> = 0.028	4.14 ± 0.43 <i>p</i> = 0.586	4.82 ± 0.13 <i>p</i> = 0.025	5.55 ± 0.06	5.67 ± 0.17 <i>p</i> = 0.001	5.50 ± 0 <i>p</i> = 0.943	5.66 ± 0.17 <i>p</i> = 0.001
rs2266788	Triglyceride	AA 1.59 ± 0.04	AG 1.92 ± 0.12	GG 1.27 ± 0	AG + GG 1.90 ± 0.12	AA 1.51 ± 0.03	AG 1.69 ± 0.07	GG 1.60 ± 0	AG + GG 1.69 ± 0.07
	Cholesterol	4.67 ± 0.06	4.84 ± 0.19 <i>p</i> = 0.008	3.90 ± 0 <i>p</i> = 0.671	4.82 ± 0.19 <i>p</i> = 0.010	5.57 ± 0.06	5.52 ± 0.18 <i>p</i> = 0.004	4.70 ± 0 <i>p</i> = 0.575	5.50 ± 0.17 <i>p</i> = 0.004

We also investigated the haplotypes with statistical probes in Roma and Hungarian populations. The structure of the probable haplotypes is summarized in Table 5. With the applied methods, we identified seven haplotypes in each population. Six of these haplotypes, APOA5*1, APOA5*2, APOA5*3, APOA5*4, APOA5*5 and ht7 were found to occur most frequently in both populations. The frequencies of the haplotypes are shown in Table 5. Significant differences were found in the presence of APOA5*2, APOA5*4, APOA5*5 and ht7 haplotypes between the Roma and Hungarian populations. However, we did not identify differences in the presence of APOA5*1 and APOA5*3 haplotypes between these populations. Ht5 haplotype in Roma and ht4 haplotype in Hungarian population could not be detected.

Discussion

In the present study, we examined the effect of the major APOA5 polymorphisms (rs662799; rs2266788; rs3135506; rs207560) on lipids, especially triglyceride levels. In our results, heterozygous carriers of rs2266788; rs3135506; rs207560 variants had higher triglyceride levels than non-carriers. Homozygous carriers of rs662799 variant have higher triglyceride levels than non-carriers in Roma subjects. To our best knowledge, such association has not yet been described. However, most of the studies do not present the homozygous and heterozygous samples separately because of the low risk allele frequencies of the APOA5 variants. In our study, after combining the homozygous and heterozygous samples, significantly elevated plasma TG levels were found in carriers of risk alleles of the APOA5 variants when compared to the non-

carriers in both Hungarian and Roma populations. All four APOA5 variants showed correlation to triglyceride levels with or without adjustment factors like age and cholesterol levels. These findings correspond to the results of previous studies [16–19, 30].

Health status is a major problem for health care systems of those countries where Romas are in significant minority [28]. In Central-Eastern Europe, Romas are likely more susceptible to metabolic syndrome and stroke, have higher morbidity rates, and lower life expectancy than other European populations [26, 31]. CVD among Romas is one of the most common causes of death [27, 32, 33] reportedly with 2.5-fold higher premature CVD mortality compared to the overall population [34] and increased prevalence of various CVD risks factors [35–38]. The situation is not restricted to the Eastern European countries [36, 37].

There are several classic risk factors that increase the development of CVD e.g.: smoking, family history with CVD, hypertension, lipid and lipoprotein abnormalities (elevated total cholesterol and low density lipoprotein (LDL)-cholesterol, high density lipoprotein (HDL)-cholesterol, hypertriglyceridemia and increased lipoprotein(a) (Lp(a)), diabetes (insulin resistance, hyperinsulinemia and elevated blood glucose level), obesity and metabolic syndromes. According to various clinical studies in Central-Eastern Europe [28], the two most common risk factors contributing to the development of CVD presented in most of the Roma populations are obesity and smoking. These are followed by diabetes, metabolic syndrome, hypertension, and increase of triglycerides. Higher prevalence of obesity may result from decreased physical activity and unhealthy dietary habits of the Romas. Smoking is strongly supported as cultural, ethnical, and individual

Table 3 Correlations among APOA5 variants in the study groups

Population	Correlation coefficient (R)	APOA5 variant	APOA5 variant			
			rs662799	rs207560	rs3135506	rs2266788
Roma	Crude	rs662799	-	0.562 <i>p</i> < 0.001 CI = 0.612–0.832	0.021 <i>p</i> = 0.684 CI = -0.092–0.140	0.552 <i>p</i> < 0.001 CI = 0.593–0.813
		rs207560	0.562 <i>p</i> < 0.001 CI = 0.612–0.832	-	0.084 <i>p</i> = 0.110 CI = -0.163–0.017	0.988 <i>p</i> < 0.001 CI = 0.980–1.013
		rs3135506	0.021 <i>p</i> = 0.684 CI = -0.092–0.140	0.084 <i>p</i> = 0.110 CI = -0.163–0.017	-	0.087 <i>p</i> = 0.098 CI = -0.167–0.014
		rs2266788	0.552 <i>p</i> < 0.001 CI = 0.593–0.813	0.988 <i>p</i> < 0.001 CI = 0.980–1.013	0.087 <i>p</i> = 0.098 CI = -0.167–0.014	-
		rs662799	-	0.636 <i>p</i> < 0.001 CI = 0.665–0.883	0.119 <i>p</i> = 0.913 CI = -0.119–0.133	0.625 <i>p</i> < 0.001 CI = 0.642–0.860
		rs207560	0.636 <i>p</i> < 0.001 CI = 0.665–0.883	-	0.138 <i>p</i> = 0.110 CI = -0.185–0.019	0.985 <i>p</i> < 0.001 CI = 0.977–1.016
		rs3135506	0.119 <i>p</i> = 0.913 CI = -0.119–0.133	0.138 <i>p</i> = 0.110 CI = -0.185–0.019	-	0.137 <i>p</i> = 0.099 CI = -0.190–0.016
		rs2266788	0.625 <i>p</i> < 0.001 CI = 0.642–0.860	0.985 <i>p</i> < 0.001 CI = 0.977–1.016	0.137 <i>p</i> = 0.099 CI = -0.190–0.016	-
	Adjusted [†]	rs662799	-	0.780 <i>p</i> < 0.001 CI = 0.826–0.967	0.073 <i>p</i> = 0.143 CI = -0.173–0.025	0.485 <i>p</i> < 0.001 CI = 0.328–0.469
		rs207560	0.780 <i>p</i> < 0.001 CI = 0.826–0.967	-	0.019 <i>p</i> = 0.702 CI = -0.133–0.090	0.626 <i>p</i> < 0.001 CI = 0.769–0.984
		rs3135506	0.073 <i>p</i> = 0.143 CI = -0.173–0.025	0.019 <i>p</i> = 0.702 CI = -0.133–0.090	-	0.084 <i>p</i> = 0.090 CI = -0.224–0.016
		rs2266788	0.485 <i>p</i> < 0.001 CI = 0.328–0.469	0.626 <i>p</i> < 0.001 CI = 0.769–0.984	0.084 <i>p</i> = 0.090 CI = -0.224–0.016	-
Adjusted [†]	rs662799	-	0.803 <i>p</i> < 0.001 CI = 0.833–0.970	0.076 <i>p</i> = 0.160 CI = -0.177–0.029	0.512 <i>p</i> < 0.001 CI = 0.345–0.488	
	rs207560	0.803 <i>p</i> < 0.001 CI = 0.833–0.970	-	0.061 <i>p</i> = 0.703 CI = -0.110–0.074	0.637 <i>p</i> < 0.001 CI = 0.769–0.986	
	rs3135506	0.076 <i>p</i> = 0.160 CI = -0.177–0.029	0.061 <i>p</i> = 0.703 CI = -0.110–0.074	-	0.090 <i>p</i> = 0.098 CI = -0.233–0.020	
	rs2266788	0.512 <i>p</i> < 0.001 CI = 0.345–0.488	0.637 <i>p</i> < 0.001 CI = 0.769–0.986	0.090 <i>p</i> = 0.098 CI = -0.233–0.020	-	

[†] Adjusted for differences in age and cholesterol levels

identity, thus, they usually start smoking in their early teens. Most of the population is exposed to these risk factors in their direct family environment [28].

Previous studies of some susceptibility genetic variants revealed Roma are a genetically special population [39–42] and their genetic constitution can differ from other populations (we supposed susceptibility alleles in the background also as genetic factors) [43, 44]. In our study, the minor allele frequencies of the studied APOA5 variants were collected in 1000Genomes and HapMap databases, to compare those found in the Roma population with those in Europeans and Asians. For rs662799, significantly different risk allele

frequencies were detected between Roma and other studied populations. The allele frequencies in Roma subjects were in between those of Europeans and Asians. We found Roma risk allele frequencies differed significantly from those of the Asian populations for rs662799, rs207560, rs2266788 variants. We found, that the risk allele frequencies were significantly higher in Roma than in Hungarian population for rs662799; rs3135506 and rs207560 variants. It is important to emphasize, that the frequencies found in Hungarians correspond with those detected in European populations [13, 45, 46]. The reasons for these differences have not yet been cleared. At the same time, the already confirmed definitive

Table 4 Correlations between carrying APOA5 risk alleles and triglyceride levels in Roma and Hungarian population samples

Population	Correlation coefficients	APOA5 variant				
		rs662799	rs207560	rs3135506	rs2266788	
Roma	Crude	R/Beta	0.102	0.149	0.124	0.149
		R ²	0.011	0.022	0.015	0.022
		95% CI	0.000–0.092	0.027–0.144	0.011–0.113	0.027–0.143
	Adjusted [†]	p	0.051	0.004	0.018	0.004
		R	0.360	0.351	0.362	0.351
		R ²	0.129	0.123	0.131	0.123
		Beta	0.138	0.111	0.142	0.113
		95% CI	0.014–0.115	0.002–0.126	0.018–0.129	0.003–0.126
		p	0.012	0.043	0.009	0.040
Hungarian	Crude	R/Beta	0.155	0.161	0.142	0.137
		R ²	0.024	0.026	0.020	0.019
		95% CI	0.024–0.106	0.031–0.125	0.019–0.102	0.014–0.081
	Adjusted [†]	p	0.002	0.001	0.004	0.006
		R	0.200	0.214	0.182	0.199
		R ²	0.040	0.046	0.033	0.039
		Beta	0.152	0.171	0.129	0.151
		95% CI	0.022–0.106	0.033–0.128	0.012–0.098	0.018–0.086
		p	0.003	0.001	0.012	0.003

[†] Adjusted for differences in age and cholesterol levels

association of susceptibility variants and the development of diseases mean that increased minor allele frequencies obligatory lead to increased vascular events [21]. Thus, the data of the present study support that elevated rates of susceptibility alleles are in relationship- at least in part- with increased prevalence of CVDs in Roma minority.

The most common APOA5 variants, like rs662799, rs207560, rs2266788 and rs3135506 are in strong linkage disequilibrium and create two major haplotype variants (APOA5*2 and *3). These two haplotypes together with wild type haplotype (APOA5*1–3) constitute approximately 98% of the average population [13]. Five common haplotypes were identified this far (APOA5*1–5) [47–49]. Additional possible haplotypes are also known (ht4, 5, 7) composing only a small portion of the population. In our study, we prospected linkage disequilibrium among the APOA5 polymorphisms in both

populations and attempted to investigate the haplotypes in Roma and Hungarian samples. Different linkage was found between the rs207560 and rs3135506 in Roma and Hungarian populations. In Roma the linkage between the variants was strong, while in Hungarians moderate, possibly because of the distinct origin of the two populations. To our best knowledge, such association has not yet been described.

The haplotype analyses for APOA5 revealed eight theoretical haplotypes, but only seven occurred in both populations. Five of these (APOA5*1, APOA5*2, APOA5*3, APOA5*4 and APOA5*5) are the most extensively studied haplotypes of the gene. Ht7 haplotype has not yet been investigated in susceptibility studies, so far. Comparison of the prevalence's in Roma and Hungarian populations revealed APOA5*2, APOA5*4 and ht7 haplotypes were significantly prevalent in Roma population, whereas APOA5*5 haplotype was more frequent in Hungarians.

Table 5 The structure of the individual APOA5 haplotype variants with percentage of Romas and Hungarians

Haplotypes	APOA5 variant				Population Roma/Hungarian (%)
	rs662799	rs207560	rs3135506	rs2266788	
APOA5*1/ ht1	A	C	C	A	77.8/85.6
APOA5*2/ ht8	G	T	C	G	5.4 [†] /3.2
APOA5*3/ ht3	A	C	G	A	7.6/4.7
APOA5*4/ ht2	G	C	C	A	6.3 [†] /2.0
APOA5*5/ ht6	A	C	C	G	0.1 [†] /4.1
ht4	G	C	G	A	1.8/–
ht5	G	T	C	A	–/0.1
ht7	A	T	C	G	1.0 [†] /0.2

[†] *p* < 0.05 vs Hungarian samples

Results of previous studies describe APOA5*2 haplotype is associated with elevated TG levels and might confer as susceptibility for metabolic syndrome and ischemic stroke in the Hungarian population [18, 22]. Our results suggest, Roma people have higher risk for hypertriglyceridemia and for vascular events because of increased prevalence of the APOA5 susceptibility alleles. Previously, Kisfali et al. did not confirm connection between the presence of APOA5*4 and the risk for metabolic syndrome in Hungarians. Moreover, APOA5*5 haplotype was found to have a protective effect against metabolic syndrome, and associated with decreased TG levels [22]. Our findings on APOA5*5 reported here also provide indirect support for APOA5 variant's having a role in the Roma susceptibility to CVD.

Acknowledgements We would like to thank Ildiko Bock-Marquette and Jon Marquette for their English review. (UTSW Dallas, Texas)

Compliance with Ethical Standards

Funding and Grants The study was supported by the grant of OTKA K103983.

Conflict of Interest The authors declare no conflict of interest.

References

- Krauss RM (1998) Atherogenicity of triglyceride-rich lipoproteins. *Am J Cardiol* 81(4A):13B–17B
- Hodis HN (1999) Triglyceride-rich lipoprotein remnant particles and risk of atherosclerosis. *Circulation* 99(22):2852–2854
- Cullen P (2000) Evidence that triglycerides are an independent coronary heart disease risk factor. *Am J Cardiol* 86(9):943–949
- Haim M, Benderly M, Brunner D, Behar S, Graff E, Reicher-Reiss H, Goldbourt U (1999) Elevated serum triglyceride levels and long-term mortality in patients with coronary heart disease: the Bezafibrate infarction prevention (BIP) registry. *Circulation* 100(5):475–482
- Pennacchio LA, Olivier M, Hubacek JA, Cohen JC, Cox DR, Fruchart JC, Krauss RM, Rubin EM (2001) An apolipoprotein influencing triglycerides in humans and mice revealed by comparative sequencing. *Science* 294(5540):169–173. doi:10.1126/science.1064852
- van der Vliet HN, Sammels MG, Leegwater AC, Levels JH, Reitsma PH, Boers W, Chamuleau RA (2001) Apolipoprotein A-V: a novel apolipoprotein associated with an early phase of liver regeneration. *J Biol Chem* 276(48):44512–44520. doi:10.1074/jbc.M106888200
- Sharma V, Ryan RO, Forte TM (2012) Apolipoprotein A-V dependent modulation of plasma triacylglycerol: a puzzlement. *Biochim Biophys Acta* 1821(5):795–799. doi:10.1016/j.bbali.2011.12.002
- Gin P, Yin L, Davies BS, Weinstein MM, Ryan RO, Bensadoun A, Fong LG, Young SG, Beigneux AP (2008) The acidic domain of GPIIb/IIIa is important for the binding of lipoprotein lipase and chylomicrons. *J Biol Chem* 283(43):29554–29562. doi:10.1074/jbc.M802579200
- Gin P, Beigneux AP, Davies B, Young MF, Ryan RO, Bensadoun A, Fong LG, Young SG (2007) Normal binding of lipoprotein lipase, chylomicrons, and apo-AV to GPIIb/IIIa containing a G56R amino acid substitution. *Biochim Biophys Acta* 1771(12):1464–1468. doi:10.1016/j.bbali.2007.10.005
- Sun G, Bi N, Li G, Zhu X, Zeng W, Wu G, Xue H, Chen B (2006) Identification of lipid binding and lipoprotein lipase activation domains of human apoAV. *Chem Phys Lipids* 143(1–2):22–28. doi:10.1016/j.chemphyslip.2006.04.004
- Lookene A, Beckstead JA, Nilsson S, Olivecrona G, Ryan RO (2005) Apolipoprotein A-V-heparin interactions: implications for plasma lipoprotein metabolism. *J Biol Chem* 280(27):25383–25387. doi:10.1074/jbc.M501589200
- Merkel M, Loeffler B, Kluger M, Fabig N, Geppert G, Pennacchio LA, Laatsch A, Heeren J (2005) Apolipoprotein AV accelerates plasma hydrolysis of triglyceride-rich lipoproteins by interaction with proteoglycan-bound lipoprotein lipase. *J Biol Chem* 280(22):21553–21560. doi:10.1074/jbc.M411412200
- Pennacchio LA, Olivier M, Hubacek JA, Krauss RM, Rubin EM, Cohen JC (2002) Two independent apolipoprotein A5 haplotypes influence human plasma triglyceride levels. *Hum Mol Genet* 11(24):3031–3038
- Pennacchio LA, Rubin EM (2003) Apolipoprotein A5, a newly identified gene that affects plasma triglyceride levels in humans and mice. *Arterioscler Thromb Vasc Biol* 23(4):529–534. doi:10.1161/01.ATV.0000054194.78240.45
- Hubacek JA, Skodova Z, Adamkova V, Lanska V, Poledne R (2004) The influence of APOAV polymorphisms (T-1131 > C and S19 > W) on plasma triglyceride levels and risk of myocardial infarction. *Clin Genet* 65(2):126–130
- Kisfali P, Mohas M, Maasz A, Hadarits F, Marko L, Horvatovich K, Oroszlan T, Bagosi Z, Bujtor Z, Gasztonyi B, Wittmann I, Melegh B (2008) Apolipoprotein A5 IVS3 + 476A allelic variant associates with increased triglyceride levels and confers risk for development of metabolic syndrome in Hungarians. *Circ J* 72(1):40–43
- Maasz A, Kisfali P, Horvatovich K, Mohas M, Marko L, Csonge V, Farago B, Jaromi L, Magyari L, Safrany E, Sipeky C, Wittmann I, Melegh B (2007) Apolipoprotein A5 T-1131C variant confers risk for metabolic syndrome. *Pathol Oncol Res* 13(3):243–247
- Maasz A, Kisfali P, Jaromi L, Horvatovich K, Szolnoki Z, Csonge V, Safrany E, Sipeky C, Hadarits F, Melegh B (2008) Apolipoprotein A5 gene IVS3 + G476A allelic variant confers susceptibility for development of ischemic stroke. *Circ J* 72(7):1065–1070
- Maasz A, Kisfali P, Szolnoki Z, Hadarits F, Melegh B (2008) Apolipoprotein A5 gene C56G variant confers risk for the development of large-vessel associated ischemic stroke. *J Neuro* 255(5):649–654. doi:10.1007/s00415-008-0768-z
- Zhang Z, Peng B, Gong RR, Gao LB, Du J, Fang DZ, Song YY, Li YH, Ou GJ (2011) Apolipoprotein A5 polymorphisms and risk of coronary artery disease: a meta-analysis. *Biosci Trends* 5(4):165–172
- Sarwar N, Sandhu MS, Ricketts SL, Butterworth AS, Di Angelantonio E, Boekholdt SM, Ouwehand W, Watkins H, Samani NJ, Saleheen D, Lawlor D, Reilly MP, Hingorani AD, Talmud PJ, Danesh J (2010) Triglyceride-mediated pathways and coronary disease: collaborative analysis of 101 studies. *Lancet* 375(9726):1634–1639. doi:10.1016/S0140-6736(10)60545-4
- Kisfali P, Mohas M, Maasz A, Polgar N, Hadarits F, Marko L, Brasnyo P, Horvatovich K, Oroszlan T, Bagosi Z, Bujtor Z, Gasztonyi B, Rinfel J, Wittmann I, Melegh B (2009) Haplotype analysis of the apolipoprotein A5 gene in patients with the metabolic syndrome. *Nutr Metab Cardiovasc Dis* 20(7):505–511. doi:10.1016/j.numecd.2009.05.001
- Kalaydjieva L, Gresham D, Calafell F (2001) Genetic studies of the Roma (gypsies): a review. *BMC Med Genet* 2:5

24. Zeman CL, Depken DE, Senchina DS (2003) Roma health issues: a review of the literature and discussion. *Ethn Health* 8(3):223–249. doi:10.1080/1355785032000136434
25. Gresham D, Morar B, Underhill PA, Passarino G, Lin AA, Wise C, Angelicheva D, Calafell F, Oefner PJ, Shen P, Tournev I, de Pablo R, Kucinskas V, Perez-Lezaun A, Marushiakova E, Popov V, Kalaydjieva L (2001) Origins and divergence of the Roma (gypsies). *Am J Hum Genet* 69(6):1314–1331. doi:10.1086/324681
26. McKee M (1997) The health of gypsies. *BMJ* 315(7117):1172–1173
27. Vozarova de Courten B, de Courten M, Hanson RL, Zahorakova A, Egyenes HP, Tataranni PA, Bennett PH, Vozar J (2003) Higher prevalence of type 2 diabetes, metabolic syndrome and cardiovascular diseases in gypsies than in non-gypsies in Slovakia. *Diabetes Res Clin Pract* 62(2):95–103. doi:10.1016/S0168822703001621
28. Dobranici M, Buzea A, Popescu R (2012) The cardiovascular risk factors of the Roma (gypsies) people in Central-Eastern Europe: a review of the published literature. *J Med Life* 5(4):382–389
29. Barrett JC, Fry B, Maller J, Daly MJ (2005) Haploview: analysis and visualization of LD and haplotype maps. *Bioinformatics* 21(2):263–265. doi:10.1093/bioinformatics/bth457
30. Havasi V, Szolnoki Z, Talian G, Bene J, Komlosi K, Maasz A, Somogyvari F, Kondacs A, Szabo M, Fodor L, Bodor A, Melegh B (2006) Apolipoprotein A5 gene promoter region T-1131C polymorphism associates with elevated circulating triglyceride levels and confers susceptibility for development of ischemic stroke. *J Mol Neurosci* 29(2):177–183. doi:10.1385/JMN:29:2:177
31. Flecha A (2013) Healthier lives for European minority groups: school and health care, lessons from the Roma. *Int J Environ Res Public Health* 10(8):3089–3111. doi:10.3390/ijerph10083089
32. Bogdanovic D, Nikic D, Petrovic B, Kocic B, Jovanovic J, Nikolic M, Milosevic Z (2007) Mortality of Roma population in Serbia, 2002–2005. *Croat Med J* 48(5):720–726
33. Masseria C, Mladovsky P, Hernandez-Quevedo C (2010) The socio-economic determinants of the health status of Roma in comparison with non-Roma in Bulgaria, Hungary and Romania. *Eur J Pub Health* 20(5):549–554. doi:10.1093/eurpub/ckq102
34. Alberty R, Albertyova D, Ahlers I (2009) Distribution and correlations of non-high-density lipoprotein cholesterol in Roma and Caucasian children: the Slovak lipid community study. *Coll Antropol* 33(4):1015–1022
35. Dolinska S, Kudlackova M, Ginter E (2007) The prevalence of female obesity in the world and in the Slovak gypsy women. *Bratisl Lek Listy* 108(4–5):207–211
36. Carrasco-Garrido P, Lopez de Andres A, Hernandez Barrera V, Jimenez-Trujillo I, Jimenez-Garcia R (2011) Health status of Roma women in Spain. *Eur J Pub Health* 21(6):793–798. doi:10.1093/eurpub/ckq153
37. Gualdi-Russo E, Zironi A, Dallari GV, Toselli S (2009) Migration and health in Italy: a multiethnic adult sample. *J Travel Med* 16(2):88–95. doi:10.1111/j.1708-8305.2008.00280.x
38. Krajcovicova-Kudlackova M, Blazicek P, Spustova V, Valachovicova M, Ginter E (2004) Cardiovascular risk factors in young gypsy population. *Bratisl Lek Listy* 105(7–8):256–259
39. Sipeky C, Weber A, Szabo M, Melegh BI, Janicsek I, Tarlos G, Szabo I, Sumegi K, Melegh B (2013) High prevalence of CYP2C19*2 allele in Roma samples: study on Roma and Hungarian population samples with review of the literature. *Mol Biol Rep* 40(8):4727–4735. doi:10.1007/s11033-013-2569-4
40. Sipeky C, Csongei V, Jaromi L, Safrany E, Maasz A, Takacs I, Beres J, Fodor L, Szabo M, Melegh B (2011) Genetic variability and haplotype profile of MDR1 (ABCB1) in Roma and Hungarian population samples with a review of the literature. *Drug Metab Pharmacokin* 26(2):206–215
41. Sipeky C, Lakner L, Szabo M, Takacs I, Tamasi V, Polgar N, Falus A, Melegh B (2009) Interethnic differences of CYP2C9 alleles in healthy Hungarian and Roma population samples: relationship to worldwide allelic frequencies. *Blood Cells Mol Dis* 43(3):239–242. doi:10.1016/j.bcmd.2009.05.005
42. Sipeky C, Csongei V, Jaromi L, Safrany E, Polgar N, Lakner L, Szabo M, Takacs I, Melegh B (2009) Vitamin K epoxide reductase complex 1 (VKORC1) haplotypes in healthy Hungarian and Roma population samples. *Pharmacogenomics* 10(6):1025–1032. doi:10.2217/pgs.09.46
43. Moorjani P, Patterson N, Loh PR, Lipson M, Kiszfali P, Melegh BI, Bonin M, Kadasi L, Riess O, Berger B, Reich D, Melegh B (2013) Reconstructing Roma history from genome-wide data. *PLoS One* 8(3):e58633. doi:10.1371/journal.pone.0058633
44. Mendizabal I, Lao O, Marigorta UM, Wollstein A, Gusmao L, Ferak V, Ioana M, Jordanova A, Kaneva R, Kouvatzi A, Kucinskas V, Makukh H, Metspalu A, Netea MG, de Pablo R, Pamjav H, Radojkovic D, Rolleston SJ, Sertic J, Macek M Jr, Comas D, Kayser M (2012) Reconstructing the population history of European Romani from genome-wide data. *Curr Biol* 22(24):2342–2349. doi:10.1016/j.cub.2012.10.039
45. Evans D, Seedorf U, Beil FU (2005) Polymorphisms in the apolipoprotein A5 (APOA5) gene and type III hyperlipidemia. *Clin Genet* 68(4):369–372. doi:10.1111/j.1399-0004.2005.00510.x
46. Dallongeville J, Cotel D, Wagner A, Ducimetiere P, Ruidavets JB, Arveiler D, Bingham A, Ferrieres J, Amouyel P, Meirhaeghe A (2008) The APOA5 Trp19 allele is associated with metabolic syndrome via its association with plasma triglycerides. *BMC Med Genet* 9:84. doi:10.1186/1471-2350-9-84
47. Melegh BI, Duga B, Sumegi K, Kiszfali P, Maasz A, Komlosi K, Hadzsiev K, Komoly S, Kosztolanyi G, Melegh B (2012) Mutations of the apolipoprotein A5 gene with inherited hypertriglyceridaemia: review of the current literature. *Curr Med Chem* 19(36):6163–6170
48. Yin RX, Li YY, Lai CQ (2011) Apolipoprotein A1/C3/A5 haplotypes and serum lipid levels. *Lipids Health Dis* 10:140. doi:10.1186/1476-511X-10-140
49. Furuya TK, Chen ES, Ota VK, Mazzotti DR, Ramos LR, Cendoroglo MS, Araujo LQ, Burbano RR, Smith MA (2013) Association of APOA1 and APOA5 polymorphisms and haplotypes with lipid parameters in a Brazilian elderly cohort. *Genet Mol Res* 12(3):3495–3499. doi:10.4238/2013.February.28.7